Tesi doctoral

STUDY OF EXTRACELLULAR MATRIX AND WATER CHANNELS IN BOVINE SPONGIFORM ENCEPHALOPATHY

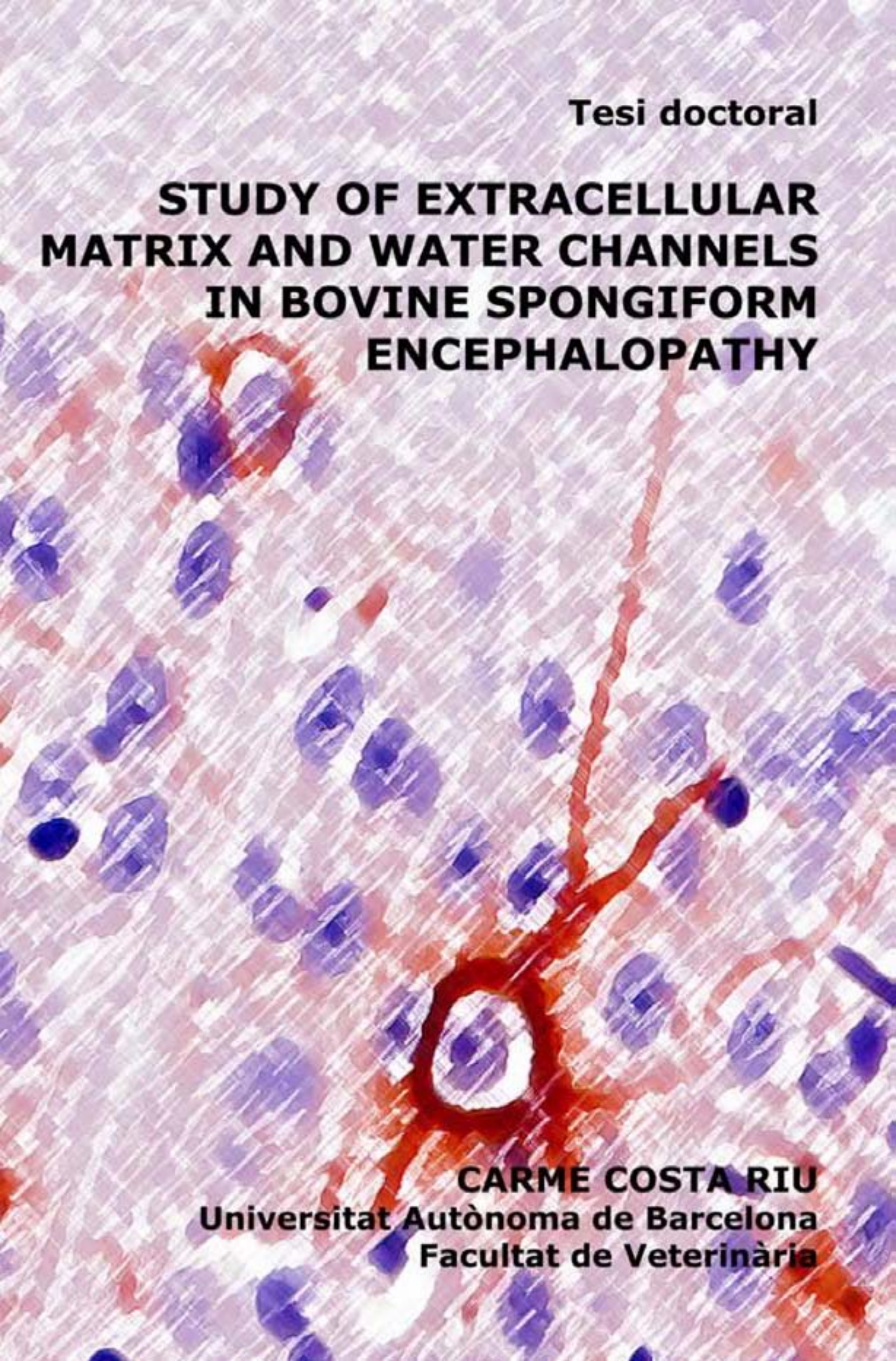

CARME COSTA RIU
Universitat Autònoma de Barcelona
Facultat de Veterinària

Universitat Autònoma de Barcelona
Facultat de Veterinària
Departament de Medicina i Cirurgia Animals

STUDY OF EXTRACELLULAR MATRIX AND WATER CHANNELS IN BOVINE SPONGIFORM ENCEPHALOPATHY

Tesi que presenta Carme Costa Riu
per optar al títol de doctora

Directors de tesi:

Martí Pumarola Batlle

Anna Bassols Teixidó

Bellaterra, Octubre 2007

Carme Costa Riu va gaudir d'una beca Predoctoral
de Formació d'Investigadors de la UAB,
des del 2003 fins al 2006.

Aquest treball s'ha portat a terme
gràcies al suport econòmic del projecte de recerca:
*Estudio Neuropatológico en un Modelo Experimental
Murino de la Encefalopatia Espongiforme Bovina*,
del *Ministerio de Ciencia y Tecnología* (EET2002-05168-C04)
i s'ha desenvolupat a les instal·lacions del laboratori Priocat-CReSA
i del Departament de Medicina i Cirurgia Animal.

AGRAÏMENTS

Quan he començat a escriure aquesta part de la tesi m'he adonat que estava tancant una etapa de treball, d'il·lusions, i també de decepcions. Però m'he adonat que acaba una període en el que, sobretot, he compartit experiències, que fa uns anys ni tan sols podia imaginar, amb moltes persones que m'han fet créixer i d'una manera o altra han fet possible aquest moment, i és a totes elles a qui vull donar les gràcies.

Primer de tot us vull agrir als directors de tesi, Martí i Anna, que hagueu confiat en mi i m'hagueu obert les portes del món de la recerca. Hi ha hagut moments de tot però al final ens en hem sortit prou bé.

Gràcies a tots els companys del "grup de Neuro", tant els que acabeu d'arribar com els que ja esteu en altres llocs, perquè heu fet que tot aquests temps fos tan especial. Gràcies Jose, per ajudar-me en els meus primers passos i per ser el meu mestre. Als meus companys de tesi: Anna, m'has contagiat la teva passió per la patologia i t'has convertit en una gran amiga; i Raül que has posat música a les hores davant de l'ordinador, ara et toca a tu. Enric, Merce, Anna, Lola, Ester, Jéssica i Laia gràcies per tot el que heu fet per mi i per totes les bones estones junts. Us trobaré molt a faltar.

Sierra, Ivan, Anna i Marta, les hores de feina al Priocat són les que han fet possible aquesta tesi, però ho he aconseguit perquè vosaltres m'hi heu ajudat, sou els millors companys de laboratori que es poden tenir.

També heu col·laborat en tota aquesta feina els companys de la Unitat d'Histologia i Anatomia Patològica: profes, personal tècnic, secretàries, residents i becaris, que sempre heu estat allà per respondre les meves preguntes i compartir el dia a dia.

Als becaris de bioquímica del grup de l'Anna: Laia, Dani, Maria José... no m'heu fallat mai.

A l'Isidre i als companys de l'INP: Agustí, Loli i Anna, que em veu acollir al vostre laboratori i em veu fer sentir una més del grup.

A los compañeros del CISA, sobre todo a Fayna que nos guiaste por los pasillos del P3 y nos ayudaste con todo el trabajo.

Thanks Uwe for giving me your patience, time and knowledge (and for the cheese plane). You, Janina, Smriti and Gunnel made me feel like home in Sweden.

I finalment vull donar les gràcies a tots els que sempre esteu al meu costat, fins i tot quan estic de mal humor, i que us ha tocat patir-me a mi i a la tesi: a tota la família, sobretot a vosaltres pares, als "meus nens", Josep i Lluís, i especialment a tu Jordi, gràcies per tot.

INDEX

ABREVIATIONS

ADAMS
a desintegrin and metalloprotease
ADAMTS
a desintegrin-like and metalloprotease domain with thrombospondin tipe 1 motifs
α-DG
α-dystroglycan
ADAMTS
thrombospondin
AQP
aquaporin
α-syn
α-syntrophin
ß-DG
ß-dystroglycan
BSE
bovine spongiform encephalopathy
CNS
central nervous sistem
CS
chondroitin sulphate
CSPG
chondroitin sulphate proteoglycan
Dp-71
dystrophin major isoform
DS
dermatan sulphate
ECM
extracellular matrix
FGF
fibroblast growth factor
GAG
glycosaminoglycans
HA
hyaluronic acid
HAS
hyaluronan synthase
HB-GAM
heparin-binding growth-associated molecule
HS
heparan sulphate
HSPG
heparan sulphate proteoglycan
IGF-II
insulin-like growth factor
KS
keratan sulphate
LYVE-1
lymphatic vessel endotelial HA receptor
MMP
matrix metalloproteinase
MP
metalloproteinase
MT-MMP
membrane-type matrix metalloproteinase
NCAM
neural cell adhesion molecule
PDGF
platelet-derived growth factor
PG
proteglycan
PNN
perineuronal nets
PrP
prion protein
PrPc
cellular prion protein
PrPres
resistant prion protein
PTN
pleitrophin
RHAMM
receptor for HA-mediated motility
RPTP-ß
receptor-type protein-tyrosin phosphatase
syn
syntrophin
TGF-ß
transforming growth factor-ß
TIMP
tissue inhibitors of metalloproteinases
TSE
transmissible spongiform encephalopaty
TSG-6
tumor necrosis factor-stimulated gene 6
uPA
urokinase-type plasminogen activator
uPAR
urokinase-type plasminogen activator receptor
VEGF
vascular endothelial cell growth factor
WFA
Wisteria floribunda agglutinina

ABSTRACT

The extracellular matrix (ECM) of the central nervous system (CNS) is found dispersed in the neuropil or forming aggregates around the neurons called perineuronal nets (PNNs). The ECM mainly contains chondroitin sulphate proteoglycans (CSPG), hyaluronic acid (HA) and tenascin-R. Heparan sulphate proteoglycans (HSPG) can also be secreted in the ECM or be part of the cell membrane. Aquaporins (AQP) are a family of transmembrane proteins that act as water selective channels. AQP1 and AQP4 are widely expressed in the CNS where they play several roles. Nevertheless the importance of these elements, their distribution in the CNS of mice is only partially known.

The histochemical distribution of PNNs, aggrecan, HA, HSPGs and AQP4 were semiquantitatively evaluated in the whole CNS of mice. The results showed that aggrecan, HA and HSPGs have a perineuronal distribution, and AQP4 has an heterogeneous distribution throughout the neuropil of the CNS. An inverse correlation between AQP4 and ECM components was observed, suggesting a complementary role in the maintenance of water homeostasis. A common location for AQP4 and HSPGs was also observed in CNS neuropil.

ECM and AQPs were studied in bovine spongiform encephalopathy (BSE) and Scrapie. Both diseases belong to the group of animal transmissible spongiform encephalopathies (TSE) or prion diseases. They are characterized by the accumulation of resistant prion protein (PrPres) in the CNS, neuronal loss, spongiform degeneration and glial cell proliferation.

The ECM was studied by immunohistochemistry in the transgenic mice boTg110, overexpresing bovine PrPc, intracranially infected with cattle BSE; and in C57BL/6 mice intraperitoneally infected with RML scrapie strain. Both of them showed dramatical ECM disturbances at latest stage of both diseases.

AQP1 and AQP4 were studied in boTg110 mice by immunohistochemistry, and in BSE field cases by immunohistochemistry and western blot. Both AQPs were overexpressed in the membrane of astrocytes at terminal stage of the disease in mice with evident clinical signs, and in pre-clinical cattle.

The ECM changes and AQPs overexpression were correlated with PrPres accumulation, and activated glial cells. Therefore we conclude that alterations in the ECM, AQP1 and AQP4 are a consequence of glial cell activation induced by PrPres, and both changes could lead to ion and water imbalance in the CNS which could contribute to trigger the typical histopathological features of TSEs.

INTRODUCTION

1.- THE EXTRACELLULAR MATRIX OF THE CENTRAL NERVOUS SYSTEM

The extracellular matrix (ECM) is a complex of macromolecules produced by the cells that are secreted towards the extracellular space. All organs and tissues have an ECM with their own characteristics and composition, but almost all of them have certain elements in common: proteoglycans (PG), glycoproteins and glycosaminoglycans (GAG), such as hyaluronic acid (HA) (1).

The amount of extracellular material in the central nervous system (CNS) is relatively small, if compared with that of other tissues, and its distribution is not homogeneous but rather varies regionally. Its components are found dispersed in the neuropile or forming aggregates that are called perineuronal nets (PNN), as they are located around the body of neurons, dendrites and initial segment of the axons of specific neuronal subpopulations (2, 3).

At the end of the XIX century, Camilo Golgi, Santiago Ramon y Cajal and other scientists, almost at the same time, used stainings and metal impregnations that enabled them to view the PNN. Golgi described them as "*a delicate cover, with a reticular structure…that surrounds the cellular body of all the nervous cells and continues all along the protoplasmatic extensions (dendrites) until the second or third arborisation order*", but they never agreed on the composition and function of these structures (4, 5, 6).

Throughout the 20th century, the use of new special staining techniques and the detailed morphological work published, allow researchers to suspect that the CNS should contain substances with a significant negative electrical charge such as GAG, chondroitin sulphates (CS), glycoproteins or HA. Nevertheless, it was not possible to demonstrate the presence of an intercellular space in the CNS, and this led to the idea, mostly accepted, that the CNS did not have any type of ECM (5).

At the end of the 70's, with the appearance of new techniques such as immunohistochemistry, it was possible to specifically identify a large number of molecules in this extracellular space, and the CNS was no longer an exception. Now we know that PNN, which were described already more than 100 years ago, are the result of ECM material deposition in the space between the neurons and the glial cell processes (4, 5, 6).

2.- COMPONENTS OF THE ECM IN THE CNS

2.1.- Proteoglycans

A PG is a complex molecule made up of a proteic nucleus with several covalently joined GAG chains. They are classified according to the type of GAG in: CS, heparan sulphate (HS), keratan sulphate (KS) and dermatan sulphate (DS) PG.

2.1.1.- Chondroitin Sulphate Proteoglycans

2.1.1.1.- Lecticans

Lecticans or hyalectans are a family of chondroitin sufate proteoglycans (CSPG), made up of 4 members: aggrecan, neurocan, brevican and versican (6, 7). All of them are proteins which are secreted to the extracellular space by glial cells and neurons (8, 9).

All members of this family have a core protein with common characteristics, which has led to the suggestion that they come from a common ancestral gene, and that diversity was introduced into this family through alternative splicing (6).

Aggrecan

Aggrecan was identified for the first time in the cartilage as one of its most important components (6). This lectican is also the most abundant in the adult brain ECM (10). The large number and variability of the glycosylations in its lateral chains give a very large molecular heterogeneity to the PNNs (11, 12).

In a study carried out on rats, it was observed that aggrecan appears in the CNS just before birth and progressively increases until it reaches the definitive adult level (10), indicating that its increase correlates with the establishment and consolidation of the synaptic connections of the mature CNS (12).

Versican

It is the most ubiquitous of the lecticans and it is mainly found in connective tissues (6). It is also very abundant in the nervous tissue and is mostly located in the white matter where it has been related to myelinization processes. (13, 14).

Four different isoforms generated by alternative splicing of the α and β domains have been identified (13, 14). The isoforms containing the α domain are little expressed during development and reach their peak a few days after birth. On the other hand, those containing the β domain are strongly expressed during development and are reduced to very low levels in the mature encephalon. Therefore the V2 isoform, which contains the α domain, is the one that predominates in the adult encephalon (10, 15), while the V1 isoform, which contains the β domain is the most abundant during the final embryonic period (10).

Brevican

Brevican is limited to the nerve tissue (6) and it is very abundant in the adult brain (16, 17, 18). Two secreted forms of 145kDa and 80kDa, which are N-terminal fragments produced by proteolysis, and a third form generated by alternative splicing which is anchored to plasma membranes (16, 19) have been identified.

Only traces are detected in the embryo and it progressively increases after birth until it reaches the definitive levels of the mature CNS (10).

Neurocan

Neurocan is exclusively limited to the nerve tissue (6). It is detected very early during embryonic development (10). During this period, the 150kDa C-terminal fragment, and 130kDa N-terminal fragments as well as the entire protein are detected. On the other hand, the entire form is barely detected in the adult and the two fragments (10, 20, 21), which exist as different core proteins, are more abundant indicating that most likely they have different functions (22, 23).

2.1.1.2.- Other Chondroitin Sulphate Proteoglycans

We can also find other CSPG in the ECM of the CNS:

RPTP β (receptor-type protein-tyrosin phosphatase)/phosphacan

It is a CSPG that is exclusive to the CNS (24). Three isoforms generated by alternative splicing of a single gene are known: the RPTP β and the sRPTP β which are transmembrane forms, and the phosphacan which is a secreted form (21, 25).

The RPTP β form begins to be expressed very early during the embryonic development, predominantly in glial progenitor cells, and decreases around birth (25). However, phosphacan begins to increase after birth and is widely expressed in the adult (7, 25, 26), mostly around the neurons that contain parvalbumin (24).

NG2

It is a transmembrane CSPG that is expressed in glial progenitor cells (27, 28).

Decorin and biglycan

They are small PG which are ubiquitously expressed and can contain both CS as well as DS lateral chains (29, 30).

Neuroglycan C

It is a transmembrane PG that is expressed in neurons and can have several CS lateral chains linked to the N-terminal half of the core protein (29, 30).

2.1.1.3.- Interactions of Chondroitin Sulphate Proteoglycans

The CSPGs may interact with several molecules (see table 1). They mostly interact with ECM and cell surface components, which strengths and expands their structural function. But it is also known that they may interact with growth factors, giving them an important role in the development of the CNS (7).

CSPG	ECM molecules	Molecules of cell surface	Growth factors
Brevican	HA Tenascin-R	Sulphatides (glycolipids)	
Neurocan	HA Tenascin-C Tenascin-R	NCAM; Ng-CAM/L1 TAG-1/axonin Sulfatides	FGF2
Versican	HA Tenascin-R Fibronectin	Sulfatides	
Aggrecan	HA	Sulfatides	
RPTP ß/phosphacan	Tenascin-R Tenascin-C HB-GAM/PTN Amphoterin	NCAM; Ng-CAM/L1 TAG-1/axonin-1 Contactin	FGF2
NG2	Collagen V, VI	PDGF-Rec-α	FGF2 PDGF-AA

Table 1: CSPG interactions according to Bandtlow CE, 2000 (7). FGF: fibroblast growth factor, PDGF-AA: platelet-derived growth factor, NCAM: neural cell adhesion molecule.

2.1.2.- Heparan Sulphate Proteoglycans

2.1.2.1.- Heparan Sulphate Proteoglycans (HSPG)

In the CNS there are several HSPG families, which are mostly found in the surface of glial cell and neurons, making up part of the cell membrane through the transmembrane domains; and very few of them are found secreted in the extracellular space (7). Among all of them, the following stand out:

Glypicans

The glypicans are one of the two most important families of the membrane-anchored HSPG (7).

Syndecans

They are a family of transmembrane proteins that mostly contain HS lateral chains. It consists of 4 different members: syndecan-1, syndecan-2 (fibroglycan), syndecan-3 (N-syndecan) and syndecan-4 (ryudocan, amphiglycan). All of them are expressed in the developing and in the adult CNS (7, 31).

All cell types can express at least one of the four types of syndecans and many express more than one. The most abundant form in the CNS and in the adult peripheral nerve is syndecan-3, whose expression rapidly increases around birth, coinciding with the period of glial cell differentiation, myelinization and formation of neural connections (32, 33). Afterwards, syndecan-3 levels decrease and in the adult it is found concentrated around the axons (31). On the other hand, syndecan-2 is located in the synaptic spines of the mature CNS (34). Despite this, it is not known exactly how these syndecans take part in all these processes (33).

Agrin

Agrin is an HSPG that is associated with basal membranes. Originally it was detected in the neuromuscular junction, but afterwards it has been identified in other non-muscular tissues such as brain where it is mainly expressed during embryonic development (33). Agrin has at least three alternative splicing sites, giving rise to multiple isoforms by insertion of small peptides. Only neurons seem to express the isoforms that include these insertions (7, 35, 36).

Perlecan

It is a secreted HSPG that is found in the extracellular space of the CNS, where it is part of the basal membranes of leptomeninges and blood vessels (37). It can be synthesized by neurons, astrocytes and possibly microglia (38). It is a powerful co-receptor of FGF1 and FGF2, which means it has a very important role during development (39).

2.1.2.2.- Interactions of Heparan Sulphate Proteoglycans

HSPGs may also interact with ECM proteins, but above all, they interact with growth factors (see table 2) (7). It is for this reason they are mainly considered as co-receptors of soluble factors (growth factors, cytokines, chemokines) given that they act by modulating the signs produced by other molecules (7). They can also participate in the internalization of receptors of these factors, and even act themselves as a paracrine soluble factors through the detachment of their ectodomains from the cell surface (29, 40).

HSPG	ECM molecule	Growth factor
Syndecan-1	Fibronectin Tenascin-C Midkine HB-GAM/PTN	FGF2 TGF-β
Syndecan-2		FGF2
Syndecan-3	HB-GAM/PTN Midkine Laminin	FGF2
Glypican-1	Laminin Slit-1 Slit-2	FGF1 FGF2 FGF7 VEGF
Glypican-2	Laminin Thromboplastin	FGF2
Glypican-3		IGF-II FGF2

Table 2: HSPG interactions according to Bandtlow CE, 2000 (7). TGF-β transforming growth factor-β, VEGF: vascular endothelial cell growth factor, IGF-II: insulin-like growth factor, HB-GAM: heparin-binding growth-associated molecule, PTN: pleitrophin.

2.2.- The glycoproteins

A large variety of glycoproteins like laminins, fibronectins, etc., are found in the CNS ECM. We will highlight the tenascins, which although they are not exclusive of the CNS, they have great structural significance and are important to development.

2.2.1.- The tenascins

Tenascins belong to a family of oligomeric glycoproteins which is made up of a minimum of 5 members: tenascin-C, tenascin-R, tenascin-X, tenascin-Y and tenascin-W (41), well conserved in all vertebrates (42). Furthermore, each one of them, except tenascin-W, can give rise to a large number of isoforms generated by alternative splicing of the FNIII domain (41).

Tenascin-C

It was the first tenascin described given that it is found in many tissues. Nowadays, we know that there is a large number of isoforms that give rise to various monomers which are naturally found forming hexamers (42).

It is detected very early in the embryo, where it is secreted by glial cells and some immature neurons (43). It is almost absent in most of the mature CNS zones, and only persists in areas with a high level of plasticity like olfactory system or hypothalamus (44). It is reexpressed in lesioned areas (45) or tumours (46).

Tenascin-R

Tenascin-R is specific to the CNS. Two different isoforms are known, which monomers are naturally found forming trimers (47, 48).

It begins to be expressed around birth, synthesized by oligodendrocytes (41, 42). It is located around the neuron bodies, where it is part of the PNNs that begin to organize (17), and participates in the myelinization (49). In the mature CNS, tenascin-R is basically found as part of the PNNs that surround some of the neuronal populations (50).

2.2.2.- Interactions of tenascins

Tenascin-R has a great capacity to bind lecticans, while tenascin-C stands out due to its ability to interact with cell surface proteins and growth factors such as N-CAM, Ng-CAM/LI, Nr-CAM, integrins, contactin, TAG-1/axonin, HB-GAM, amphoterin and collagen (41).

2.3.- Hyaluronic acid

2.3.1.- Hyaluronic acid (HA)

HA was discovered in 1934 in the vitreous humour of the eye (51). It is a non-sulphated polysaccharide, non-covalently joined to proteins, from 105 to 107Da,

which is found in almost all the ECM in the organism (52). It has high affinity for water and occupies a large hydrodynamic space where it acts as a lubricant, providing the tissues with viscosity and elasticity, and supports the ECM (51).

HA in the CNS is synthesized by glial cells. It is located in the white matter around myelinic fibres; and in the grey matter around the neuronal bodies (53, 54).

HA is synthesized by enzymes called hyaluronan synthases (HAS), 3 of which are known (52). Each one of them synthesizes forms of specific lengths, which are expressed in different developmental periods, thus suggesting that HA of various molecular weight can be found in the CNS at different times (52) (see table 3). This differential regulation can have significant consequences for cell behaviour, as HA functions vary according to its length (51).

HAS	Longitud de l'HA	Moment d'expressió
HAS1	sintetitza formes intermitges, <2x106Da.	a l'embrió; decreix després del naixement.
HAS2	sintetitza formes llargues, >4x106Da.	a l'embrió; augmenta fins assolir un nivell màxim a partir del qual es manté constant en l'adult.
HAS3	sintetitza formes curtes, <2,5x105Da.	a l'embrió.

Table 3: HAS expression according to Sherman LS, 2002 (52).

Several hyaluronidases have also been described that degrade HA into fragments of different lengths, which may potentially have different functions (51, 55). This phenomenon has been studied more in depth in pathological process such as ischemic stroke (56) and tumours (57).

2.3.2.- Interactions of hyaluronic acid

HA interacts with a large variety of molecules such as lecticans, extracellular proteins, transmembrane and intracellular receptors (see table 4). It allows them to take part in many functions, such as stabilizing the ECM, inhibiting axonal growth, influencing cellular signals, motility and cellular adhesion (52). As a consequence, HA is not just limited to being an element that fills space, but it has other significant biological roles.

Type of protein	Protein
Lecticans	Aggrecan Brevican Neurocan Versican
Extracellular proteins	TSG-6 Iαl
Transmembrana receptors	CD44 LYVE-1 Layilin
Intracellular receptors	RHAMM

Table 4: HA interactions according to Sherman LS, 2002 (52). TSG-6: tumor necrosis factor-stimulated gene 6, LYVE-1: lymphatic vessel endothelial HA receptor, RHAMM: receptor for HA-mediated motility.

3.- ECM ORGANIZATION: THE HTL MODEL

Given that the different ECM components are found distributed heterogeneously, that they interact among each other and these interactions condition their functions, it was thought that the ECM must be a very well organized structure. To explain their organization, the HTL model has been proposed (6). According to this model, the HA, lecticans and tenascin-R organize to form a ternary complex, where the lecticans interact with the other two creating a network structure that gives rise to the PNNs (4, 6, 17, 58). Although this model does not explain the organization of all the ECM, it does explain the organization of the PNNs and moreover, it does it in a functional way as it takes the biochemical properties of the elements that make it up into consideration and allows for an explanation of processes such as CNS maturation.

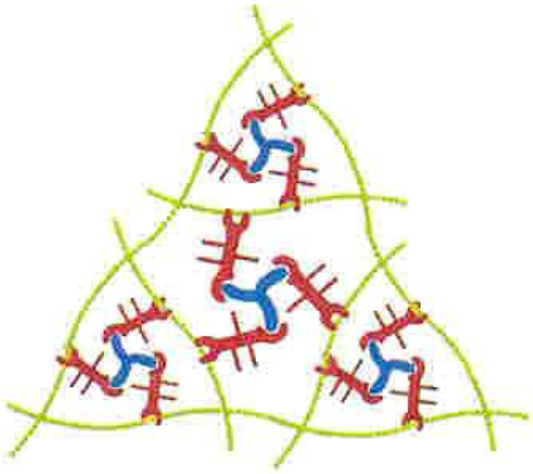

Fig 1: Diagram of PNN organization, according to Yamaguchi Y, 2000 (6): HA in green, tenascin-R in blue and lecticans in red.

4.- FUNCTIONS OF THE ECM IN THE CNS

Several functions are attributed to the ECM and its components during the development and maturation of the CNS, in the mature CNS and in post-lesional regeneration.

4.1.- Embryonic development and post-natal maturation

ECM during the embryonic development of the CNS has been widely studied. It is known that during this period it is made up of fibronectin, collagen and laminins, that are later restricted to the basal membranes of the blood vessels and meninges (6). There are also found CSPGs, HSPGs, HA and tenascins, that intervene, mainly at the end of CNS development, in several processes that are later described (7, 10, 26, 49, 59, 60, 61):

4.1.1.- Neurogenesis, gliogenesis and cellular migration

Neurogenesis and gliogenesis are phenomena that begin in the embryonic period and finish around birth in many parts of the CNS in mammals. During this period, several HSPG, like glypican or perlecan are expressed. Its maximum synthesis coincides with the period of glial cell differentiation, myelinization and formation of neuronal connections, and then their level decreases (7). It seems that they may act as FGF co-receptors and reservoir in the extracellular space during neurogenesis and gliogenesis (31, 37).

Also some CSPGs like phosphacan are expressed in the embryonic CNS in the areas with the most proliferative cellular activity and thus it is believed that they may promote the mitogenic activity of growth factors (7).

HA is very important during embryonic development as it promotes cellular proliferation and motility: the neural crest cells of the neuroectoderm migrate through HA rich matrices; when these reach their target, the HA is degraded, thus preventing the cells from going further (62). HA also influences cellular differentiation in such a way that while a very rich HA environment is maintained, the cells do not differentiate, and when it is degraded by the hyaluronidases, they acquire the characteristics of differentiated cells (63).

4.1.2.- Growth of neurites and axons

The HSPG are intimately associated with neuritogenesis, as they can interact with a large variety of growth factors, acting as co-receptors or modulators of its signals (64, 65). However, the role of the CSPG is more controversial as they can work by inhibiting or favouring the growth of the neurites, depending on the spatial and temporal conditions, and the interactions with other molecules. In general, they are believed to have a repulsive role on the growth of dendrites and axons, conditioning their growth direction (30).

4.1.3.- Synaptic modulation and structural plasticity: post-natal maturation

PNNs appear late in the development of the CNS and condition the synaptic plasticity, because as they increase, the plasticity of the CNS decreases, difficulting the formation of new synapses and stabilizing those that already exist (66). They are involved in the functional maturation of the brain (12, 17, 66, 67), as their appearance represents the conversion of a very fluid embryonic matrix to a more rigid adult matrix. This ECM conversion can at least partly be explained by the expression of different CSPG with a different number of CS chains, and HA of different lengths which retain varying volumes of water, thus regulating the fluency of the extracellular space without altering its basic molecular organization (6).

With respect to HSPGs, it is known that syndecan-2 plays an important role in the morphogenesis of the dendritic spines, given that it concentrates into the synapses as these mature morphologically (33, 34).

4.2.- The ECM in the adult CNS

In the adult CNS, very different functions have been attributed to the ECM, despite most of them being related to the ionic and hydrophilic properties of PGs and HA.

4.2.1.- Maintenance of the ionic balance in the extracellular space

The ECM, especially the PNNs, contribute to the maintenance of the electrophysical properties surrounding different cellular domains (3). The PNN components are markedly anionic, and therefore they have a high capacity to link cations. They can

act as a reservoir of Na^+, Ca^{2+} and K^+ around very active neurons, acting as a buffer of ions and facilitating their diffusion (2, 3, 59, 68). For this reason, it has been proposed that the PNNs, associated with fast-spiking neurons (very active neurons), could act as an ionic buffer when an action potential occurs (see fig. 2) and complement other cellular mechanisms of homeostasis maintenance, normally attributed to the glia (68).

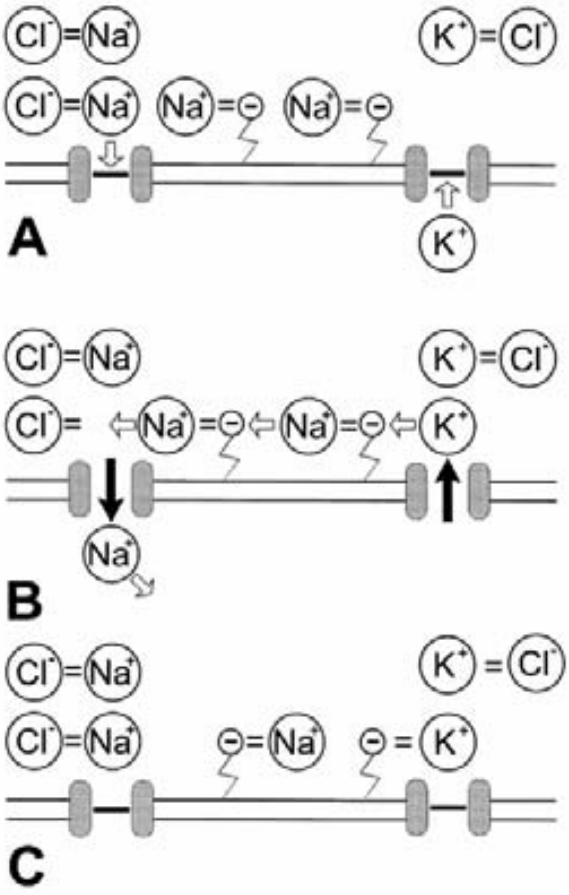

Fig 2: Diagram of the hypothetical role of the anionic sites of PNN, according to Hartig W, 1999 (68): (A) Under resting conditions in the extracellular space, there are Na^+ and K^+ which can be balanced by Cl^-, or linked to the anionic sites of the ECM components. (B) When the membrane generates an action potential the Na^+ ions enter into the neurons and K^+ leaves, thus producing a local unbalance of charges in the extracellular space. (C) The anionic sites of the ECM can buffer it in such a way that where the Na^+ was bound before, the excess of K^+ can now be bound and thus the charges can be quickly redistributed.

4.2.2.- Maintenance of mature synapses

The PNNs have been related to the stabilization and maturation of the synapses, given that their formation period, around birth, coincides with the end of synaptogenesis (66). This is also because their enzymatic digestion with chondroitinases or hyaluronidases reactivates the neuronal plasticity (67, 69, 70, 71, 72, 73).

It seems that the CSPGs of the PNNs are capable of retaining a certain amount of water, forming a layer around the synapses without fully occupying them, thus preventing the molecules from freely flowing and therefore compartmentalizing the extracellular space (74).

4.2.3.- Neuroprotection

Neuroprotective effects against oxidative stress have also been attributed to the PNNs (75). The polyanionic elements of the ECM can interact with ions like iron, involved in the generation of oxidative stress; intervene in their homeostasis; and neutralize their oxidative charge, which could cause oxidative stress (76), as well as the intracellular accumulation of products like lipofuscin (75, 77, 78).

The ECM study on knock-out animals helped better understand the function of some of its elements. For example, animals that do not express brevican and neurocan

show anomalies in one form of plasticity, the long term potentiation, in spite of not showing any learning or memory problems (69). Knock-out mice for tenascin-C (79) and tenascin-R show reduced speed of axonal conduction (80). Even mice with a lack of brevican, neurocan, tenascin-C and tenascin-R are viable as it seems that fibulin-1 and fibulin-2 can be substitutes for the tenascins, and that aggrecan and versican can replace the lack of neurocan and brevican, thus suggesting that the brain ECM is highly flexible and only needs to maintain its basic organization (81). Mutations in versican or aggrecan are lethal in the embryonic and perinatal period respectively (82, 83) and, therefore, it still has not been possible to study their function on the adult brain using animal models.

4.3.- The ECM and post-lesional regeneration

The HTL complex also allows to explain the ability of the mature ECM to inhibit synaptogenesis and axonal regeneration after a lesion, given that it acts as a barrier making the approximation of the axons and dendrites difficult, thus preventing new synapses from forming and inhibiting the axonal growth cones.

Axonal regeneration is not a problem for the axon itself. But the reactive gliosis that forms in the adult CNS after a lesion is in fact a problem given that it repairs injuries, but blocks axonal regenerative growth due, in part, to the expression of inhibitory molecules on the surface of the damaged tissue such as tenascins, CSPGs and class III semaphorins (84).

CSPGs generate a type of barrier that prevents axonal growth due to their repulsive effects, as they block the growth promoting properties of laminins and other ECM proteins (7, 29, 85, 86).

Little is known about the regulation and function of the HSPGs after CNS lesions and it is not known whether they play a positive or negative role (31).

In general, high molecular weight HA is the most abundant in the adult CNS, its function is basically structural and maintains the level of tissue hydration (51). When a lesion occurs, the glia is activated and hyaluronidases are generated, which degrade the HA into smaller fragments that have the ability to stimulate the synthesis of inflammatory cytokines (87). This small HA fragments are powerful dendritic cell activators (88, 89), and can be angiogenic, inflammatory and immunostimulators (55).

5.- HOW THE ECM IS DEGRADED

5.1.- How the ECM proteins in the CNS are degraded

In physiological as well as pathological processes glial cells, neurons and endothelial cells can produce proteolytic enzymes able to degrade the ECM components, which are called metalloproteases (MP) (90, 91, 92, 93, 94). There are different MP families:

- Matrix MP (MMP) includes many sub-families: collagenases, gelatinases, stromelysin and membrane type-MMP (MT-MMP). Their main function is believed to be

that of degrading ECM components, although they can act on other substrates such as growth factors that are linked to the ECM or the cell surface, thus releasing them into the medium (95).

- ADAM (a desintegrin and metalloprotease) is a family made up of more than 30 members. They are transmembrane proteins that act as sheddases, that is, their principal substrates are other cell surface proteins (95, 96).

- ADAMTS (a desintegrin-like and metalloprotease domain with thrombospondin type 1 motifs) is a family made up of 19 members which, once secreted, are located near the cell surface or the ECM, probably through their interaction with GAGs. Their principal substrates are found on the cell surface and in the ECM (97).

Physiologically, the MP are involved in embryonic development, wound healing and angiogenesis, but they also have a significant role in pathological processes such as tumour invasion and metastasis, post-lesional recovery, axonal growth and inflammatory processes (94).

As the MP catalyze the degradation of many ECM proteins, it is very important to keep their activity under very strict control, therefore they are regulated at 3 levels: gene transcription, proenzyme activation and action of specific inhibitors, the tissue inhibitors of metalloproteinases (TIMPs) (94, 98). Most of the MPs are not constitutively expressed, and they are expressed as proenzymes which must be activated to be functional. Once activated, the MPs are regulated by the formation of non-covalent 1:1 complexes with TIMPs (94, 99).

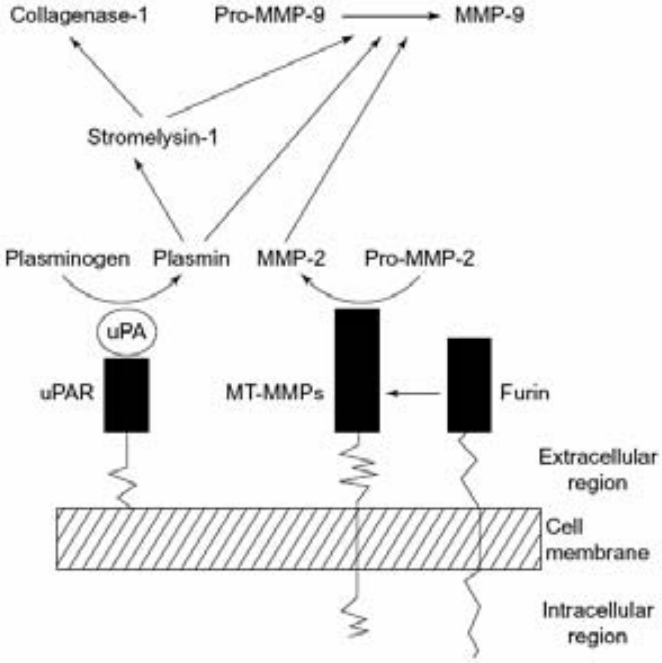

Fig 3: MMP activation cascade on the cell surface, according to Yong V, 1998 (94). The coordinated activation of several MMPs begins with the formation of plasmin, which is first generated from plasminogen which has been degraded by urokinase-type plasminogen activator (uPA) which are anchored to the membrane by its receptor (uPAR). The plasmin can activate the MMP-9 and the stromelysin-1, and the latter, can activate other MMPs, including the MMP-9 and the collagenase-1. On the other hand, the MMP-9 can be activated by MMP2, which has been activated through MT-MMP, which has been first activated by furin protease, thus making the activation cascade even larger.

The activation machinery is located on the cell surface and as a result the most important proteolysis takes place in the most immediate pericellular setting, where it can influence the ECM cell-cell interactions (94, 98). It is for this reason that in physiological conditions, the MPs are very precisely controlled as excessive MP production and activation could play a key role in the pathogenesis of many inflammatory diseases and tumours (94).

MPs	Grup	Member	MP num.	Main substrate
MMP	Collagenases	Intersticial collagenase	MMP-1	Collagens I, II, III, VI, VIII i X, aggrecan, PG, MMP-2, MMP-9
		Neutrophil collagenase	MMP-8	Collagens I, II, III, V, VII, VIII and X, aggrecan, fibronectin, gelatin.
		Collagenase-3	MMP-13	Collagens I, II, IV, IX, X and XIV, gelatin, plasminogen, aggrecan, perlecan, fibronectin, MMP-9.
	Gelatinases	Gelatinase A	MMP-2	Collagens I, IV, V, VII, X, XI and XIV, fibronectin, gelatin, elastin, aggrecan, myelin basic protein, laminin-1, MMP-1, MMP-9, MMP-13.
		Gelatinase B	MMP-9	Collagens IV, V, VII, X and XIV, gelatin, enactin, aggrecan, elastin, fibronectin, plasminogen, myelin basic protein, ILß
	Stromelysins	Stromelysin-1	MMP-3	Collagen III, IV, V and IX, gelatin, aggrecan, perlecan, decorin. Laminin, elastin, casein, plasminogen, myelin basic protein, IL-ß, MMP-2/TIMP-2, MMP-7, MMP-8, MMP-9, MMP-13.
		Stromelysin-2	MMP-10	Collagens III, IV, V, gelatin, casein, aggrecan, elastin, MMP-1, MMP-8
		Matrilysin	MMP-7	Collagens IV and X, gelatin, aggrecan, decorin, fibronectin, laminin, elastin, plasminogen, myelin basic protein, b4-integrin, MMP-1, MMP-2, MMP-9, MMP-9/TIMP-1
		Stromelysin-3	MMP-11	α I proteinase inhibitor (serpin)
	MT-MMPs	MT1-MMP	MMP-14	Collagen I, II and III, gelatin, fibronectin, lamin, vitronectin, PG, MMP-2, MMP-13
		MT2-MMP	MMP-15	Fiboronectin, enactin, laminin, perlecan, MMP-2
		MT3-MMP	MMP-16	Collagen III, gelatin, casein, fibronectin, MMP-2
		MT4-MMP	MMP-17	Pro-MMP-2, collagens, gelatin
	Others	Macrophage metalloelastase	MMP-12	Collagen IV, gelatin, elastin, casein, fibronectin, vitronectin, laminin, enactin, myelin basic protein, fibrinogen, fibrin, MMP-9
		Enamelysin	MMP-20	Amelogrenein, aggrecan
		RASI-1	MMP-19	Gelatin, aggrecan, fibronectin
ADAM			ADAM-8	Cytokines, cell surface receptors, adhesion proteins
			ADAM-9	Cytokines, Growth factors, cell surface receptors, proteinases, APP, collagen XVII,
			ADAM-10	Cytokines, Growth factors, adhesion proteins, proteinases, APP, collagen XVII, Notch, PrP
			ADAM-12	Growth factors, proteinases
			ADAM-15	Growth factors, cell surface receptors
			ADAM-17	Cytokines, growth factors, cell surface receptors, adhesion proteins, proteinases, APP, collagen XVII, Notch, PrP
ADAMTS			ADAMTS-1	Aggrecan, versican
			ADAMTS-2	Procollagens I, II and III
			ADAMTS-3	Procollagens I, II and III
			ADAMTS-4	Aggrecan, versican, brevican
			ADAMTS-5	Aggrecan, versican
			ADAMTS-9	Aggrecan, versican
			ADAMTS-14	Procollagens I, II and III

Table 5: Types of MPs and their substrates (94, 95, 96, 97).

5.2.- How HA is degraded

Although less well known, there are also many different enzymes that are able to degrade HA. The hyaluronidases 1 and 2 are the most abundant, are expressed constitutively, and can be found free in the extracellular space, like hyaluronidase-1, or anchored to cytoplasmic membranes, like hyaluronidase-2 (100). Moreover, when these enzymes degrade an HA molecule, generate other HA of specific lengths and with new functions. For this reason it is believed that the expression as well as the function of these enzymes must be very well-regulated (55).

6.- THE AQUAPORINS

Aquaporins (AQP) are a family of integral membrane proteins that act as water channels (101). They have been identified in bacteria, yeasts, unicellular eukaryotes, plants and animals (101). AQP1 was the first AQP to be identified at the beginning of the 90's. It was located in erythrocytes in mammals (102, 103). Since then, in mammals alone, up to 13 different AQPs have been identified in several tissues (104).

All of them have a very similar molecular structure. They contain six alpha-helix domains which make up a structure in the form of pores, where the first three and last three helices have inverted symmetry. They also have two conserved motifs Asn-Pro-Ala (NPA) on each side of the monomer, which allow water but not small solutes to pass across the pores (105, 106). Each AQP monomer can function as an independent channel in the membrane, but the monomers have been observed by freeze-facture electron microscopy assembled in membranes as tetramers (see fig. 4) (104, 107, 108).

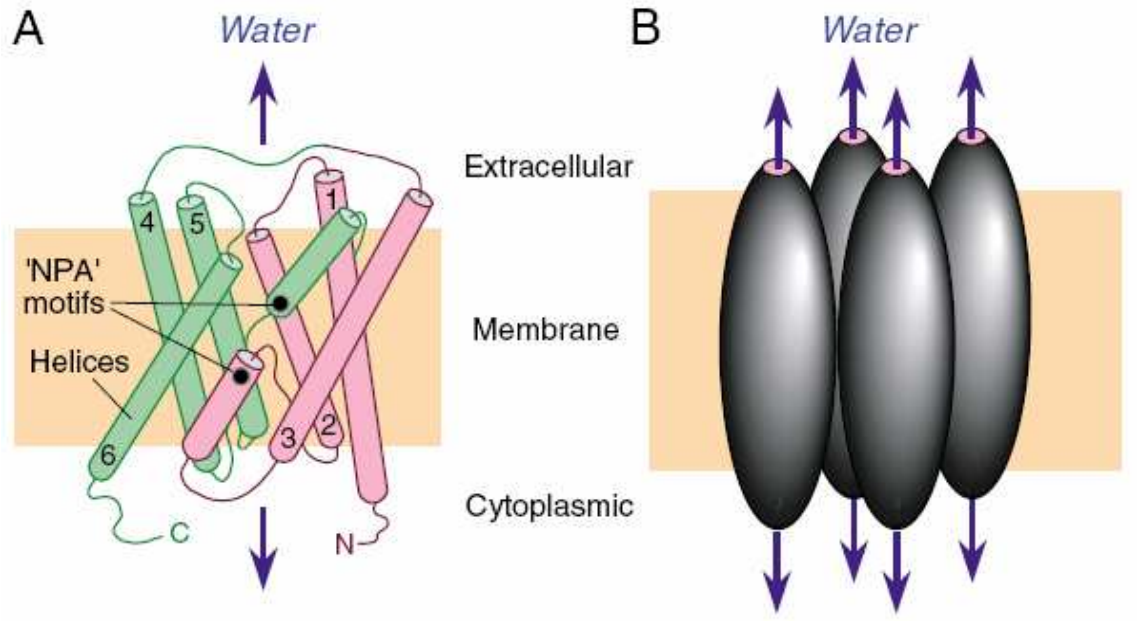

Fig 4: Structure of the AQP1 monomers and their tetrameric assembly in the membrane according to Verkman AS, 2005 (104). (A) Crystal structure of an AQP1 monomer with the helical domains (1-6) surrounding a water pore, with two "NPA" motifs. (B) Tetrameric assembly of AQP1 in the membrane, where each monomer forms its own water channel.

The AQPs have been subdivided into 3 functional groups according to their permeability characteristics:

- Aquaporins: AQP0, 1, 2, 4, 5 and 6, which are permeable to water (109).
- Aquaglyceroporins: AQP 3, 7 and 8, which are permeable to water, glycerol and urea (109).
- Neutral solutes channel: AQP 9, which is permeable to water, glycerol, urea, purines, pyrimidines and carboxylates, and AQP10 which is permeable like AQP9 except to urea and glycerol (109).

The AQPs are ubiquitously distributed in mammal tissues (Table 5). Up until now, only 6 different AQPs have been located in the brain, but the most abundant are AQP1, AQP4, and AQP9 (110, 111, 112, 113).

AQP	Permebility	Organ	Cell/Tissue Type
AQP1	Water	**Brain** Endothelium Eye Kidney Lung Blood	Choroid plexus, nociceptive and ganglionar neurons Variety of tissues. Ciliary body, iris, lens epithelium. Descending loop Hendle, vasa recta, renal proximal tubular epithelium. Pulmonary vascular endothelium. Red blood cells
AQP2	Water	Kidney	Collecting duct
AQP3	Water, glycerol, urea	Eye Kidney	Conjuctiva Collecting duct
AQP4	Water	**Brain** Colon Eye Inner ear Muscle Skin Stomach	Ependyma, astroglia. Epithelial cells. Retinal glia. Inner sulcus cells. Muscle fiber cells. Keratinocytes. Parietal cells.
AQP5	Water	Eye Lacrimal glands Lung Salivary glands Skin	Corneal epithelium Acinar cells, apical membrane. Submucosal glands, type I pneumocytes. Acinar cells, apical membrane. Sweat glands.
AQP6	Water	Kidney	Collecting duct.
AQP7	Water, glycerol, urea	Fat pad Kidney	Adipocytes Renal proximal tubular epithelium.
AQP8	Water, glycerol, urea	Colon Kigney Large inestine Liver, pancreas Salivary glands Small intestine	Not determined Not determined Not determined Not determined Not determined Not determined
AQP9	Water, glycerol, urea, purines, pyrimidines, and monocarboxylates.	**Brain**	Astrocytes, ependyma.
AQP10	Water, purines, pyrimidines, and monocarboxylates.	Duodenum and jejunum	Not determined.

Table 6: Distribution of the AQPs in mammal tissues, modified from Wasson K, 2006 (101).

6.1.- Aquaporin 1

AQP1 was the first human AQP identified and functionally characterized (103). Originally it was called channel-forming integral protein 28 (CHIP28), because it has a molecular weight of 28kDa, although later other glycosylated forms with higher molecular weights were identified (114). It is thought to act as a water channel (104), in spite of being also described in a recent study that it can act as a NO transporter, facilitating its passage through the cell membranes (115).

AQP1 has been located in the membrane of erythrocytes, renal proximal tubular epithelium, the eye, lung and in endothelial cells, except in the brain (101). In the CNS it is located in the apical pole of the choroid plexus (116), in the ependymocytes (117, 118). Very recently it has been described in dorsal ganglionar neurons and nociceptive afferent neurons in the spinal cord (119).

Under physiological conditions, the function of secreting the cerebrospinal fluid has been attributed to AQP1 (120, 121). Under pathological conditions, it is also expressed in the membrane of astrocytes and microglia thus favouring cell migration (122, 123); and neoplastic cells can induce their expression in endothelial cells (118, 124).

6.2.- Aquaporin 4

AQP4 was cloned later, in 1994, from pulmonary tissue (125). Presently, 2 isoforms generated by alternative splicing and weighing 31 and 34 kDa are known. Both specifically act as water channels.

AQP4 has been located in kidney, skin, stomach, colon, eye, muscle and CNS (101). In the CNS, it is the predominant AQP (123, 126, 127). Above all it is expressed in the astrocyte end-feet that form the internal and external glia limitans, in endothelial cells and in the basolateral membranes of the ependymocytes (128).

AQP4 has a very polarized expression in the membrane of the astrocytes. This is due to the fact that it is intracellularly bound to a-syntrophins, which are bound to dystrophin, which is in turn bound to dystroglycan. Dystroglycan interacts extracellulary with agrins and laminins of the basal membranes, forming the dystroglycan complex (128) (see fig 4). Together with AQP4, other proteins such as the K^+ Kir4.1 channel are specifically located (128). In any case, AQP4 can also be distributed throughout the entire astrocyte membrane without being bound to this complex, as occurs with the astrocytes of osmosensitive organs such as the supraoptic nuclei (128).

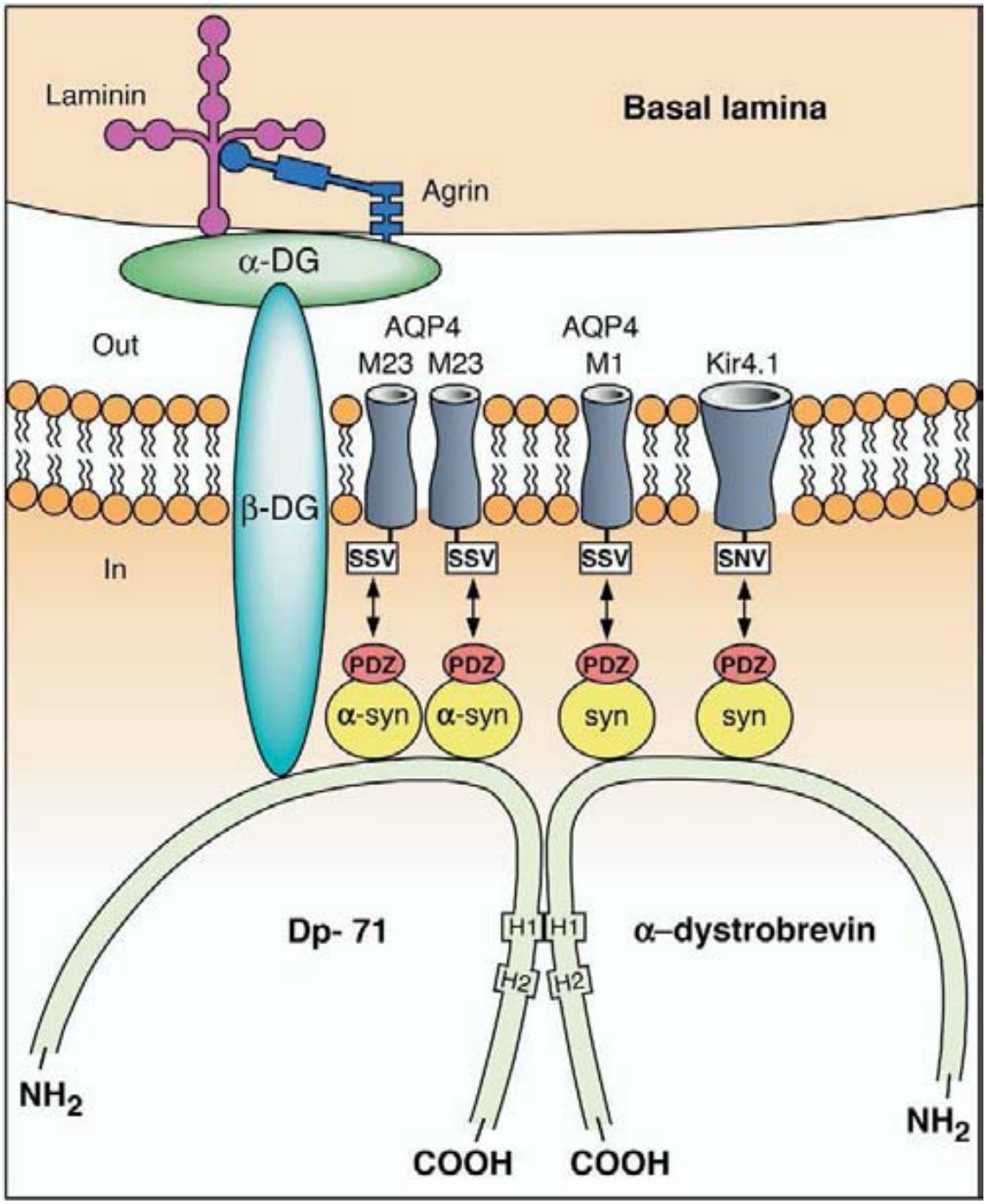

Fig 5: Dystroglycan complex, according to Amiry-Moghaddam M, 2004 (128). The dystroglycan complex (α-DG i β-DG) anchors itself in the basal membrane through interaction with laminins and agrins, and bounds AQP4 and other molecules with a SXV sequence such as that of the Kir4.1 channels through α-syntrophin (α-syn) and other syntrophins (syn). The union between AQP4 and α-syn or the syn is indirect (arrows). It is assumed that the α-syn is mostly involved in anchoring the M23 isoform of AQP4. However, other syn are involved in anchoring the M1 isoform of AQP4. Dp-71 is the largest dystrophin isoform in the encephalon, PDZ are the binding domains of syn and H1 indicates the coiled-coil motif of interaction between Dp71 and α-dystrobrevin.

Thanks to the use of knock-out mice for AQP4 or for syntrophin, it has been possible to determine the different functions of AQP4 in the CNS (123, 128):

- Selective water transport: it has been proposed that the water generated by cell metabolism and from the blood vessels is gathered by the astrocytes which release it in the subarachnoidal space and in the ventricles (123, 128).

- Neuronal signal transduction through K^+: AQP4 can alter the ionic concentration of the extracellular space as it is located in the membranes along with K^+ Kir4.1 channels, thus AQP4 could modify the transport of K^+ towards the inside of the astrocytes based on its absorption of water. Therefore, AQP4 may condition the rapid changes in the K^+ concentration that take place in the extracellular space during neuronal depolarization (104, 123, 128, 129, 130).

- Cell migration: during cell migration, AQP4 is located on the end of the lamellipodia where the water enters due to an osmotic gradient, therefore the membrane expands and a space is created where the actin polymerizes and increases cell motility (131). Under pathological conditions, it has been proven that the reactive astrocytes constitutively express AQP4 and that this is related to its migration (104, 123).

7.- STUDIES ON THE ECM AND WATER CHANNELS IN THE CNS OF MAMMALS

There are few immunohistochemical studies on the normal distribution of ECM and the AQPs in the CNS, and moreover, they have been conducted on very diverse species and in general are very partial. It has been proven that the ECM and PNN have great heterogeneity in the composition and proportion in which their components are expressed according to their location (67, 132).

7.1.- The PNN

The distribution of PNNs has been described using lectins such as Wisteria floribunda or Vicia villosa, which recognize N-acetyl-galactosamine, a disaccharide that is found in CSPGs (133, 134). It has been described in a variety of species: mouse (132, 135), rat (24, 136, 137), guinea pig (138), Monodelphis domestica (139) and humans (140, 141). All these studies focus on very specific areas of the encephalon and most of them refer to the cerebral cortex or the hippocampus, and in very few cases, the brain stem (137).

7.2.- CSPGs

The distribution of CSPGs in the ECM of the mouse brain is little known. The most well-studied are phosphacan and the lecticans, but their description is restricted to a few areas of the encephalon in a variety of species (12, 17, 24, 26).

A PNN component as significant as aggrecan has only been described in the hippocampus (132) and in the superior colliculus in the mouse (3). In other animals its

distribution has been described in the neocortex of rat (12) and guinea pig (138), in the coclear nuclei, olivary nuclei and trapezoid body of gerbils(142) and in the lateral geniculat nuclie of cats (143). There are still many encephalic areas in which none of these CSPG has been studied.

7.3.- HSPGs

Only two general descriptions about the distribution of the HSPG with few details have been reported on rat CNS (144, 145) and on the mesencephalon of mice (146).

7.4.- HA

On the other hand, HA distribution has been described with quite a few details in the mouse CNS (132, 135) and a few studies have also been performed on the rat CNS (53, 54).

7.5.- AQPs

Despite the fact that the location of the AQPs in cell membranes have been ultrastructurally studied and the functions are known thanks to the use of transgenic mice (101, 111, 147), their anatomical distribution in the mouse CNS has not been very accurately described, only some areas such as the spinal cord (148, 149), or the glia limitans (128, 150, 151, 152) have been studied. Its location in other areas of the brain is not at all detailed or has not even been carried out (118, 153, 154).

As it can be seen, all of these studies only provide partial knowledge of the ECM components and AQPs, and are very restricted with respect to their distribution. For this reason, we were required first to optimize the identification techniques to study the ECM components and the water channels in paraffin embedded nervous tissue. Afterwards, we studied the complete distribution of each one of these markers in CD1 mouse, giving rise to the first study of this thesis.

8.- TRANSMISSIBLE SPONGIFORM ENCEPHALOPATHIES

In veterinary neuropathology, the Transmissible Spongiform Encephalopathies (TSE) or prionic diseases were originally included within the group of inflammatory diseases (155). Currently, the TSEs are considered, in veterinary as well as human medicine, to be neurodegenerative diseases (156, 157).

The prionic diseases have been referred to as TSEs due to the vacuolar degeneration that occurs during the disease and because they can be transmitted, despite the possibility of also being inherited. When the agent causing the disease was discovered, it was called prion protein (PrP), which is the abbreviation for “proteinaceuous and infection” in order to differentiate it from the conventional infectious agents (156). This group of diseases include Creutzfeldt-Jakob disease (158,

159), kuru (160, 161), Fatal Familial Insomnia (162), Gerstmann-Sträussler-Scheinker disease; the animal encephalopathies such as Scrapie (163), Transmissible Mink Encephalopathy, Chronic Wasting Disease (164, 165), Bovine Spongiform Encephalopathy (BSE) (166); and their variants: Feline Spongiform Encephalopathy (167) and the variant of Creutzfeldt-Jakob disease (168).

All of the prionic diseases have common neuropathological characteristics: spongiform degeneration of the neuropile and the neurons, neuronal loss, reactive astrogliosis and accumulation of resistant PrP (PrPres) (169).

8.1.- The causal agent: the prion protein

The etiological agent of the TSEs is still wrapped up in a certain controversy. For the time being, the most accepted theory on the cause of the prionic diseases is the "protein only hypothesis", postulated by S.B. Prusiner in 1982. According to this theory, the causal agent is only a protein, the PrPres, which is capable of transmitting the disease without any kind of association with nucleic material (170, 171) and it has been experimentally proven based on the recombined PrPres that the disease can reproduce (172), but despite this, some authors defend the possibility that it could be a type of slow virus (173, 174).

The mature cellular PrP (PrPc) is a sialoprotein of 209 amino acids, where the alpha-helix structure predominates (175, 176), anchored to the plasma membrane with a glycosylphosphatidylinositol link (177, 178). It is expressed in most cells in the organism such as lymphocytes, follicular dendritic cells (179), neurons (180), glial cells (181) and other cells in the organism.

The PrPc in the CNS has been linked to the presynaptic and postsynaptic membranes (182, 183, 184), and therefore can interact with ECM components such as GAGs (185), HSPGs (186) and laminins (187). All of this suggests that it could be involved in the growth of neurites and the establishment of the synapsis (188). On the other hand, PrP is also linked to metals and could act as a transporter of these metals, intervening in oxidative stress phenomena (189).

The PrPc can undergo a conformational post-translational change by which it becomes PrPres. This can occur spontaneously, due to treatments with denaturalizing agents (190), pressure (191), through the introduction of specific mutations in the gene that codifies for PrPc, or induced by PrPres itself. The PrPres differs from the PrPc only due to its final conformation with domains folded into ß-sheets (177, 192), which gives it a series of properties such as being insoluble, polymerizing to form amyloid fibres and also the resistance to digestion with proteases (177, 193), thus becoming pathological.

8.2.- Bovine Spongiform Encephalopathy

This disease which is the subject of the study for this thesis is BSE, popularly known as the mad cow disease. It was described for the first time in the United Kingdom in 1986 (166), and affected bovines. Later on it was proven to be the origin of Feline

Spongiform Encephalopathy (167) and the variant of Creutzfeldt-Jakob disease (168). Experimentally, it was proven that the BSE could affect small ruminants (194) and more recently the first natural case of BSE in goats was described (195).

The BSE lesional profile is located in the central nervous system, and is characterized by the spongiform changes that consist of the vacuolization of the neuropile and the neuronal bodies, reactive gliosis, neuronal loss and the accumulation of PrPres (196).

8.2.1.- The BSE pathogeny

Neuroinvasion

Natural infection is caused by the ingestion of materials contaminated by prions of bovine origin. The entry points implicate the immune system (197), the first entry point is the palatine tonsil, the second entry point is the small intestine, especially in the ileum, which is where the Peyer's patches or lymphoid tissue associated with the intestine are concentrated. Therefore, the M cells (enterocytes modified by the presence of subjacent B lymphocytes) capture proteins to identify antigens and thus the PrPres passes through to the lymphoid tissue, where it accumulates and replicates in macrophage cells and follicular dendritic cells (197). Once the PrPres has been established in the intestinal lymphoid tissue, it passes to the enteric nervous system, from where it expands proximally and distally through the gastrointestinal tract (198). From here, the PrPres can reach the central nervous system by means of nerve structures of the parasympathetic nerve system (198, 199, 200, 201). In any case, the neuroinvasion process can not be so simplified, given that it can not be ruled out that a fraction of PrPres circulates through the blood (202).

Neurodegeneration and glial cell activation

According to the protein only hypothesis, PrPres is the etiological agent (177). The PrPres deposition is one of the common characteristics that define all the TSE and all of them have been linked to the appearance of lesions and the proliferation of glial cells.

The most significant changes that take place in the glial cells and neurons associated with the PrPres deposition include:

- Astrocytes: astrocytosis refers to the proliferation and hypertrophy of the astrocytes, and is one of the changes that are consistently described in many TSE, and in particular, in BSE (196). The astrocyte reaction is associated with the PrPres deposit and precedes the appearance of spongiform lesions (203, 204, 205).

- Microglia: it has been proven that the microglia is an important component of the gliosis (206) and PrPres deposits have been identified in microglia cells (207). In cell cultures, the PrPres has been seen as capable of inducing the proliferation of the microglia. In fact, it seems that the proliferation of astrocytes depends on the presence of activated microglial cells (which would release interleukins 1 and 6, which are responsible for the activation of astrocytes) (205). In cell culture, neurons

and astrocytes, in the presence of PrPres, have been observed to activate the microglial cells by means of the expression of cytokines (208).

- Oligodendrocytes: while some studies show that a very important part of the RNAm of the PrPc that is expressed in the CNS comes from the oligodendrocytes and therefore they could play a very significant role in the pathogeny of the disease (181, 209, 210), others point out that this cell type presents a certain resistance to prion infection (211).

- Neurons: one of the characteristic lesions of BSE is vacuolization (196, 212, 213). During the course of the disease, the neurons adopt a vacuolated appearance, which has given to the disease the name of spongiform encephalopathy. In spite of it not being clear how they are formed, it has been suggested that the vacuoles may come from dilated organelles (mitochondria and endoplasmic reticulum) (214).

As the disease progresses, the neurons progressively die. Despite that the mechanisms that cause their death are still not well-defined, it has been published that apoptosis participates in neuronal loss in murine models (206, 215, 216, 217, 218) and in natural cases of BSE and Scrapie (219, 220). PrP peptides have been observed in cell cultures as causing apoptosis (221). In any case, the relevance that apoptosis could have on TSE pathogeny has been questioned (222). From the sequence of facts that take place in prion-induced neurodegeneration it can be first found an alteration of the dendritic spines (223), followed by the loss of synapsis (224, 225), which precede the neuronal loss.

9.- THE ECM, AQPs AND BSE

9.1.- The ECM and BSE

If there were already few studies on ECM in the CNS, there are even less that consider ECM and PrPres together.

In studies conducted in cell cultures, it has been proven that in order for the conformational change of the PrPc to PrPres to occur, additional factors are necessary such as the presence of Cu^{2+} and GAGs from the ECM (226). Moreover, the GAGs could act as a bridge between the cell surface PrPc and the PrPres, and favour the internalization of both forms (185, 227).

A study on GAGs conducted on the brain stem of BSE-affected cattle describes that the amount of HS, CS, AH and DS is decreased, which suggests that there could be some type of link between the GAGs and BSE pathogeny (228). Also in histochemical studies using Vicia villosa, Wisteria floribunda agglutinin or anti-CSPG antibodies as markers conducted on nervous tissue from patients affected by human prionic diseases, there is evidence of a decrease in the PNN related to a decrease in the GABAergic neurons, above all in the subset of parvalbumins neurons (229, 230, 231), and its has been postulated that the loss of PNN facilitates PrPres deposition in the extracellular space and it induces neuronal death (230, 231).

9.2.- The AQPs and BSE

For a few years it has been suspected that alterations in the content and distribution of CNS water may occur during the course of the TSEs. It was first suspected in Creutzfeldt-Jakob patients, from whom magnetic resonances were obtained where an increase of the signal was observed in some areas of the brain, and that this could be compatible with viscosity changes around and in the cells or in their membrane (232, 233, 234, 235).

The AQPs, due to their function, have quickly become candidates for being responsible for these changes in the water contents, given that, at the same time, studies based on DNA microarrays have shown an overexpression of AQP4 in mice and hamsters experimentally infected with Scrapie (236, 237, 238), and in Creutzfeldt-Jakob patients (239).

More recently, overexpression of AQP1 and AQP4 has been shown by western blot and immunohistochemistry in Creutzfeldt-Jakob patients, and also by western blot in mice experimentally infected with BSE (240).

10.- THE boTg110 TRANSGENIC MOUSE MODEL

Due to the long incubation period for these diseases, the experimental models in mice have proven to be very important and effective in the study of TSEs.

Thanks to the research project entitled Neuropathologic Study of the Bovine Spongiform Encephalopathy in a Murine Experimental Model, by the Spanish Ministry of Science and Technology (EET2002-05168-C04), the study of the BSE pathogeny was carried out on the transgenic mouse line boTg110. These mice come from crossing the B6CBAfl and 129/Ola lines, carrying a null mutation for the endogenous PrPc and several copies of the gene that codifies for the bovine PrPc under the murine promoter prnp, so that these animals showed a expression of bovine PrPc 8-fold higher than the levels that are normally found in the encephalon of cattle (241).

The susceptibility of these animals to intracranial infection with BSE and Scrapie was characterized by the use of two inoculums from bovine encephalon homogenates, BSE1 and BSE2, another from encephalon homogenates of boTg110 mice previously infected with BSE1, and with encephalon homogenates from sheep affected by Scrapie, and in all cases, susceptibility to the disease was observed (241, 242). It has also been shown that in this transgenic mouse line, vertical transmission of BSE can occur, despite not being able to conclude how it takes place (243).

The histopathological and immunochemical study of these animals, infected with the BSE1 inoculum showed a lesional distribution and PrPres deposition pattern indistinguishable from the classic BSE pattern (241).

The studies on the ECM and AQPs during the course of the BSE were carried out on the boTg110 transgenic mouse line, infected with the BSE1 inoculum, and lead to studies 2 and 3.

OBJECTIVES

The general objective of the research work was to delve further into knowledge of the ECM and water channels in the CNS under physiological conditions, as well as its role in the pathogeny of animal prionic diseases.

Based on these considerations, the specific objectives were:

1 – Study the distribution of ECM and water channels in the CNS of healthy mice:

* Describe the immunohistochemical distribution of the PNN using the Wisteria floribunda lectin and some of the ECM components: aggrecan, HA and the HSPG, and AQP4, using specific antibodies.

* Evaluate the possible relationship between these elements.

2 – Histochemical study of the ECM alterations in BSE pathogeny using the boTg110 transgenic mouse infected intracranially with the BSE1 inoculum:

* Evaluate the affectation of the PNN and some of the ECM components: aggrecan and HA.

* Correlate the changes of the different ECM components with the PrPres deposition, and the activation of the astrocytes and microglia.

3 - Histochemical study of the ECM alterations in Scrapie pathogeny in C57BL/6 mice infected intraperitoneally with RML scrapie strain:

* Evaluate the affectation of the PNN and some of the ECM components: tenascin-R, brevican, neurocan and HA.

* Correlate the changes of the different ECM components with the activation of the astrocytes.

4 - Histochemical study of the water channel alterations in BSE pathogeny:

* Immunohistochemical study of AQP1 and AQP4 expression in the boTg110 transgenic mouse line infected intracranially with BSE1:

* Immunohistochemical and western blot study of the AQP1 and AQP4 expression in BSE field cases.

* Correlate the AQP1 and AQP4 expression with the PrPres distribution and glial activation in mice and bovines.

STUDY 1

MAPPING OF AGGRECAN, HYALURONIC ACID, HEPARAN SULPHATE PROTEOGLYCANS AND AQUAPORIN 4 IN THE CENTRAL NERVOUS SYSTEM OF THE MOUSE

Carme Costa, Raül Tortosa, Anna Domènech, Enric Vidal, Martí Pumarola, Anna Bassols.

Journal of Chemical Neuroanatomy 33, 111–123, January 2007.

Available online at www.sciencedirect.com
ScienceDirect
Journal of Chemical Neuroanatomy 33 (2007) 111–123
Journal of CHEMICAL NEUROANATOMY
www.elsevier.com/locate/jchemneu

Mapping of aggrecan, hyaluronic acid, heparan sulphate proteoglycans and aquaporin 4 in the central nervous system of the mouse

Carme Costa [a], Raul Tortosa [a], Anna Domènech [a], Enric Vidal [b], Martí Pumarola [a,b], Anna Bassols [c,*]

[a] *Department of Animal Medicine and Surgery, Veterinary Faculty, Universitat Autònoma de Barcelona, 08193 Bellaterra (Cerdanyola del Vallès), Barcelona, Spain*
[b] *PRIOCAT Laboratory, CReSA, Veterinary Faculty, Universitat Autònoma de Barcelona, 08193 Bellaterra (Cerdanyola del Vallès), Barcelona, Spain*
[c] *Department of Biochemistry and Molecular Biology, Veterinary Faculty, Universitat Autònoma de Barcelona, 08193 Bellaterra (Cerdanyola del Vallès), Barcelona, Spain*

Received 16 November 2006; received in revised form 11 January 2007; accepted 17 January 2007
Available online 2 February 2007

Abstract

The extracellular matrix (ECM) of the central nervous system (CNS) is found dispersed in the neuropil or forming aggregates around the neurons called perineuronal nets (PNNs). The ECM mainly contains chondroitin sulphate proteoglycans (CSPG), hyaluronic acid (HA) and tenascin-R. Heparan sulphate proteoglycans (HSPG) can also be secreted in the ECM or be part of the cell membrane. The ECM has a heterogeneous distribution which has been linked to several functions, such as specific regional maintenance of hydrodynamic properties in the CNS, in which aquaporins (AQP) play an important role. AQP are a family of membrane proteins which acts as a water channel and AQP4 is the most abundant isoform in the brain.

Nevertheless the importance of these proteins, their distribution and correlation in the whole CNS of mice is only partially known. In the present study, the histochemical and immunohistochemical distribution of PNNs, using *Wisteria floribunda* agglutinin (WFA), aggrecan, HA, HSPGs and AQP4 is described, and their perineuronal and neuropil staining has been semi-quantitatively evaluated in the whole CNS of mice.

The results showed that the aggrecan, HA and HSPGs perineuronal distribution coincided partially and this could be related to ECM functional properties. AQP4 showed a heterogeneous distribution throughout the CNS. In some areas, an inverse correlation between AQP4 and ECM components has been observed, suggesting a complementary role for both in the maintenance of water homeostasis. A common location for AQP4 and HSPGs has also been observed in CNS neuropil.

Keywords: Perineuronal nets; *Wisteria floribunda* agglutinin; Chondroitin sulphate proteoglycan; Immunohistochemistry; Histochemistry; Water homeostasis

1. Introduction

The extracellular matrix (ECM) of brain was first described by Camilo Golgi and Santiago Ramón y Cajal, late in the 19th century, when iron and silver impregnation techniques allowed them to visualise the perineuronal nets (PNN) (Celio et al., 1998; Yamaguchi, 2000). Despite this early discovery, knowledge about the real significance and functions of the ECM did not surface until late in the 20th century by means of biochemical and structural studies (Brauer et al., 1982; Celio and Blumcke, 1994; Yamaguchi, 2000).

The various components of the central nervous system (CNS) ECM are found in the neuropil, either dispersed or forming the PNNs. The molecules mainly present in the CNS ECM are hyaluronic acid (HA), tenascin-R and chondroitin sulphate proteoglycans (CSPG). It has been proposed that the PNNs arise from a ternary complex formed by these components (Celio and Blumcke, 1994; Hagihara et al., 1999; Yamaguchi, 2000; Murakami and Ohtsuka, 2003; Morawski et al., 2004). HA is a non-sulphated polysaccharide lacking covalent bonds to any protein that is synthesised by glial cells in the CNS (Bignami and Asher, 1992). Besides CSPGs, HA is able to interact with other extracellular proteins and transmembrane and intracellular receptors (Bignami and Asher, 1992; Bignami et al., 1992; Carulli et al., 2006; Deepa et al., 2006). The CSPGs in the CNS mainly correspond to the

* Corresponding author. Tel.: +34 93 581 10 42; fax: +34 93 581 20 06.
E-mail address: anna.bassols@uab.es (A. Bassols).

0891-0618/$ – see front matter © 2007 Elsevier B.V. All rights reserved.
doi:10.1016/j.jchemneu.2007.01.006

lectican family, which is composed of four members: aggrecan, neurocan, brevican and versican (Bandtlow and Zimmermann, 2000; Yamaguchi, 2000). All of them are secreted by glial cells and neurones to the extracellular space (Carulli et al., 2006; Deepa et al., 2006). Aggrecan is one of the most abundant lecticans in the adult rat brain (Milev et al., 1998) and, due to the existence of glycoforms, it contributes to the molecular heterogeneity of the PNNs (Matthews et al., 2002).

Through all of these interactions, the ECM is responsible for modulating cell behaviour in different ways, such as neurogenesis, gliogenesis, axonal growth regulation, cell signalling, cell motility, cell adhesion, neuronal plasticity, neuroprotection and the extracellular hydric and ion homeostasis (Hagihara et al., 1999; Haunso et al., 1999; Bandtlow and Zimmermann, 2000; Yamaguchi, 2000; Sherman et al., 2002; Tammi et al., 2002; Morawski et al., 2004; Deepa et al., 2006).

In the water homeostasis context, an important role has also been attributed to aquaporins (Verkman et al., 2006). Aquaporins (AQP) are a family of integral membrane proteins that function as water channels in many cell types of the organism (Agre et al., 2002; Nielsen et al., 2002), being AQP4 the most abundant isoform in the CNS. Its expression is mainly confined to the astrocyte end-feet forming the internal and external glial limitans (blood–brain and brain–cerebrospinal fluid barriers) contributing to the osmotic regulation with its water transport functions (Nielsen et al., 1997; Venero et al., 1999, 2001; Neely et al., 2001; Badaut et al., 2002). Despite the fact that AQP4 in the CNS has been studied at structural and functional level (Nielsen et al., 1997; Bloch et al., 2006; Wasson, 2006), its immunohistochemical distribution in the mouse CNS has not yet been fully reported, since a detailed description only exists in spinal cord (Oshio et al., 2004; Vitellaro-Zuccarello et al., 2005) and glia limitans (Inoue et al., 2002; Amiry-Moghaddam et al., 2003), and their location in other brain areas is only partially described (Frigeri et al., 2001; Nagy et al., 2002; Manley et al., 2004). Moreover, it has been recently described in the spinal cord that the distribution of CSPGs show a complementary distribution to that of AQP4, and that both structures, AQP4 and the extracellular matrix, may represent complementary mechanisms for the control of water and ion homeostasis (Vitellaro-Zuccarello et al., 2005).

Finally, AQP4 has also been related to other kind of proteoglycans, the heparan sulphate proteoglycans (HSPGs), since AQP4 interacts with the dystrophin complex in the astrocyte membrane, which binds to the basal lamina via the HSPG agrin (Amiry-Moghaddam et al., 2004), and agrin is necessary for the polarized distribution of AQP4 in the astrocyte (Warth et al., 2004).

Despite to the numerous biological functions of ECM components and AQP4, and their implications in several pathologies, such as spongiform encephalopathies (Belichenko et al., 1999; Rodriguez et al., 2006), only a few partial immunohistochemical studies have been published regarding their distribution in the CNS. Moreover, these studies focus on specific brain regions, mainly the hippocampus and cerebral cortex and, in a few cases, the brain stem (Bertolotto et al., 1991; Bruckner et al., 1996, 2003; Ojima et al., 1998; Haunso et al., 1999; Nowicka et al., 2003). As a consequence, the distribution of PNNs and HA in the mouse CNS has been described (Bertolotto et al., 1996; Bruckner et al., 2000, 2003), whereas the immunohistochemical location of aggrecan, HSPGs and AQP4 is still lacking.

The main objective of the present study is to describe in detail the immunohistochemical distribution of aggrecan, HSPGs and AQP4 in the CNS of healthy adult mice. Moreover, they are compared with the distribution of PNNs, labelled with *Wisteria floribunda* agglutinin, and HA, the most abundant component of the ECM (Sherman et al., 2002), since all of them are related in different way to water imbalance and ion homeostasis in the CNS.

2. Material and methods

2.1. Animals euthanasia and sample collection

CD1 male mice were used, aged 2 ($n = 4$) and 9 ($n = 4$) months. The animals were kept under standard light conditions and at a constant temperature (23 °C), water and food were supplied ad libitum.

Mice were injected intraperitoneally with sodium pentobarbital. Intracardiac perfusion was performed with 4% paraformaldehyde in 0.1 M phosphate buffer saline (PBS), pH 7.4) before collection of the brain and spinal cord. Tissues were then immersed in 4% paraformaldehyde in PBS at 4 °C for 4 h, followed by three 1-h wash steps in PBS. Coronal sections of the brain were obtained at the level of the optic chiasm, piriform cortex and medulla oblongata, as well as spinal cord sections. Samples were dehydrated by increasing alcohol concentrations and were embedded in xylene and paraffin. Four micrometer sections were obtained and mounted in 3-triethoxysilylpropylamine coated glass slides for histochemical and immunohistochemical studies.

2.2. Histochemistry and immunohistochemsitry

Sections were deparaffinised and rehydrated. Endogenous peroxidase activity was blocked by incubating the sections for 20 min in hydrogen peroxide (2%), methanol (70%) and PBS. Sections for the aggrecan study were incubated with 0.5 U/ml of chondroitinase ABC (Sigma, Madrid, Spain) diluted in a buffer containing 16.5 mM Tris and 16.5 mM sodium acetate, for 4 h at 37 °C. For HSPGs detection, sections were digested with 5 mU/ml of heparitinase (from *Flavobacterium heparinum*, Seikagaku Corporation, Tokyo, Japan) diluted in a buffer containing 100 mM sodium chloride and 1 mM calcium chloride for 3 h at 37 °C.

Non-specific protein binding was blocked with 2% bovine albumin in PBS (blocking solution) for 1 h at room temperature. Sections were incubated overnight at 4 °C with the following primary antibodies: rabbit anti-aggrecan polyclonal antibody (1:400, Chemicon International Inc., Madrid, Spain), anti-Δ-heparan sulphate monoclonal antibody (3G10) (1:100, Seikagaku Corporation, Tokyo, Japan), which binds the desaturated hexuronate (glucuronate) that is present at the non-reducing end of the heparan sulphate fragments generated by digesting with heparitinase from *Flavobacterium heparinum*, therefore this antibody recognizes whatever HSPG and it is not specific for any core protein (David et al., 1992); and rabbit anti-aquaporin 4 polyclonal antibody (1:200, Chemicon International Inc., Madrid, Spain). For histochemistry, the overnight incubations were carried out with the biotinylated hyaluronic acid binding protein (1:100, Seikagaku Corporation, Tokyo, Japan), which binds specifically HA (Girard et al., 1986); and the biotinylated *Wisteria floribunda* agglutinin (1:200, Vector Laboratories, Barcelona, Spain) which recognises *N*-acetylgalactosamine, a sugar that is found in the glycosaminoglycan chains of CSPGs (Murakami et al., 1999), and it is used as specific marker for PNNs (Hartig et al., 1992; Seeger et al., 1994). All antibodies and affinity reagents were diluted in blocking solution.

After 1 h incubation with the secondary antibody anti-rabbit biotinylated IgG (DAKO, Barcelona, Spain) or anti-mouse biotinylated IgG (DAKO, Barcelona, Spain) diluted 1:200 in blocking solution at room temperature, the avidin–biotin-peroxidase complex (ImmunoPure ABC Peroxidase Staining Kits, Pierce, Madrid, Spain) was applied, diluted 1:100 in PBS, for 1 h at room temperature. The peroxidase reaction was visualized with 2.5 μg/ml of 3,3′-diaminobenzidine and 0.05% hydrogen peroxide. Sections were counterstained with haematoxylin.

Several controls were included in the experiments. As a background control the primary antibody incubation was omitted. The specificity of anti-Δ-heparan sulphate and anti-aggrecan antibodies was confirmed by omitting the digestion steps with *Flavobacterium heparinum* heparinitase and chondroitinase ABC, respectively. The WFA signalling specificity was assessed by digesting the sections with 0.5 U/ml chondroitinase ABC for 4 h at 37 °C.

The specificity of the hyaluronic acid binding protein signalling was demonstrated by digesting sections with 10 U/ml hyaluronidase from *Streptomyces hyalurolyticus* (Sigma, Madrid, Spain) for 1 h at 37 °C and also by incubating sections with the biotinylated hyaluronic acid binding protein previously blocked with 100 μg/ml HA (Sigma, Madrid, Spain). No signal was observed in any of the control slides.

2.3. Microscopy and results evaluation

A semi-quantitative assessment of the intensity of the neuropil signalling pattern and the perineuronal signalling pattern was scored as 0: no signal, 1: mild, 2: moderate and 3: maximal, in several CNS regions, which were identified according to the stereotaxic atlas of (Paxinos and Franklin, 1997).

Photographs were taken with an Olympus Vanox-S optical microscope with a Leica DFC480 digital camera and Leica IM50, Version 4.0 Release 117 software.

3. Results

The distribution pattern and intensity of the five markers were heterogeneous along the different CNS regions evaluated (Table 1). No differences were observed between the two age groups studied (2 and 9 months).

WFA, aggrecan, HA and HSPGs yielded two different staining patterns: the first one was defined as a neuropil pattern and corresponded to a reticular diffuse neuropil staining, and the second was the perineuronal pattern strongly staining the periphery of neural perikarya and proximal neurites, which corresponds to PNNs. These patterns could be observed separately or together depending on the region studied (Fig. 1A–C). AQP4 labelling patterns consisted of a diffuse neuropil immunostaining and a well defined astrocyte end-feet labelling in the internal and external glial limitans (Fig. 1E).

3.1. Wisteria floribunda *agglutinin and aggrecan*

The distribution of the staining obtained with WFA and with the anti-aggrecan antibody was very similar. Both markers mainly presented a perineuronal staining pattern which was, to a lesser extent in the case of aggrecan, accompanied by a mild neuropil staining.

In the white matter tracts of the brain, WFA also showed a mild neuropil staining, whereas no immunoreactivity was detected with aggrecan, as it was observed in corpus callosum (Fig. 3A–F).

In the hippocampal formation, perineuronal labelling was observed around non-pyramidal neurons of the oriens and pyramidal cell layers from CA1 and 3, and of the subiculum. Conversely, the neuropil staining was much more intense in CA2 and fasciola cinereum (Fig. 2A).

In the neocortex, the labelling mostly evidenced the PNNs of pyramidal and non-pyramidal neurons of layers III and V and, to a lesser extent layer IV, being heterogeneously distributed depending on the cortical area (Fig. 3A–F).

In the piriform cortex perineuronal labelling was observed at layer III, while layer I showed an intense neuropil staining.

In the thalamus, the reticular thalamic nucleus and the zona incerta stood out given that both the perineuronal and neuropil staining were too intense to be distinguished from each other. Nevertheless, hypothalamus staining of PNNs and neuropil was rather mild.

In the mesencephalon, a perineuronal labelling was observed in the superior (Fig. 4A and B) and inferior colliculus. Both signalling patterns were intensely present in the red, oculomotor and trochlear nuclei, as well as in the reticular part of the substantia nigra (Fig. 5A). In the pontine nuclei and rostral periolivary region the staining was so intense that it was hard to distinguish both patterns.

In the cerebellum, the perineuronal pattern was observed around the granular layer Golgi neurons (Fig. 6A) and around many perikarya of the deep cerebellar nuclei.

In the medulla oblongata, the trapezoid bodies, the parapyramidal and olive nuclei presented intense neuropil and perineuronal staining, while in others such as the cochlear, reticular, vestibular and the trigeminal nuclei the predominant pattern was perineuronal. Nuclei lacking labelling were also observed: facial, prepositus and solitary tract nuclei and locus coeruleus.

In the spinal cord grey matter, the PNNs staining prevailed, particularly in the dorsal horn, but was totally absent in laminae I and II (Fig. 7A).

3.2. Hyaluronic acid

The HA labelling was widely distributed adopting mainly the diffuse neuropil pattern and, less frequently, stained PNNs in some areas. In the white matter tracts of the brain, HA showed moderate to intense, and diffuse staining.

In the hippocampal formation, the neuropil was widely stained except for the stratum lucidum which lacked this pattern and the subiculum where the perineuronal pattern predominated (Fig. 2B).

In the neocortex the signalling was observed surrounding pyramidal and non-pyramidal neurons of layer V and, to a lesser extent, of layers III and IV (Fig. 3G–I).

In the thalamus and mesencephalon, the reticular thalamic, red, oculomotor, trochlear and pontine nuclei and the rostral periolivary region stood out due to the marked intensity of both the perineuronal and neuropil patterns. In the superior and inferior colliculi and in the substantia nigra, the neuropil staining pattern prevailed (Fig. 5B).

In the cerebellar cortex, neuropil staining was observed in the molecular and granular layers, whereas a marked perineuronal pattern could be observed surrounding the Purkinje neurons (Fig. 6B). In the cerebellar deep nuclei both patterns could be identified.

Table 1
Distribution and semiquantification of WFA, aggrecan, HA, HSPGs and AQP4 in the mouse CNS

	WFA		Aggrecan		HA		HSPG		AQP4
	N	P	N	P	N	P	N	P	N
Neocortex									
Cingulate cortex	1	3	0	3	3	3	1	2	2
Indusium griseum	3	0	3	0	0	0	2	0	1
Motor cortex	0	2	0	2	3	0	1	0	2
Parietal association cortex	0	2	0	2	3	0	1	0	2
Retrosplenial cortex	1	3	1	3	3	3	1	2	2
Somatosensory cortex	1	3	1	3	3	3	1	3	2
Visual cortex	0	3	0	3	3	0	1	3	2
Piriform cortex									
Layer I	3	0	3	0	3	0	2	0	3
Neuronal layer	0	2	0	2	2	0	2	0	0
Hippocampal formation									
CA1–CA3	0	3	0	3	2	0	2	0	0
CA2	3	3	3	3	2	0	2	2	0
Fasciola cinereum	3	0	3	0	2	0	2	0	0
Lacunosum moleculare layer	0	0	0	0	1	0	1	0	3
Molecular layer of the dentate gyrus	1	0	1	0	1	0	1	0	2
Oriens layer	0	3	0	3	2	0	2	0	0
Polymorph layer of the dentate gyrus	1	0	1	0	1	0	3	0	1
Stratum lucidem	0	0	0	0	0	0	3	0	0
Stratum radiatum	0	3	0	3	2	0	2	0	0
Subiculum and presubiculum	0	3	0	3	2	2	1	3	1
Cerebellum									
Golgi cells		3		3		0		3	0
Granular layer	0		0		1		1		3
Interposed cerebellar nucleus	1	2	1	2	2	3	1	2	0
Lateral cerebellar nucleus (dentate)	2	3	2	3	2	3	2	3	0
Medial cerebellar nucleus (Fastigi)	1	2	1	2	2	3	1	2	0
Molecular layer	0	0	0	0	2	0	1	0	1
Purkinje neurons		0		0		3		0	0
Subcortical forebrain									
Amigdaloid area	1	3	1	3	3	0	3	0	2
Caudate-Putamen nuclei	0	1	0	1	1	0	1	0	1
Diagonal band	0	2	0	1	1	0	0	0	0
Lateral globus pallidus	1	2	1	2	2	0	2	2	2
Lateral septal nucleus, dorsal part	0	0	0	0	1	0	2	0	3
Lateral septal nuclues, intermediate	0	2	0	2	2	0	2	0	0
Medial septal nucleus	0	2	0	1	1	0	0	0	0
Diencephalon									
Hypothalamic nuclei	1	2	0	1	2	0	2	0	2
Lateral habenular nucelus	1	2	0	1	2	0	2	0	1
Medial havenular nucleus	0	0	0	0	2	0	2	0	2
Reticular thalamaic nuclei and zona incerta	3	3	3	3	2	0	3	3	1
Mesencephalon									
Deep grey layer	0	2	0	2	1	2	1	2	1
Deep mesencephalic nucleus	1	2	1	2	2	0	1	0	1
Inferior colliculus	2	3	2	3	2	0	1	3	1
Intermediate grey layer	0	2	0	2	1	2	1	2	1
Interpeduncular nucleus	0	0	0	0	1	0	1	0	3
Lateral lemniscus nuclei	0	2	0	2	2	0	3	0	3
Oculomotor and trochlear nuclei	3	3	2	3	3	3	0	0	0
Optic layer	0	1	0	1	2	0	1	0	1
Periaqueductal grey	0	0	0	0	1	0	3	0	2
Pontine nuclei	3	3	2	2	3	3	3	0	3
Pontine reticular nucleus	1	2	0	2	2	0	1	0	1
Raphe nucleus	0	0	0	0	1	0	3	0	3
Red nucleus	3	3	2	3	3	3	0	0	0
Rostral periolivary region	2	3	1	2	3	3	3	0	3
Subbrachial nucleus	1	2	1	3	1	0	1	0	1

Table 1 (*Continued*)

	WFA		Aggrecan		HA		HSPG		AQP4
	N	P	N	P	N	P	N	P	N
Substanci nigra, reticular part	1	3	0	3	3	0	3	0	3
Superficial grey layer	0	0	0	0	1	0	1	0	2
Tegmental nuclei	1	2	0	2	1	0	1	0	2
Pons and medulla oblongata									
Dorsal cochlear nucleus	0	2	0	1	2	0	2	0	2
Facial nucleus	0	0	0	0	3	0	2	0	1
Gigantoellular reticular nuclei	1	2	1	2	2	0	1	0	0
Locus coeruleus	0	0	0	0	0	0	1	0	0
Nucleus of solitary tract	0	0	0	0	1	0	1	0	0
Olive nuclei	2	2	2	2	2	2	3	3	3
Prepositus nucleus	0	0	0	0	2	0	1	0	1
Raphe obscurus nucleus	1	2	0	2	1	0	2	0	0
Reticular nuclei	1	2	0	2	1	0	1	0	0
Trapezoid body and parapyramidal nuclei	2	3	1	2	3	3	3	3	2
Trigeminal nucleus	2	3	1	3	2	0	1	0	1
Ventral cochlear nucleus	1	2	1	3	2	0	1	0	3
Vestibular nuclei	2	3	1	3	2	0	1	0	1
Spinal cord									
Grey matter	1	2	1	3	2	2	2	2	2
Laminae I and II of dorsal horn	0	0	0	0	0	0	3	0	3
White matter	1	0	1	0	1	0	1	0	1

Labelling intensity of the perineuronal (P) and neuropil (N) patterns was scored as follows: 0—no signal, 1—mild, 2—moderate and 3—maximal.

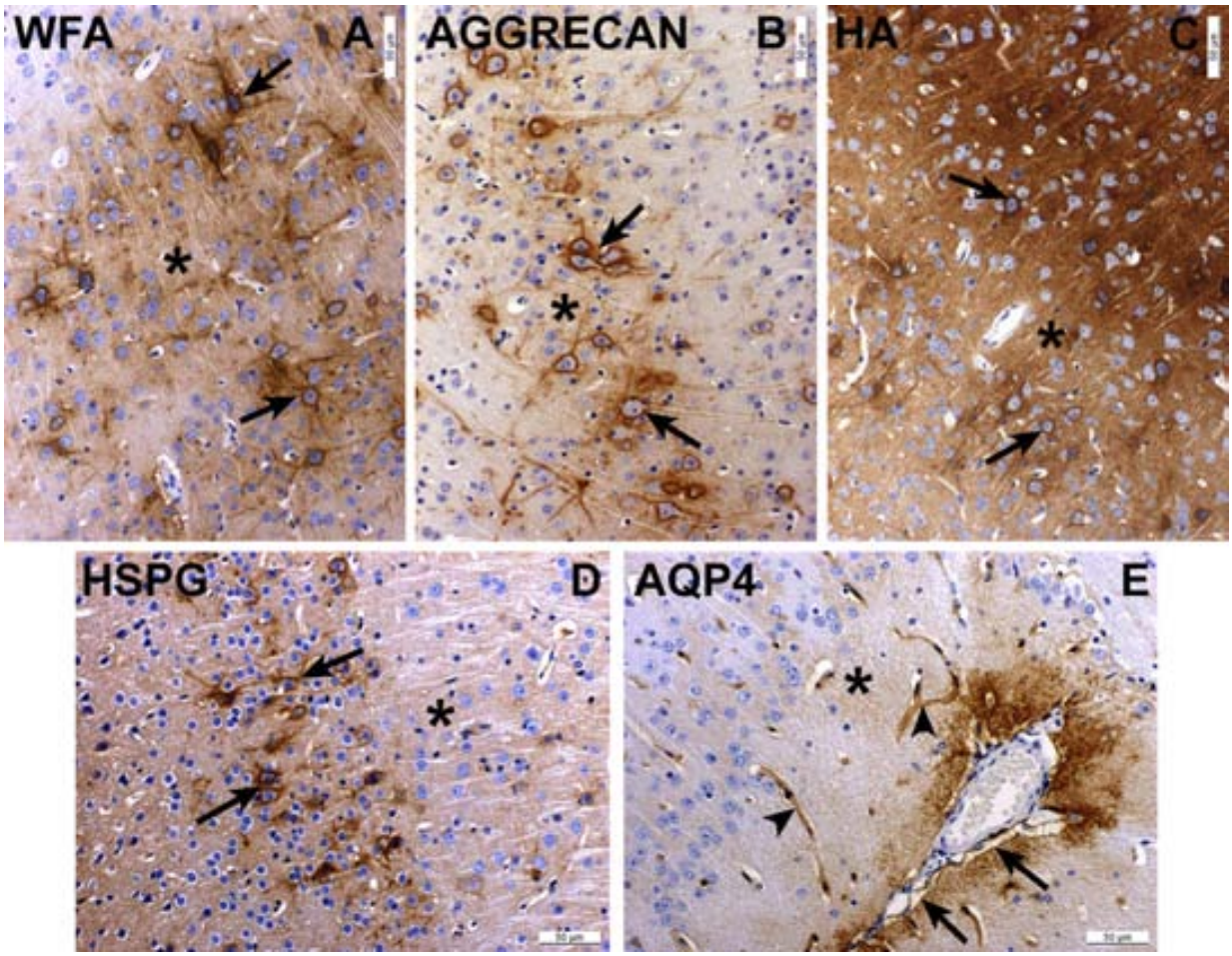

Fig. 1. Detail of WFA (A), aggrecan (B), HA (C) and HSPGs (D) perineuronal (arrows) and neuropil staining (*). AQP4 (E) location in the neuropil (*), in the internal glia limitans (blood–brain barrier) (arrowsheads) and in the external glia limitans (brain–cerebrospinal fluid barrier) (arrows). Scale bars = 50 μm.

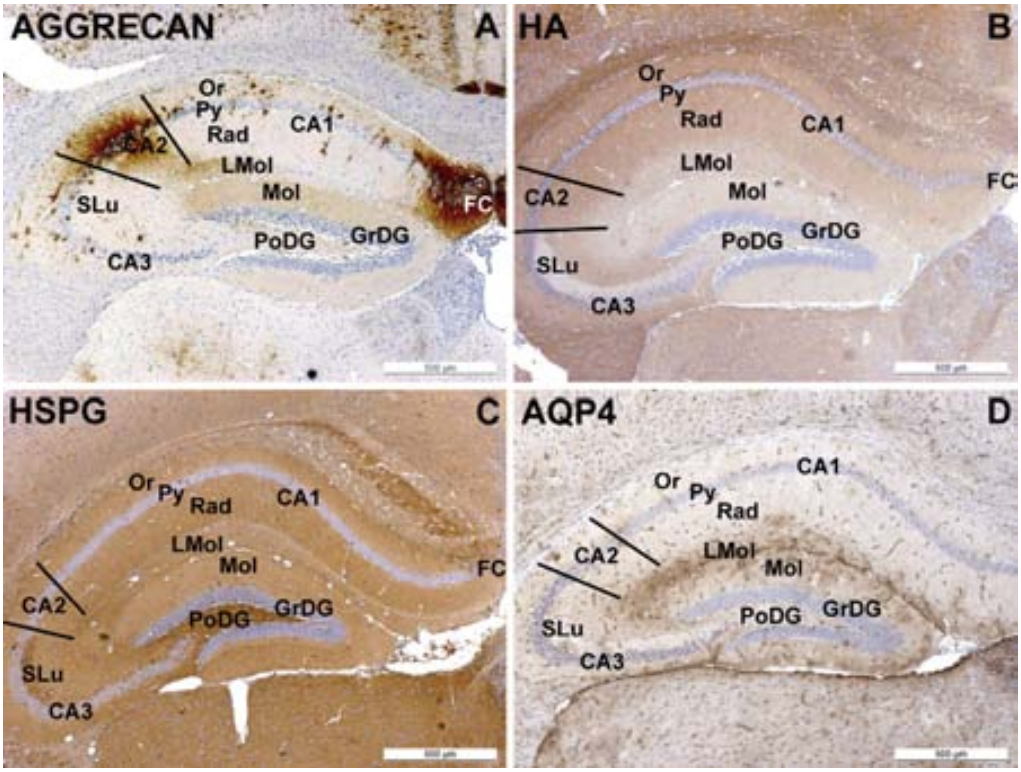

Fig. 2. Distribution in the hippocampal formation of aggrecan (A), HA (B), HSPGs (C) and AQP4 (D). PNNs in the oriens (Or) and pyramidal cell (Py) layers in the regions CA1 and CA3 contained aggrecan and the neuropil showed immunoreactivity for HA and HSPGs. The neuropil in CA2 region was intensely stained for aggrecan, comprising the oriens (Or) and pyramidal cell (Py) layers and parts of the stratum radiatum (Rad). In the stratum lucidum (SLu), the granular layer of the dentate gyrus (GrDG) and the polymorph layer of the dentate gyrus (PoDG), HSPGs were more intensely located in the neuropil. AQP4 were mainly found in the molecular layer of the dentate gyrus (Mol) and in the lacunosum moleculare layer (LMol). The neuropil of the fasciola cinereum (FC) is sharply delineated and intensely stained with anti-aggrecan antibody. Scale bars = 500 μm.

In the medulla oblongata, the neuropil pattern outweighed the PNNs that showed a mild intensity. This was conspicuous in the facial, trapezoid body, parapyramidal and olive nuclei where, on occasion, it was difficult to distinguish the PNNs from the intense neuropil staining.

In the spinal cord the situation was similar, although some PNNs labelling could also be observed in the grey matter and laminae I and II lacked staining (Fig. 7B).

3.3. Heparan sulphate proteoglycans

The staining was mainly of the neuropil type and could be observed throughout the whole CNS, being coincident in some areas with the perineuronal pattern. In the white matter tracts of the brain, HSPGs showed mild and diffuse mark.

In the hippocampal formation, an intense neuropil staining of the stratum lucidum and the polymorph layer of the dentate girus was observed. Conversely, the perineuronal pattern was present in the subiculum and the CA2 (Fig. 2C).

In the neocortex, perineuronal labelling around pyramidal neurones was observed, mainly in layer V, but variably distributed along the different cortical areas (Fig. 3J–L).

In the cerebellum, a marked immunoreactivity was detected surrounding Golgi neurons (Fig. 6C) and some perikarya of the deep cerebellar nuclei, where a strong neuropil signalling could also be noticed.

In the subcortical forebrain and in the brain stem, an intense neuropil and perineuronal immunostaining was observed in the lateral globus pallidus, the reticular thalamic, trapezoid body, the parapyramidal and the olive nuclei. Conversely, other regions such as the substantia nigra (Fig. 5C), lateral lemniscus, pontine nuclei, rostral periolivary region, periaqueductal grey (Fig. 4C), raphe nucleus, raphe obscurus and facial nucleus also showed intense staining but only of the neuropil type.

In the spinal cord immunoreactivity was seen perineuronally and in the neuropil of the grey matter, being particularly intense in laminae I and II (Fig. 7C).

3.4. Aquaporin 4

A remarkable and well defined staining was observed in the internal glial limitans, depicting the astrocyte end-feet surrounding blood vessels throughout the nervous parenchyma. The external glial limitans was also intensely immunostained where the astrocyte feet contact the leptomeningeal cells and also, albeit in a less uniform manner, the basal pole of the ependimocytes lining the ventricles.

The nervous parenchyma presented a diffuse neuropil staining of varying intensity depending on the region. In the neocortex (Fig. 3M–O) and in the piriform cortex, a marked signalling was observed in layer I, while the lacunosum moleculare layer was the most intensely labelled in the

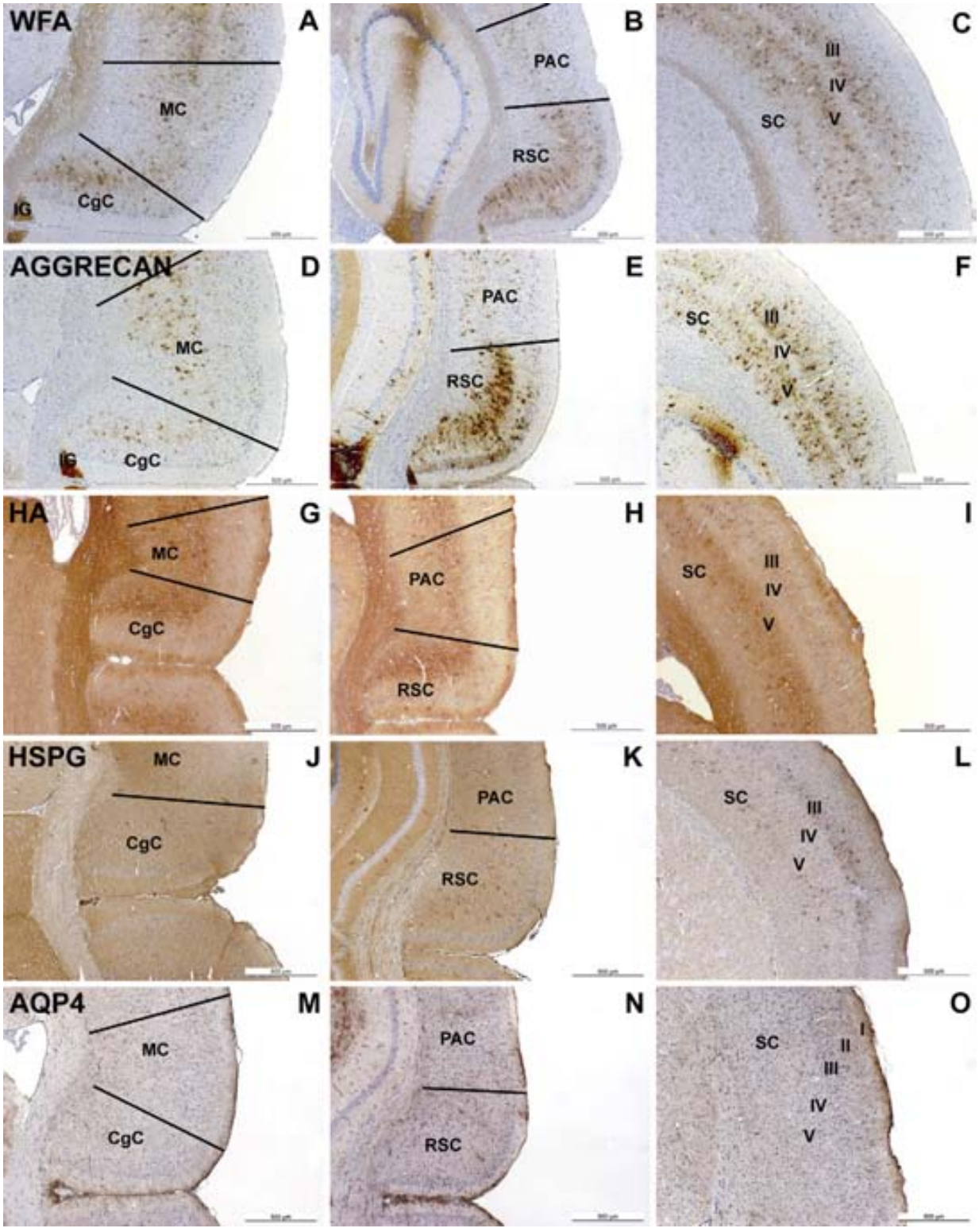

Fig. 3. Distribution in the neocortex of WFA (A–C), aggrecan (D–F), HA (G–I), HSPGs (J–L) and AQP4 (M–O). PNNs that contain WFA, aggrecan, HA and less HSPGs were observed in the cingulate cortex (CgC), retrosplenial cortex (RSC) and somatosensory cortex (SC), located mainly in the layers V–III. In the motor cortex (MC) and parietal association cortex (PAC), PNNs showed reaction for WFA, aggrecan and HA, which were mainly located in the layer V. In the neuropil, HSPGs and HA were widely located, and AQP4 was mainly observed in the layer I. Indusium griseum (IG) was intensely stained with WFA and anti-aggrecan antibody. Scale bars = 500 μm.

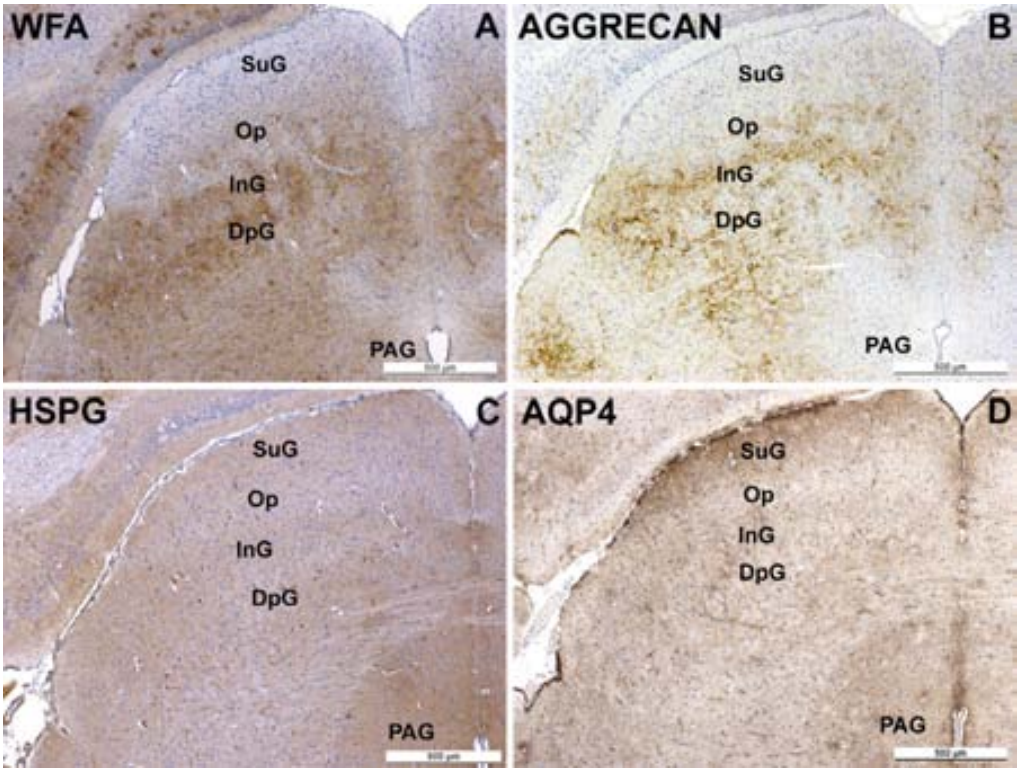

Fig. 4. Distribution in the superior colliculus of WFA (A), aggrecan (B), HSPGs (C) and AQP4 (D). In the optic layer (Op), intermediate grey layer (InG) and deep grey layer (DpG), a perineuronal pattern with WFA, aggrecan and less intensely with HSPGs was observed. AQP4 was mainly found in the neuropil of the superficial grey layer (SuG). The periaqueductal grey (PAG) contained AQP4 and HSPGs in the neuropil. Scale bars = 500 μm.

hippocampal formation (Fig. 2D). In the cerebellar cortex, AQP4 staining was observed in the granular layer and surrounding Purkinje cells (Fig. 6D).

In the subcortical forebrain and in the brain stem, the most intense immunoreactivity was seen in the following locations: lateral septal nucleus dorsal part, lateral globus pallidus, hypothalamus, substantia nigra, lateral lemniscus, pontine nuclei, rostral periolivary region, periaqueductal grey, raphe nuclei, interpeduncular nuclei, trapezoid body, parapyramidal nucleus and olive nuclei (Figs. 4 and 5D).

In the spinal cord immunolabelling was observed in both grey and white matter. Yet, the staining in laminae I and II was particularly remarkable (Fig. 7D).

4. Discussion

This study reports the complete mapping of the whole CNS in mice using several ECM markers, such as WFA, aggrecan and HA, and compares this distribution with that of AQP4 and HSPGs. The most remarkable finding is the heterogeneous distribution throughout the nervous parenchyma regarding both the perineuronal and the neuropil staining patterns, suggesting definite roles for these molecules.

4.1. The extracellular matrix

The distribution of PNNs as stained with WFA coincides with previous descriptions performed by using the same lectin or *Vicia villosa* agglutinin, another marker of PNNs, reported in mice (Bruckner et al., 2000, 2003) and in other species such as rat (Hartig et al., 1992; Fernaud-Espinosa et al., 1996; Haunso et al., 1999), guinea pig (Ojima et al., 1998), short-tailed opossum (Bruckner et al., 1998) or in humans (Bertolotto et al., 1991; Adams et al., 2001).

Aggrecan staining was widely distributed throughout the PNNs of the CNS. Previous immunohistochemical studies described the presence of aggrecan-positive PNNs in the rat (Matthews et al., 2002) and guinea pig (Ojima et al., 1998) neocortex, in the mouse hippocampus (Bruckner et al., 2003) and superior colliculus (Bruckner et al., 2006), in the cochlear, the olive nuclei and the trapezoid body of the gerbil (Lurie et al., 1997), and in the lateral geniculate nuclei of the cat (Kalb and Hockfield, 1990). In the present study, performed on mice, aggrecan immunostaining was observed in all of these areas and also in others where it had not previously been described, such as in the piriform cortex, cerebellar cortex, lateral globus pallidus, reticular thalamic nucleus, inferior colliculus, substantia nigra and spinal cord.

The distribution of both aggrecan and WFA stained PNNs is analogous throughout the CNS, except in the white matter tracts where WFA showed a mild staining but no immunoreactivity was observed with aggrecan. This parallelism had previously been demonstrated in the guinea pig neocortex using *Vicia villosa* agglutinin as a PNNs marker and Cat-301 as a specific anti-aggrecan antibody (Ojima et al., 1998). The results presented here indicate that the same similarity occurs in the

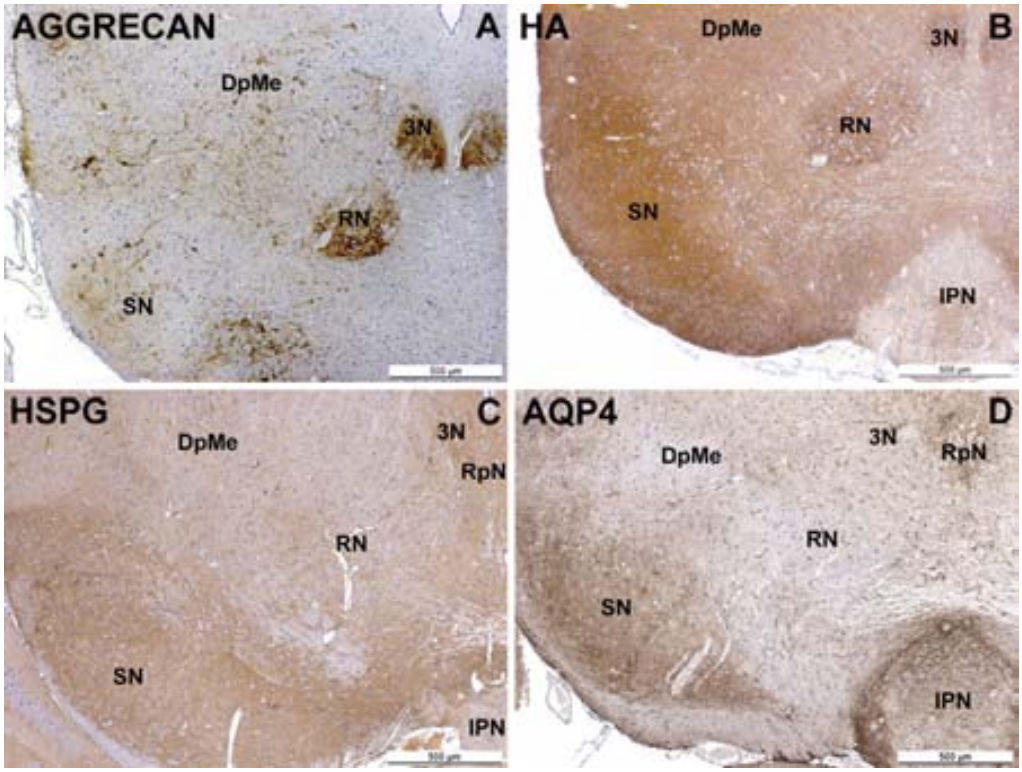

Fig. 5. Distribution in the ventral mesencephalon of aggrecan (A), HA (B), HSPGs (C) and AQP4 (D). In the oculomotor (3N) and red nuclei (RN), aggrecan and HA showed intense perineuronal and neuropil patterns, while HSPGs were only observed in the neuropil. In the deep mesencephalic nucleus (DpMe), aggrecan was located in PNNs whereas HA, HSPGs and AQP4 were lightly distributed in the neuropil. In the substantia nigra (SN), aggrecan showed a perineuronal pattern and HA, HSPGs and AQP4 showed an intense neuropil pattern. In the raphe nuclei (RpN), HSPGs and AQP4 were located in the neuropil. The interpeduncular nucleus (IPN) was mainly stained in the neuropil with anti-AQP4 antibody. Scale bars = 500 μm.

mouse CNS. It has not been possible to confirm such colocalisation by double immunohistochemistry since the protocol used for the anti-aggrecan antibody requires the use of chondroitinase ABC, an enzyme that removes *N*-acetylgalactosamine that is recognized by WFA. This coincidence suggests that aggrecan contains a significant amount of the *N*-acetylgalactosamine present in the PNN. Nevertheless, the WFA labelling could also correspond to other CSPGs which have been identified by biochemical approaches in the brain PNNs, such as the other lecticans (versican V2, neurocan, brevican) and phosphacan (Carulli et al., 2006; Deepa et al., 2006). The neuropil staining with WFA could be also due, besides the lecticans, to other CSPGs such as phosphacan or NG2, which are found mostly secreted or associated to the cell membranes (Deepa et al., 2006).

HA is widely distributed in the mouse CNS both in the PNNs and in the neuropil. The results of the present study coincide with previous immunohistochemical studies performed in mouse CNS (Bruckner et al., 2000, 2003) and in the rat neocortex (Bignami and Asher, 1992; Bignami et al., 1992), where it is described as one of the main ECM elements (Sherman et al., 2002).

4.2. HSPGs and aquaporin 4

The 3G10 antibody recognizes the desaturated uronate residues generated by a heparitinase treatment. Although it has been pointed out that this desaturated uronate residue is recognized in a specific context, only one residue per chain will remain linked to the core protein. The extent to which 3G10 reacts with heparitinase-treated tissue sections will therefore trace the number of HS chains carried by any protein core bearing HS chains rather than the mass of heparan sulphate that was originally present (David et al., 1992).

The HSPGs distribution in the mouse CNS assessed with the 3G10 antibody has been found to be similar to that found in rats using the same antibody with immunofluorescence techniques, such as neocortex and CA2 (Fuxe et al., 1994, 1997). In the present study, however, the perineuronal and neuropil HSPG signalling is stronger than in the rat, as it was observed in several areas as red and substantia nigra. This strong signal had previously been shown in the mouse mesencephalon using 3,3′-diaminobenzidine to visualize the binding (McBride et al., 1998) instead of the immunofluorescence. This suggests that the differences were due to technical procedures used to visualize the antibody binding.

In the present study, HSPGs staining has been also observed in regions where it had not been formerly described, such as surrounding the Golgi neurons or in the laminae I and II of the spinal cord dorsal horn.

It is difficult to determine whether 3G10 immunostaining is mainly related with some specific type of HSPG, since the 3G10 antibody recognizes any molecule carrying HS chains. Syndecans and glypicans are the main cell surface HSPGs,

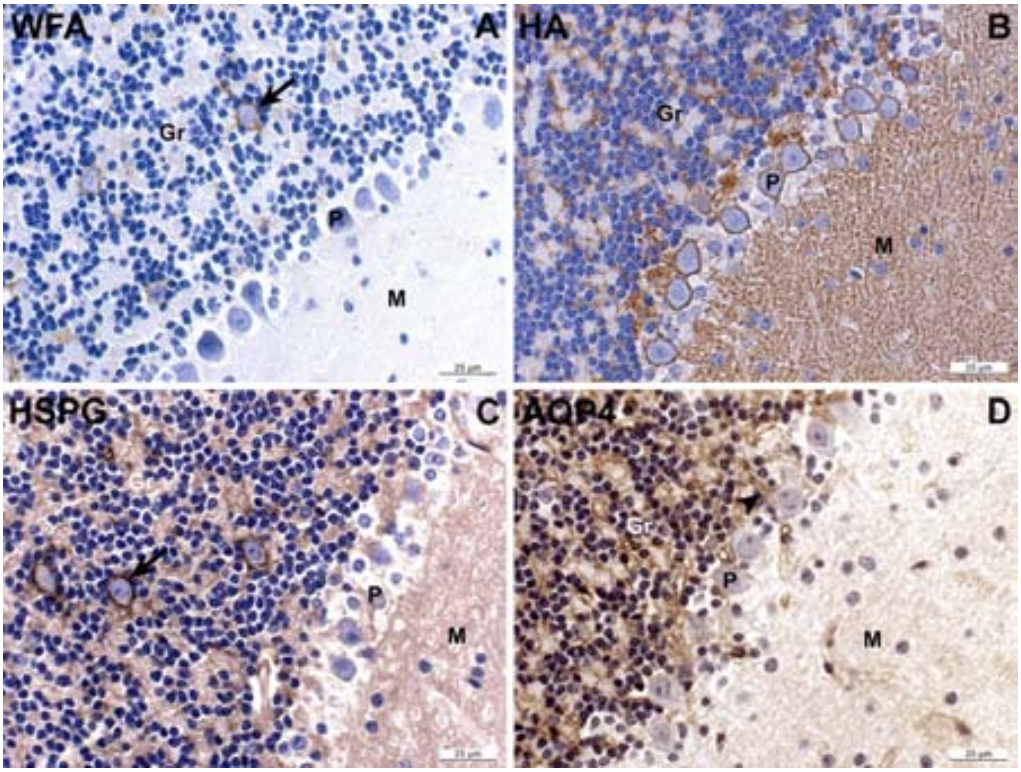

Fig. 6. Distributions in the cerebellar cortex of WFA (A), HA (B), HSPG (C) and AQP4 (D). In the granular layer (Gr), the neuropil was labelled with HA, HSPG and AQP4, and the Golgi cells (arrows) were surrounded by PNNs wich also contained HSPG. The Purkinje (P) neurons were intensely surrounded by HA reactivity, and anti-AQP4 antibody showed a mild mark close to its axonal part (arrowhead). In the molecular layer (M), HA showed intense mark, and HSPG and AQP4 presented less intense staining in the neuropil. Scale bars = 500 μm.

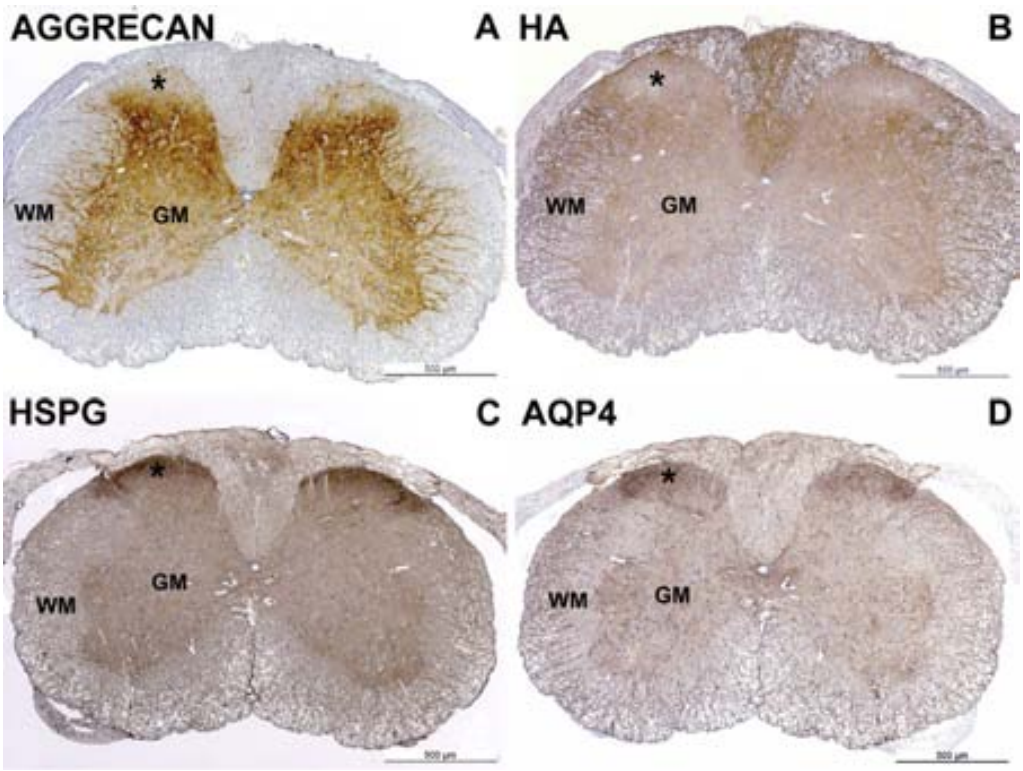

Fig. 7. Distribution in the spinal cord of aggrecan (A), HA (B), HSPGs (C) and AQP4 (D). In the grey matter (GM), the PNNs displayed aggrecan-immunoreactivity and showed a less intense of HA and HSPGs. In laminae I and II (*), only an intense mark with anti-AQP4 and anti-HSPG was observed. The white matter (WM) contained HA, HSPGs and AQP4. Scale bars = 500 μm.

whereas agrin and perlecan are found in the extracellular space (Rhiner and Hengartner, 2006), but there is scarce information about the mapping of these molecules in the CNS areas: syndecans and glypicans have been reported in developing and adult CNS neurons and glia (Karthikeyan et al., 1994; Litwack et al., 1994; Iseki et al., 2002; Winkler et al., 2002), whereas agrin is mainly localized in the synapsis, and perlecan in the perivascular astrocyte feet (Leadbeater et al., 2006). Further work is necessary to identify the particular HSPGs from the 3G10-positive areas.

A heterogeneous distribution of AQP4 throughout the mouse CNS has been demonstrated. The results of the present study support the previously described location in the astrocyte end-feet forming the external glial limitans (Amiry-Moghaddam et al., 2003, 2004; Bragg et al., 2006). Nevertheless, our study contributes to the complete knowledge of its immunohistochemical distribution in the whole murine CNS since previously published studies were confined to the spinal cord of mouse (Oshio et al., 2004; Vitellaro-Zuccarello et al., 2005) and only a few references exist about the neocortex and other areas (Frigeri et al., 2001; Nagy et al., 2002; Manley et al., 2004). Although the observed distribution is in accordance with the cited publications, a noticeable AQP4 immunostaining has also been detected in the neuropil of other areas such as the piriform cortex, lacunosum moleculare of the hippocampal formation, dorsal part of the lateral septal nucleus, superficial grey layer of the superior colliculus, reticular part of the substantia nigra, lateral lemniscus, pontine nuclei, rostral periolivary region, periaqueductal grey, raphe nuclei and the interpeduncular nuclei.

Several regions with a marked AQP4 staining concomitantly with an intense HSPGs neuropil labelling have been observed: laminae I and II of the spinal cord, granular layer of the cerebellar cortex, periaqueductal grey and dorsal part of the lateral septal nuclei. It has been suggested that, in the perivascular and subpial astrocyte feet, the dystrophin complex binds to the basal lamina via agrin (which is an HSPG) and laminin and, simultaneously, binds to astrocyte membrane AQP4 by means of syntrophins (Amiry-Moghaddam et al., 2004). The common location of AQP4 and HSPGs observed in the present study might be explained by the formation of a complex similar to the one formerly mentioned. Hence, it would be interesting to assess whether the HSPG identified in these locations is actually agrin or any other.

4.3. Connections between extracellular matrix, heparan sulphate proteoglycans and aquaporin 4

Previous reports on the mouse brain (Hartig et al., 1992) demonstrated a close relationship between the distribution of WFA positive PNNs and that of the GABAergic neuronal subpopulation. On the other hand, it has been proved on rat brains that numerous HSPGs positive neurones are indeed GABAergic (Fuxe et al., 1997). Our results support the fact that GABAergic nuclei display aggrecan and HA-positive PPNs, and are usually positive for HSPGs. In contrast, in the present study it has been observed that aminergic nuclei, such as the solitary tract nucleus, prepositus nucleus and the locus coeruleus, lack PNNs and that the amount of HSPGs detected in the neuropil on those nuclei was minimal. Similar results have been reported previously (King, 1987; Hobohm et al., 1998).

All these studies indicate that PNNs, enriched in CSPGs and HA, as well as the presence of HSPGs, surrounds specific neuronal subpopulations and that, possibly, these elements are related to the particular functional properties of such subpopulations. However, it has not yet been possible to establish a clear relationship between the various neuronal subpopulations, and the ECM and the HSPGs associated to them.

The various ECM components are believed to contribute to the hydrodynamic properties that allow the maintenance of water and specific ion concentrations in the extracellular space (Bruckner et al., 1996, 2003; Hobohm et al., 1998). Along with those elements, AQP4 also has a role in water metabolism in the CNS since it is the chief water channel of the blood brain barrier (Badaut et al., 2002; Amiry-Moghaddam et al., 2003, 2004; Vitellaro-Zuccarello et al., 2005; Bragg et al., 2006).

In the present study a lack of aggrecan and WFA signalling in laminae I and II of the dorsal horn of the spinal cord has been observed in contrast to a marked AQP4 immunolabelling; this is in accordance with previous descriptions in mice and rats (Vitellaro-Zuccarello et al., 2005). Additionally a lack of HA in this region has been observed. We have also observed an enrichment of AQP4 concomitantly to a lack of PNNs, aggrecan and HA staining in other regions such as: neocortex layer I, dorsal part of the lateral septal nucleus, lacunosum moleculare layer of the hippocampus, hypothalamus, superficial grey layer of the superior colliculus, periaqueductal grey, interpenduncular nucleus, raphe nuclei, and in the granular layer of the cerebellar cortex. Thus, the results of the present study reinforce the hypothesis presented in the cited reference (Vitellaro-Zuccarello et al., 2005), by which the regions with an ECM enriched in highly hydrophilic molecules, such as CSPGs and HA, allow an easier circulation of the water through the extracellular space, whereas in regions with a scarcer presence of ECM, thus having closer cellular contacts that limit the size of the intercellular space, AQP4 could facilitate the water and potassium diffusion. Therefore, both mechanisms would complement each other in the maintenance of the water homeostasis.

On the other hand, regions where the four markers (WFA, aggrecan, HA, and AQP4) were extensively and simultaneously expressed were also observed. Noticeable examples of such were the layer I of the piriform cortex, lateral globus pallidus, substantia nigra, pontine nuclei, olive nuclei and the ventral cochlear nuclei.

In conclusion, the results described here suggest that, while in certain regions the lack of ECM might be compensated by the AQP4 and vice versa, in others both mechanisms may function complementarily.

Acknowledgements

The authors would like to thank Marta Valle and Sierra Espinar for their excellent technical assistance. This work has been economically supported by the Spanish *Ministerio de*

Ciencia y Tecnología (Grant ref. EET2002-05168-C04-01). C.C. was supported by a fellowship from the *Universitat Autònoma de Barcelona*, A.D. was supported by a fellowship from the Spanish *Ministerio de Educación* and R.T. was supported by the fellowship attached to the grant EET2002-05168-C04-01 (to M.P.) from the *Ministerio de Ciencia y Tecnología*.

References

Adams, I., Brauer, K., Arelin, C., Hartig, W., Fine, A., Mader, M., Arendt, T., Bruckner, G., 2001. Perineuronal nets in the rhesus monkey and human basal forebrain including basal ganglia. Neuroscience 108, 285–298.

Agre, P., King, L.S., Yasui, M., Guggino, W.B., Ottersen, O.P., Fujiyoshi, Y., Engel, A., Nielsen, S., 2002. Aquaporin water channels–from atomic structure to clinical medicine. J. Physiol. 542, 3–16.

Amiry-Moghaddam, M., Frydenlund, D.S., Ottersen, O.P., 2004. Anchoring of aquaporin-4 in brain: molecular mechanisms and implications for the physiology and pathophysiology of water transport. Neuroscience 129, 999–1010.

Amiry-Moghaddam, M., Otsuka, T., Hurn, P.D., Traystman, R.J., Haug, F.M., Froehner, S.C., Adams, M.E., Neely, J.D., Agre, P., Ottersen, O.P., Bhardwaj, A., 2003. An alpha-syntrophin-dependent pool of AQP4 in astroglial end-feet confers bidirectional water flow between blood and brain. Proc. Natl. Acad. Sci. U.S.A. 100, 2106–2111.

Badaut, J., Lasbennes, F., Magistretti, P.J., Regli, L., 2002. Aquaporins in brain: distribution, physiology, and pathophysiology. J. Cereb. Blood Flow. Metab. 22, 367–378.

Bandtlow, C.E., Zimmermann, D.R., 2000. Proteoglycans in the developing brain: new conceptual insights for old proteins. Physiol. Rev. 80, 1267–1290.

Belichenko, P.V., Miklossy, J., Belser, B., Budka, H., Celio, M.R., 1999. Early destruction of the extracellular matrix around parvalbumin-immunoreactive interneurons in Creutzfeldt-Jakob disease. Neurobiol. Dis. 6, 269–279.

Bertolotto, A., Manzardo, E., Guglielmone, R., 1996. Immunohistochemical mapping of perineuronal nets containing chondroitin unsulfated proteoglycan in the rat central nervous system. Cell Tissue Res. 283, 283–295.

Bertolotto, A., Rocca, G., Canavese, G., Migheli, A., Schiffer, D., 1991. Chondroitin sulfate proteoglycan surrounds a subset of human and rat CNS neurons. J. Neurosci. Res. 29, 225–234.

Bignami, A., Asher, R., 1992. Some observations on the localization of hyaluronic acid in adult, newborn and embryonal rat brain. Int. J. Dev. Neurosci. 10, 45–57.

Bignami, A., Asher, R., Perides, G., 1992. Co-localization of hyaluronic acid and chondroitin sulfate proteoglycan in rat cerebral cortex. Brain Res. 579, 173–177.

Bloch, O., Auguste, K.I., Manley, G.T., Verkman, A.S., 2006. Accelerated progression of kaolin-induced hydrocephalus in aquaporin-4-deficient mice. J. Cereb. Blood Flow. Metab..

Bragg, A.D., Amiry-Moghaddam, M., Ottersen, O.P., Adams, M.E., Froehner, S.C., 2006. Assembly of a perivascular astrocyte protein scaffold at the mammalian blood-brain barrier is dependent on alpha-syntrophin. Glia 53, 879–890.

Brauer, K., Werner, L., Leibnitz, L., 1982. Perineuronal nets of glia. J. Hirnforsch 23, 701–708.

Bruckner, G., Grosche, J., Hartlage-Rubsamen, M., Schmidt, S., Schachner, M., 2003. Region and lamina-specific distribution of extracellular matrix proteoglycans, hyaluronan and tenascin-R in the mouse hippocampal formation. J. Chem. Neuroanat. 26, 37–50.

Bruckner, G., Grosche, J., Schmidt, S., Hartig, W., Margolis, R.U., Delpech, B., Seidenbecher, C.I., Czaniera, R., Schachner, M., 2000. Postnatal development of perineuronal nets in wild-type mice and in a mutant deficient in tenascin-R. J. Comp. Neurol. 428, 616–629.

Bruckner, G., Hartig, W., Kacza, J., Seeger, J., Welt, K., Brauer, K., 1996. Extracellular matrix organization in various regions of rat brain grey matter. J. Neurocytol. 25, 333–346.

Bruckner, G., Hartig, W., Seeger, J., Rubsamen, R., Reimer, K., Brauer, K., 1998. Cortical perineuronal nets in the gray short-tailed opossum (Monodelphis domestica): a distribution pattern contrasting with that shown in placental mammals. Anat. Embryol. (Berl.) 197, 249–262.

Bruckner, G., Szeoke, S., Pavlica, S., Grosche, J., Kacza, J., 2006. Axon initial segment ensheathed by extracellular matrix in perineuronal nets. Neuroscience 138, 365–375.

Carulli, D., Rhodes, K.E., Brown, D.J., Bonnert, T.P., Pollack, S.J., Oliver, K., Strata, P., Fawcett, J.W., 2006. Composition of perineuronal nets in the adult rat cerebellum and the cellular origin of their components. J. Comp. Neurol. 494, 559–577.

Celio, M.R., Blumcke, I., 1994. Perineuronal nets–a specialized form of extracellular matrix in the adult nervous system. Brain Res. Brain Res. Rev. 19, 128–145.

Celio, M.R., Spreafico, R., De Biasi, S., Vitellaro-Zuccarello, L., 1998. Perineuronal nets: past and present. Trends Neurosci. 21, 510–515.

David, G., Bai, X.M., Van der Schueren, B., Cassiman, J.J., Van den Berghe, H., 1992. Developmental changes in heparan sulfate expression: in situ detection with mAbs. J. Cell Biol. 119, 961–975.

Deepa, S.S., Carulli, D., Galtrey, C., Rhodes, K., Fukuda, J., Mikami, T., Sugahara, K., Fawcett, J.W., 2006. Composition of perineuronal net extracellular matrix in rat brain: a different disaccharide composition for the net-associated proteoglycans. J. Biol. Chem. 281, 17789–17800.

Fernaud-Espinosa, I., Nieto-Sampedro, M., Bovolenta, P., 1996. Developmental distribution of glycosaminoglycans in embryonic rat brain: relationship to axonal tract formation. J. Neurobiol. 30, 410–424.

Frigeri, A., Nicchia, G.P., Nico, B., Quondamatteo, F., Herken, R., Roncali, L., Svelto, M., 2001. Aquaporin-4 deficiency in skeletal muscle and brain of dystrophic mdx mice. Faseb J. 15, 90–98.

Fuxe, K., Chadi, G., Tinner, B., Agnati, L.F., Pettersson, R., David, G., 1994. On the regional distribution of heparan sulfate proteoglycan immunoreactivity in the rat brain. Brain Res. 636, 131–138.

Fuxe, K., Tinner, B., Staines, W., David, G., Agnati, L.F., 1997. Regional distribution of neural cell adhesion molecule immunoreactivity in the adult rat telencephalon and diencephalon. Partial colocalization with heparan sulfate proteoglycan immunoreactivity. Brain Res. 746, 25–33.

Girard, N., Delpech, A., Delpech, B., 1986. Characterization of hyaluronic acid on tissue sections with hyaluronectin. J. Histochem. Cytochem. 34, 539–541.

Hagihara, K., Miura, R., Kosaki, R., Berglund, E., Ranscht, B., Yamaguchi, Y., 1999. Immunohistochemical evidence for the brevican-tenascin-R interaction: colocalization in perineuronal nets suggests a physiological role for the interaction in the adult rat brain. J. Comp. Neurol. 410, 256–264.

Hartig, W., Brauer, K., Bruckner, G., 1992. Wisteria floribunda agglutinin-labelled nets surround parvalbumin-containing neurons. Neuroreport 3, 869–872.

Haunso, A., Celio, M.R., Margolis, R.K., Menoud, P.A., 1999. Phosphacan immunoreactivity is associated with perineuronal nets around parvalbumin-expressing neurones. Brain Res. 834, 219–222.

Hobohm, C., Hartig, W., Brauer, K., Bruckner, G., 1998. Low expression of extracellular matrix components in rat brain stem regions containing modulatory aminergic neurons. J. Chem. Neuroanat. 15, 135–142.

Inoue, M., Wakayama, Y., Liu, J.W., Murahashi, M., Shibuya, S., Oniki, H., 2002. Ultrastructural localization of aquaporin 4 and alpha1-syntrophin in the vascular feet of brain astrocytes. Tohoku J. Exp. Med. 197, 87–93.

Iseki, K., Hagino, S., Mori, T., Zhang, Y., Yokoya, S., Takaki, H., Tase, C., Murakawa, M., Wanaka, A., 2002. Increased syndecan expression by pleiotrophin and FGF receptor-expressing astrocytes in injured brain tissue. Glia 39, 1–9.

Kalb, R.G., Hockfield, S., 1990. Large diameter primary afferent input is required for expression of the Cat-301 proteoglycan on the surface of motor neurons. Neuroscience 34, 391–401.

Karthikeyan, L., Flad, M., Engel, M., Meyer-Puttlitz, B., Margolis, R.U., Margolis, R.K., 1994. Immunocytochemical and in situ hybridization studies of the heparan sulfate proteoglycan, glypican, in nervous tissue. J. Cell. Sci. 107 (Pt 11), 3213–3222.

King, A.S., 1987. Physiological and Clinical Anatomy of the Domestic Mammals. Oxford Science Publications, p. 1.

Leadbeater, W.E., Gonzalez, A.M., Logaras, N., Berry, M., Turnbull, J.E., Logan, A., 2006. Intracellular trafficking in neurones and glia of fibroblast growth factor-2, fibroblast growth factor receptor 1 and heparan sulphate proteoglycans in the injured adult rat cerebral cortex. J. Neurochem. 96, 1189–1200.

Litwack, E.D., Stipp, C.S., Kumbasar, A., Lander, A.D., 1994. Neuronal expression of glypican, a cell-surface glycosylphosphatidylinositol-anchored heparan sulfate proteoglycan, in the adult rat nervous system. J. Neurosci. 14, 3713–3724.

Lurie, D.I., Pasic, T.R., Hockfield, S.J., Rubel, E.W., 1997. Development of Cat-301 immunoreactivity in auditory brainstem nuclei of the gerbil. J. Comp. Neurol. 380, 319–334.

Manley, G.T., Binder, D.K., Papadopoulos, M.C., Verkman, A.S., 2004. New insights into water transport and edema in the central nervous system from phenotype analysis of aquaporin-4 null mice. Neuroscience 129, 983–991.

Matthews, R.T., Kelly, G.M., Zerillo, C.A., Gray, G., Tiemeyer, M., Hockfield, S., 2002. Aggrecan glycoforms contribute to the molecular heterogeneity of perineuronal nets. Neuroscience 22, 7536–7547.

McBride, P.A., Wilson, M.I., Eikelenboom, P., Tunstall, A., Bruce, M.E., 1998. Heparan sulfate proteoglycan is associated with amyloid plaques and neuroanatomically targeted PrP pathology throughout the incubation period of scrapie-infected mice. Exp. Neurol. 149, 447–454.

Milev, P., Maurel, P., Chiba, A., Mevissen, M., Popp, S., Yamaguchi, Y., Margolis, R.K., Margolis, R.U., 1998. Differential regulation of expression of hyaluronan-binding proteoglycans in developing brain: aggrecan, versican, neurocan, and brevican. Biochem. Biophys. Res. Commun. 247, 207–212.

Morawski, M., Bruckner, M.K., Riederer, P., Bruckner, G., Arendt, T., 2004. Perineuronal nets potentially protect against oxidative stress. Exp. Neurol. 188, 309–315.

Murakami, T., Ohtsuka, A., 2003. Perisynaptic barrier of proteoglycans in the mature brain and spinal cord. Arch. Histol. Cytol. 66, 195–207.

Murakami, T., Ohtsuka, A., Su, W.D., Taguchi, T., Oohashi, T., Abe, K., Ninomiya, Y., 1999. The extracellular matrix in the mouse brain: its reactions to endo-alpha-N-acetylgalactosaminidase and certain other enzymes. Arch. Histol. Cytol. 62, 273–281.

Nagy, G., Szekeres, G., Kvell, K., Berki, T., Nemeth, P., 2002. Development and characterisation of a monoclonal antibody family against aquaporin 1 (AQP1) and aquaporin 4 (AQP4). Pathol. Oncol. Res. 8, 115–124.

Neely, J.D., Amiry-Moghaddam, M., Ottersen, O.P., Froehner, S.C., Agre, P., Adams, M.E., 2001. Syntrophin-dependent expression and localization of Aquaporin-4 water channel protein. Proc. Natl. Acad. Sci. U.S.A. 98, 14108–14113.

Nielsen, S., Frokiaer, J., Marples, D., Kwon, T.H., Agre, P., Knepper, M.A., 2002. Aquaporins in the kidney: from molecules to medicine. Physiol. Rev. 82, 205–244.

Nielsen, S., Nagelhus, E.A., Amiry-Moghaddam, M., Bourque, C., Agre, P., Ottersen, O.P., 1997. Specialized membrane domains for water transport in glial cells: high-resolution immunogold cytochemistry of aquaporin-4 in rat brain. J. Neurosci. 17, 171–180.

Nowicka, D., Liguz-Lecznar, M., Skangiel-Kramska, J., 2003. A surface antigen delineating a subset of neurons in the primary somatosensory cortex of the mouse. Acta. Neurobiol. Exp. (Wars) 63, 185–195.

Ojima, H., Sakai, M., Ohyama, J., 1998. Molecular heterogeneity of Vicia villosa-recognized perineuronal nets surrounding pyramidal and nonpyramidal neurons in the guinea pig cerebral cortex. Brain Res. 786, 274–280.

Oshio, K., Binder, D.K., Yang, B., Schecter, S., Verkman, A.S., Manley, G.T., 2004. Expression of aquaporin water channels in mouse spinal cord. Neuroscience 127, 685–693.

Paxinos, G., Franklin, K.B.J., 1997. The Mouse Brain in Stereotaxic Coordinates. Elsevier Academic Press, London.

Rhiner, C., Hengartner, M.O., 2006. Sugar antennae for guidance signals: syndecans and glypicans integrate directional cues for navigating neurons. ScientificWorld J. 6, 1024–1036.

Rodriguez, A., Perez-Gracia, E., Espinosa, J.C., Pumarola, M., Torres, J.M., Ferrer, I., 2006. Increased expression of water channel aquaporin 1 and aquaporin 4 in Creutzfeldt-Jakob disease and in bovine spongiform encephalopathy-infected bovine-PrP transgenic mice. Acta Neuropathol. (Berl.) 112, 573–585.

Seeger, G., Brauer, K., Hartig, W., Bruckner, G., 1994. Mapping of perineuronal nets in the rat brain stained by colloidal iron hydroxide histochemistry and lectin cytochemistry. Neuroscience 58, 371–388.

Sherman, L.S., Struve, J.N., Rangwala, R., Wallingford, N.M., Tuohy, T.M., Kuntz, C.T., 2002. Hyaluronate-based extracellular matrix: keeping glia in their place. Glia 38, 93–102.

Tammi, M.I., Day, A.J., Turley, E.A., 2002. Hyaluronan and homeostasis: a balancing act. J. Biol. Chem. 277, 4581–4584.

Venero, J.L., Vizuete, M.L., Ilundain, A.A., Machado, A., Echevarria, M., Cano, J., 1999. Detailed localization of aquaporin-4 messenger RNA in the CNS: preferential expression in periventricular organs. Neuroscience 94, 239–250.

Venero, J.L., Vizuete, M.L., Machado, A., Cano, J., 2001. Aquaporins in the central nervous system. Prog. Neurobiol. 63, 321–336.

Verkman, A.S., Binder, D.K., Bloch, O., Auguste, K., Papadopoulos, M.C., 2006. Three distinct roles of aquaporin-4 in brain function revealed by knockout mice. Biochim. Biophys. Acta 1758, 1085–1093.

Vitellaro-Zuccarello, L., Mazzetti, S., Bosisio, P., Monti, C., De Biasi, S., 2005. Distribution of Aquaporin 4 in rodent spinal cord: relationship with astrocyte markers and chondroitin sulfate proteoglycans. Glia 51, 148–159.

Warth, A., Kroger, S., Wolburg, H., 2004. Redistribution of aquaporin-4 in human glioblastoma correlates with loss of agrin immunoreactivity from brain capillary basal laminae. Acta Neuropathol. (Berl.) 107, 311–318.

Wasson, K., 2006. Phenotypes of aquaporin mutants in genetically altered mice. Comp. Med. 56, 96–104.

Winkler, S., Stahl, R.C., Carey, D.J., Bansal, R., 2002. Syndecan-3 and perlecan are differentially expressed by progenitors and mature oligodendrocytes and accumulate in the extracellular matrix. J. Neurosci. Res. 69, 477–487.

Yamaguchi, Y., 2000. Lecticans: organizers of the brain extracellular matrix. Cell. Mol. Life Sci. 57, 276–289.

STUDY 2

CENTRAL NERVOUS SYSTEM EXTRACELLULAR MATRIX CHANGES IN A TRANSGENIC MOUSE MODEL OF BOVINE SPONGIFORM ENCEPHALOPATHY

Carme Costa, Raül Tortosa, Enric Vidal, Danielle Padilla, Juan Maria Torres, Isidre Ferrer, Martí Pumarola and Anna Bassols.

Summited to **The Veterinary Journal**.

CENTRAL NERVOUS SYSTEM EXTRACELLULAR MATRIX CHANGES IN A TRANSGENIC MOUSE MODEL OF BOVINE SPONGIFORM ENCEPHALOPATHY

Carme Costa[1], Raül Tortosa[1], Enric Vidal[2], Danielle Padilla[4], Juan Maria Torres[4], Isidre Ferrer[5], Martí Pumarola[1, 2] and Anna Bassols[3]

[1] Departament de Medicina i Cirurgia Animals.

[2] Laboratori Priocat, CReSA.

[3] Departament de Bioquímica i Biologia Molecular.

Universitat Autònoma de Barcelona, 08193 Bellaterra (Cerdanyola del Vallès), Barcelona, Spain.

[4] Centro de Investigación en Sanidad Animal (CISA), INIA, 28130 Valdeolmos (Madrid), Spain.

[5] Institut de Neuropatologia, Servei Anatomia Patològica, IDIBELL-Hospital de Bellvitge, Universitat de Barcelona, 08907 Hospitalet de Llobregat, Barcelona, Spain.

ABSTRACT

Bovine spongiform encephalopathy (BSE) is a disease that belongs to the group of transmissible spongiform encephalopathies (TSE), which are characterized by the accumulation of resistant prion protein (PrPres) in the central nervous system, neuronal loss, spongiform degeneration and glial cell proliferation. In human TSEs the neuronal loss has been attributed to extracellular matrix (ECM) disturbances, before the PrPres deposition. This study has been developed in a transgenic strain of mice overexpressing the bovine cellular prion protein, infected with cattle BSE. By immunohistochemistry the PrPres accumulation, and activated astrocytes and microglia, were correlated with ECM impairment, using Wisteria floribunda agglutinin as a specific marker for perineuronal nets (PNN), an antibody against-aggrecan and a hyaluronic acid binding protein. PrPres accumulation and glial cell activation were detected from the earliest stages of the disease, and they increased at the terminal stage. Otherwise, only at the terminal stage, a decrease of the PNN, aggrecan, and an alteration of hyaluronic acid were observed and correlated with the distribution of activated glial cells and PrPres accumulation. This study suggests that the loss of PNNs, aggrecan and hyaluronic acid should be considered a consequence of PrPres accumulation, which activates glial cells and the secretion of degradative enzymes, which in turn would digest the ECM.

Key words:

Transmissible spongiform encephalopathy / aggrecan / hyaluronic acid / perineuronal nets / prion disease / bovine spongiform encephalopathy

1.- INTRODUCTION

Transmissible spongiform encephalopathies (TSEs) or prion diseases are a group of neurodegenerative disorders of sporadic, genetic or infectious origin (1). This group of diseases includes bovine spongiform encephalopathy (BSE) in cattle, scrapie in sheep and goat (2), chronic wasting disease in wild ruminants (3, 4), and Creutzfeldt-Jakob disease, Gerstmann-Sträussler-Scheinker disease, kuru and fatal familial insomnia in humans (5, 6, 7, 8, 9).

TSEs are characterized by the conversion of the normal prion protein (PrPc) into the resistant prion protein (PrPres), an abnormally folded isoform of the PrPc (10). PrPres is considered to be the only component of the infectious agent responsible for the TSEs transmissibility (11, 12). Its accumulation in the brain induces neuronal loss, spongiform degeneration and glial cell proliferation (1, 10), which are the classical pathological hallmarks of TSEs.

The extracellular matrix (ECM) of central nervous system (CNS) is a mixture of macromolecules which can be dispersed in the neuropil or which can form aggregates called perineuronal nets (PNN). The PNNs are a specialized form of ECM which envelope the neuronal pericaria, dendrites and proximal part of the axons from specific neuronal subpopulations (13, 14, 15), and which contribute to creating a specialized microenvironment around them (16, 17, 18, 19). In human TSEs, the neuronal loss has been related with the disturbance or disappearance of the PNNs of the ECM surrounding neurons before their death (20, 21, 22).

PNNs are mainly composed of multiple chondroitin-sulphate proteoglycans (CSPG), hyaluronic acid (HA) and tenascin-R. The most important CSPGs of the PNN belong to the lectican family, which is composed of four members: aggrecan, neurocan, brevican and versican (14). Aggrecan is the most abundant lectican in the adult brain and its glycoforms are partially responsible for the heterogeneity of PNNs (23, 24). HA is a non-sulphated polysaccharide lacking covalent bonds to any protein. It is known to interact with lecticans, other extracellular and transmembrane proteins, and intracellular receptors (25, 26). Electron microscopy studies have demonstrated that HA-aggrecan cross-links tenascin-R (27) complexes, resulting in a net-like ternary complex that gives rise to the PNNs (14).

Several studies have shown that PrPres induces proliferation and activation of astrocytes and microglia (28, 29, 30). Upon activation, these glial cells produce and secrete several enzymes to the extracellular space, such as metalloproteases and hyaluronidases (31, 32), which digest ECM components, inducing PNNs loss.

In the present study a transgenic mouse line overexpressing the bovine PrPc (boTg110) (33) has been used to study the ECM disturbances that take place during BSE infection, with special attention paid to specific ECM components such as aggrecan and HA, and their correlations with PrPres deposition and glial activation.

2. MATERIAL AND METHODS

2.1.- Animals and general procedures

The study was developed in the transgenic mouse line boTg110 which was established as previously described (33). These mice express bovine PrPc under the murine prnp promoter in a murine PrP0/0 background. Bovine PrPc expression levels in this mouse line are 8 times higher than the PrPc levels found in cattle brain homogenates. The characteristics of these transgenic mice, the susceptibility to different prion strain and the incubation time following BSE inoculation, as well as the behavioral and neuropathological findings in inoculated mice, have been described in detail elsewhere (33, 34, 35).

For BSE infection, boTg110 mice (6-7 weeks old) were inoculated in the right parietal lobe using a 25 gauge disposable hypodermic needle with 20¤l of 10% brain homogenate (TSE/08/59 inoculum). The TSE/08/59 inoculum was obtained from a pool from the brainstem of 49 BSE infected cattle and supplied by Veterinary Laboratory Agency (New Haw, Addlestone, Surrey, UK). The procedure was carried out at CISA-INIA (Madrid, Spain).

All mice were maintained under identical environmental conditions and received food and water ad libitum. To evaluate the clinical signs appearing after inoculation, mice were observed daily and their neurological status was assessed twice a week. The presence of three signs of neurological dysfunction, using ten different items (10, 36), was necessary for a mouse to score positive for prion disease.

A brain PrPres deposition kinetic in these mice was previously reported. (33). Out of this kinetic, two different stages in the disease progression were used for the present study: one group of mice were sacrificed early in the incubation period, at 150 days post inoculation (dpi) (n=4), when the first deposits of PrPres are detected but clinical sing are not observed yet; and a second group was terminally ill mice with evident clinical signs, between 290 and 320dpi (n=8). Uninoculated age-matched control animals were also included: 150dpi (n=4) and 285-350 dpi (n=6).

Mice were culled following the recommendations and approval of the ethics committee. Necropsy was carried out; brains were immediately removed from the skull and fixed by immersion in 10% buffered formalin. The brains were cut in coronal sections at the level of the optic chiasm, piriform cortex and medulla oblongata. Samples were dehydrated by increasing alcohol concentrations, and then embedded in xylene and paraffin. Four-micrometer sections were obtained and haematoxylin-eosin stained for morphological evaluation, while further sections were mounted on 3-trietoxysilil-propilamine coated glass slides for histochemical and immunohistochemical studies.

2.2.- Histochemistry and immunohistochemistry

2.2.1.- Prion Protein

Immunohistochemistry against PrPres was performed as previously described (37). Briefly, sections were immersed in formic acid and boiled at low pH in a pressure cooker, and endogenous peroxidase activity was blocked with 2% hydroxide peroxide in PBS. After pre-treatment with proteinase K, the sections were incubated overnight with the anti-PrP mAb 6H4 as the primary antibody (1:2000, kindly provided by Prionics AG), and finally, developed using DAKO EnVision system and 3,3'diaminobenzidine as chromogen.

2.2.2- Glial cell markers

Heat-induced epitope retrieval with citrate buffer (pH 6.0) was the pre-treatment used before endogenous peroxidase activity was blocked by incubating the sections for 20 minutes with 2% hydrogen peroxide in PBS. Non-specific protein binding was blocked with 2% bovine albumin in PBS (blocking solution) for 1 hour at room temperature. For astrocyte labelling, the sections were incubated overnight at 4ºC with rabbit polyclonal antibody against glial fibrillary acidic protein (GFAP) (Dakocytomation, Barcelona Spain) at dilution 1:500. The antibody binding was visualized with DAKO EnVision Plus System anti-rabbit, and 3,3'diaminobenzidine as the chromogen substrate (Dakocytomation, Barcelona Spain).

Microglial cells were marked with the biotinylated lectin Licopersicon esculentum (LEA) (Sigma, Madrid, Spain), used at dilution 1:200 and incubated overnight at room temperature. The washing buffer was supplemented with 0.75 mM $CaCl_2$, 1mM $MgCl_2 \cdot 6H_2O$ and 1mM $MnCl_2 \cdot 4H_2O$. Finally, the binding was visualized with the avidin-biotin-peroxidase complex (ImmunoPure ABC Peroxidase Staining Kits, Pierce, Madrid, Spain) and developed with 3,3'diaminobenzidine. Omission of the primary antibody or lectin was used as a background control.

2.2.3.- Double immunostaining of GFAP and extracellular matrix

Sections were deparaffinised and rehydrated. Sections for aggrecan detection were pre-treated with 0.5 U/ml of chondroitinase ABC (Sigma, Madrid, Spain) diluted in a buffer containing 16.5 mM Tris and 16.5 mM sodium acetate, for 4 hours at 37ºC. Non-specific protein binding was blocked with 2% bovine albumin in PBS for 1 hour at room temperature. All sections were incubated overnight at 4ºC with mouse anti-GFAP marked with Cy3 (Sigma, Madrid, Spain) diluted 1:200, and at the same time with rabbit anti-aggrecan polyclonal antibody (Chemicon International Inc., Madrid, Spain) diluted 1:400, biotinylated Hyaluronic Acid Binding Protein (HABP) (Seikagaku Corporation, Tokyo, Japan) diluted 1:100, or biotinylated lectin Wisteria floribunda (WFA) (Vector Laboratories, Barcelona, Spain) diluted 1:200. All antibodies and affinity reagents were diluted in blocking solution. Aggrecan sections were incubated with the secondary antibody goat anti-rabbit biotinylated IgG (Dakocytomation, Barcelona, Spain) diluted 1:200 in blocking solution at room temperature. Streptavidin-FITC (Sigma, Madrid, Spain) was applied to all sections for 1 hour diluted at 1:200, in order to visualize the anti-aggrecan antibody, WFA and HABP.

Several controls were included in the experiments. As a background control the primary antibody incubation was omitted. The specificity of anti-aggrecan antibody was confirmed by omitting the digestion step with chondroitinase ABC. The WFA signalling specificity was assessed by digesting the sections with 0.5 U/ml chondroitinase ABC for 4h at 37ºC.

The specificity of hyaluronic acid binding protein signalling was demonstrated by digesting sections with 10 U/ml hyaluronidase from Streptomyces hyalurolyticus (Sigma, Madrid, Spain) for 1 hour at 37ºC and also by incubating sections with the biotinylated hyaluronic acid binding protein previously blocked with 100 µg/ml HA (Sigma, Madrid, Spain). No signal was observed in any of the control slides.

3.- RESULTS

3.1.- PrPres immunohistochemistry

In BSE-inoculated BoTg110 mice, positive immunostaining against PrPres was first detected at 150 dpi in all the examined animals; the mark was observed as a mild punctuated pattern in the neuropil around lateral ventricles of diencephalon, mesencephalon, pons, medulla oblongata and deep cerebellar nuclei. In the terminal group (290-320dpi), the PrPres deposition was much more intense in the periventricular areas of the diencephalon, brain stem and cerebellar nuclei, where not only were a punctuated neuropil and plaque-like structures observed (Figure 1), but also intraneuronal and glial staining. Moderate immunoreactivity was observed in hippocampus and caudate nuclei, and mild punctuated immunostaining was observed in the neocortex, mainly in the deepest cortical layers. In control animals no immunostaining against PrPres was observed at any time.

3.2.- Glial response

A generalized increase of the Glial Fibrillary Acidic Protein (GFAP) immunostained astrocytes was observed in the brains of both BSE-infected groups of mice but never in their corresponding uninoculated control mice. At the earliest stages of the disease, 150 dpi, the increase in GFAP-positive astrocytes was observed in thalamus, mesencephalon, pons, medulla oblongata and deep cerebellar nuclei. The GFAP immunostaining was increased at terminal stage, associated with the increased number and hypertrophy of astrocytes (Figure 1). The immunolabelling was mainly located in the brain stem, hippocampus and cerebellar cortex; and it was slightly observed in the caudate nuclei and the deepest layers of the neocortex.

Similarly, LEA histochemistry showed moderate staining of activated microglia in 150 dpi infected animals, located at brain stem, deep cerebellar nuclei and cerebellar cortex. The reactive microglia increased during the disease and was also observed in other locations such as hippocampus, deeper layers of the neocortex and caudate nuclei at the terminal stage (Figure 1). In control animals only a few scattered cells were observed labelled with LEA.

Distribution of reactive astrocytes and activated microglia showed correlation with the PrPres deposition.

3.3.- Double histochemistry of perineuronal nets, aggrecan, hyaluronic acid and GFAP

PNNs were specifically marked with WFA (38), a lectin that recognises N-acetylgalactosamine found in the glycosaminoglycan chains of CSPGs (39).

No significant differences in the PNNs and neuropil staining were observed in the BSE infected mice when compared to their controls at 150 dpi. At the terminal stage of the disease, BSE-infected mice showed a dramatic loss of PNN in the whole brain, showing a direct relationship with the presence of reactive astrocytosis. The loss was especially intense in thalamus, mesencephalon, pons, medulla oblongata and deep

cerebellar nuclei, where GFAP immunostaining was higher (Figure 3 and 4). It was less severe in CA2 of hippocampus and neocortex (Figure 3); in layer I of the piriform lobe, a mild decrease in the neuropil staining was also observed, in which less reactive astrocytes were observed. In contrast, the group of control mice showed intense well-preserved staining of the PNN and neuropil, similar to the staining seen in the other groups of controls.

In spite of the intense affectation of the PNNs, they were partially preserved in some areas such as neocortex, although these had a less compacted appearance and a decrease in the intensity of labelling around the proximal portion of neurites.

Since aggrecan and HA are the main components of the PNNs, the next step was to analyze whether any particular component of these structures was responsible for their disappearance.

As observed with WFA, the anti-aggrecan antibody visualized well structured-PNNs in 150 dpi BSE-infected mice when compared to their age-matched control group. At the terminal stage, the BSE-infected animals showed a dramatic loss of aggrecan immunostaining in the PNNs (Figures 3 and 4), at the same locations observed with WFA, which also showed the greatest increase of astrocytes marked with GFAP. Only a few PNNs were preserved but these showed a more diffuse and less intense staining, as well as a loss of marking around neurites.

Regarding HA, no differences in the staining of PNNs and the neuropil were observed in BSE-infected mice when compared to their controls at the beginning (150 dpi) of the disease. In the terminal stage group, BSE-infected mice, when compared to their controls, showed a moderate decrease of HA surrounding neurons, mainly in the thalamus, mesencephalon, pons, medulla oblongata and deep cerebellar nuclei (Figures 3 and 4). In other areas such as hippocampus and neocortex, the loss of PNNs was even slighter (Figures 3 and 4). The preserved PNNs showed a more diffuse HA staining than those observed in control mice and the marking was easily confused with the neuropil.

Although HA staining was considerably less affected than WFA and aggrecan, it was also clear in this case that the areas with more intense GFAP immunostaining also showed more evident changes in the HA content of the PNNs and the neuropil

4.- DISCUSSION

In the present study, a dramatic loss of PNNs has been shown at the terminal stages of the disease in the boTg 110 mouse model expressing bovine PrPc and inoculated with a brain homogenate from BSE-affected cattle. It has also been described by the first time that the PNN loss is due to a total loss of aggrecan and a partial loss and disorganization of HA, two important components of the PNNs, and that this process happens after PrPres deposition and chronic glial activation.

Two previous studies have described the disappearance of PNNs in several human spongiform encephalopathies, such as Creutzfeldt-Jacob disease (20), Gerstmann-Sträussler-Scheinker disease, Fatal Familial Insomnia and Kuru (21), as a morphological sign of disturbed brain integrity. As a conclusion of these findings, where tissues coming from terminally ill human autopsy cases were used, it was proposed that PNN loss precedes the deposition of PrPres and the retraction of synapses from their surface, finally leading to neuronal death (20, 21). Nevertheless, the use of autopsy cases hampered a more detailed study of the kinetics of both processes. Furthermore, in a more recent study developed in cattle BSE field cases without detectable clinical sings, the PNNs were not noticeably altered, although PrPres deposition was detected (40).

In the present work, we have used the transgenic mouse line boTg110 as a model of BSE infection, which has been previously characterized (33). In the present work, this characterization has been extended by showing that it responds to PrPres deposition with a progressive increase of astroglia and microglia, as it would be expected in any TSE.

Two time points in the progression of the disease were chosen: an early-stage of the disease, 150 dpi, with no clinical signs but already with a consistent presence of PrPres deposition and moderate glial activation; and a terminal-stage of the disease, 290-320dpi, with remarkable clinical signs, PrPres deposition and glial activation. Both time points would allow analyzing the relationship betwen PrPres deposition and ECM disorganization. The present study shows that in the early-stage of the disease, not only the PNNs, but also their components, aggrecan and HA, were still intact. Well preserved PNNs had been similarly described in cattle BSE field cases without detectable clinical sings (40). In both cases, well preserved PNNs were observed surrounding neurons with PrPres deposition or even around vacuolated neurons. In the late-stage of the disease, an almost complete loss of the PNNs was observed, similar to that described in humans autopsy cases (20, 21). Concomitantly to the PNNs loss, a marked loss of aggrecan and a partial loss and disorganization of HA have been showed, all of them correlated with an intense PrPres deposition and glial cell activation.

So the present study has shown that the previous observations in human TSEs (20, 21) and cattle BSE field cases (40) which could seem contradictories, reflect different moments in the evolutions of the TSEs pathogeny. The findings observed in mice at early stage of the disease were equivalent to the findings observed in cattle BSE field

cases; and the observations from the late-stage group of mice were comparable to the features described in human TSEs.

From the molecular point of view we have observed that aggrecan almost disappears during the BSE progression and HA also suffers important alterations. Since both of them are main components of the PNN in the adult SNC (14, 41, 42), their lack or impairment are probably responsible of the PNN disassembly.

Regarding the mechanism, more data are actually needed, but our results indicate that PrPres deposition and gliosis precede PNN and aggrecan loss and HA alterations thus supporting the hypothesis that PrPres accumulation triggers the activation of glial cells (28, 29, 30), which would be responsible for the degradation of the ECM around neurons (31, 32). Furthermore, we have observed a relationship between the loss of PNNs and their components, and the presence of GFAP-positive astrocytes and microglia. Thus, in areas with major glial activation the loss of PNNs was almost complete (thalamus, mesencephalon, pons, medulla oblongata and deep cerebellar nuclei), whereas in areas where the number of microglial cells and GFAP-marked astrocytes was lower, as well as PrPres deposition, some PNNs and their components were still preserved (hippocampus and neocortex). In this regard, in vitro studies have reported that, during the progression of BSE, PrPres deposition activates neurons and astrocytes (29, 30), thus promoting microglia recruitment (28). Activated astrocytes and microglia have been shown to produce metalloproteases, which might be the responsible for the degradation of the PNN components, such as aggrecan and others (31). Similar features have been showed in other chronic inflammatory encephalitis, like human immunodeficiency virus infection and in macaques after experimental lentiviral infection, and in prion disease Creutzfeldt-Jacob disease (20, 43, 44). Regarding the polysaccharide HA, our results are in accordance with those reported by (45), who described a reduction in the amount of HA in the brain stem of BSE-infected cattle using HPLC analysis. It is possible that an increase in hyaluronidase activity, similar to that described in stroke-affected tissue (46), would be responsible for the loss of HA.

The PNNs and their components play an important role in the maintenance of the homeostasis in the extracellular space of the CNS. They are highly hydrophilic and can bind cations, acting as a buffer in the extracellular space (15, 16, 18). According to that, their loss or alteration can modify the microenvironment around neurons, and lead to neuronal dysfunctions and even death. Otherwise, it is also well reported that aggrecan play an important role in the formation and maintenance of the synapses in the maturation of the CNS (19), so its loss can play an important role in the loss of synaptic buttons and the synaptic retraction which has been previously described (47, 48, 49).

In summary, this study has showed that PrPres accumulation starts before the loss of the PNNs and their components: aggrecan and HA. So, we suggest that the loss of aggrecan, HA and the PNNs is a late change in BSE progression and should be mainly considered as a consequence of the process initiated by PrPres deposition, which activates glial cells and the secretion of degradative enzymes, which in turn digest

the ECM. The results also suggest that these loss of ECM components lead to an alteration of the extracellular space homeostasis, altering the neuronal function and the synaptic stability which in turn could lead to the neuronal death.

ACKNOWLEDGMENTS

The authors wish to acknowledge the excellent technical assistance of Maria Sierra Espinar and Marta Valle of the Priocat Laboratory, CReSA. We also thank Tom Yohannan for editorial help. This study has been financially supported by the Spanish Ministerio de Ciencia y Tecnología (Grant ref. EET2002-05168-C04). C.C. was supported by a fellowship from the Universitat Autònoma de Barcelona, R.T. was supported by a fellowship attached to the grant EET2002-05168-C04-01 (to M.P.) from the Ministerio de Ciencia y Tecnología, and D.P. was supported by the Programme Alban, the European Union Programme of High Level Scholarships for Latin America, scholarship no. E05D056378CL.

FIGURES

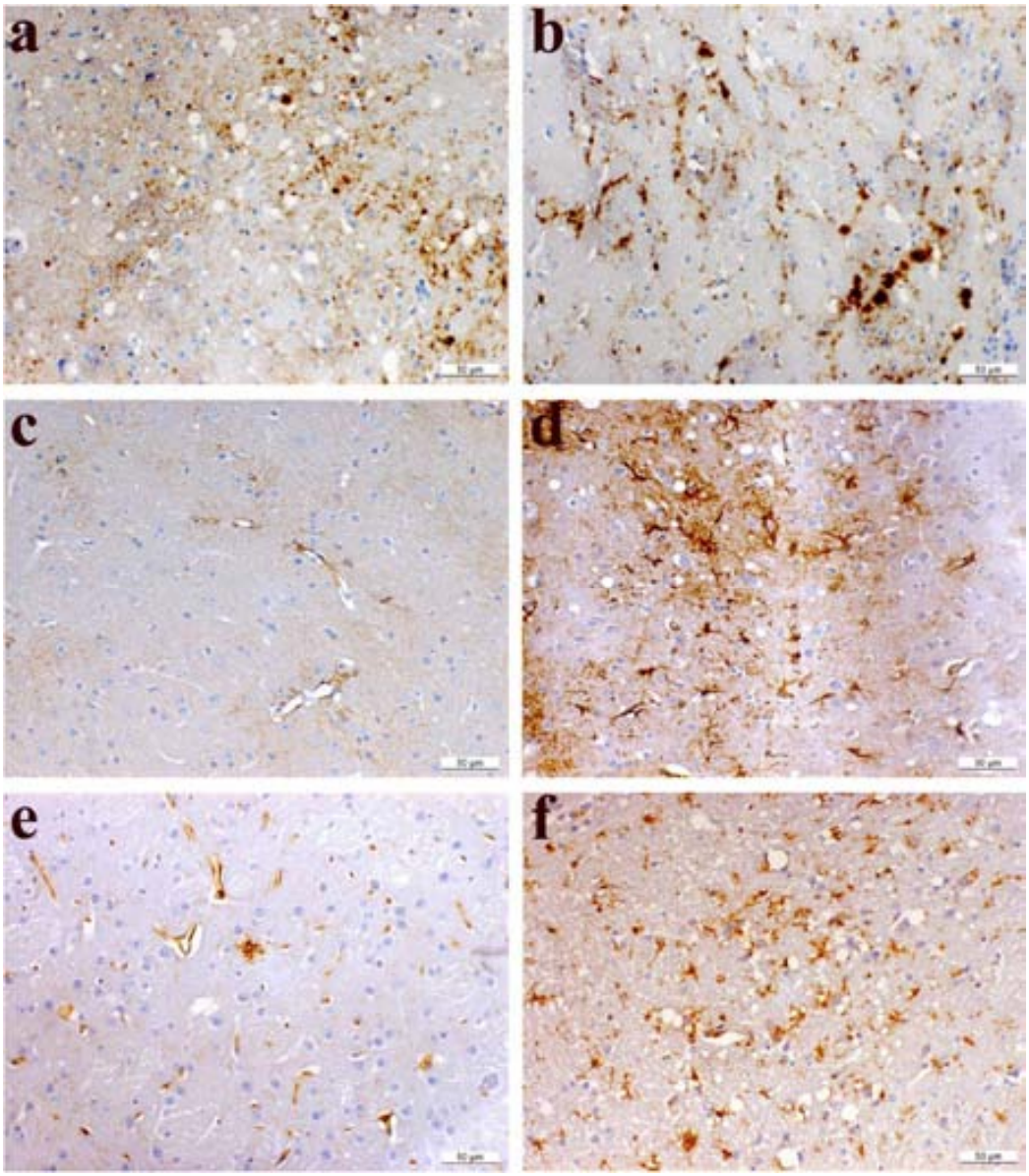

Figure 1: Immunohistochemistry of PrPres (a, b) and GFAP (c, d), and histochemistry of LEA (e, f) in brain from both control (c, e) and BSE-inoculated mice (a, b, d, f) of the terminal group (290-320 dpi). Note the punctuated pattern in the neuropil of thalamus (a) and plaque-like deposits in medulla oblongata (b) of a BSE-infected mouse. A marked increase of the GFAP immunostaining is observed in medulla oblongata of BSE-inoculated mice (d) in comparison to uninoculated control mice (c). Microglia cells marked with LEA are increased in thalamus from BSE-infected (f) mouse when compared to those from control animals (e). Scale bar 50 µm.

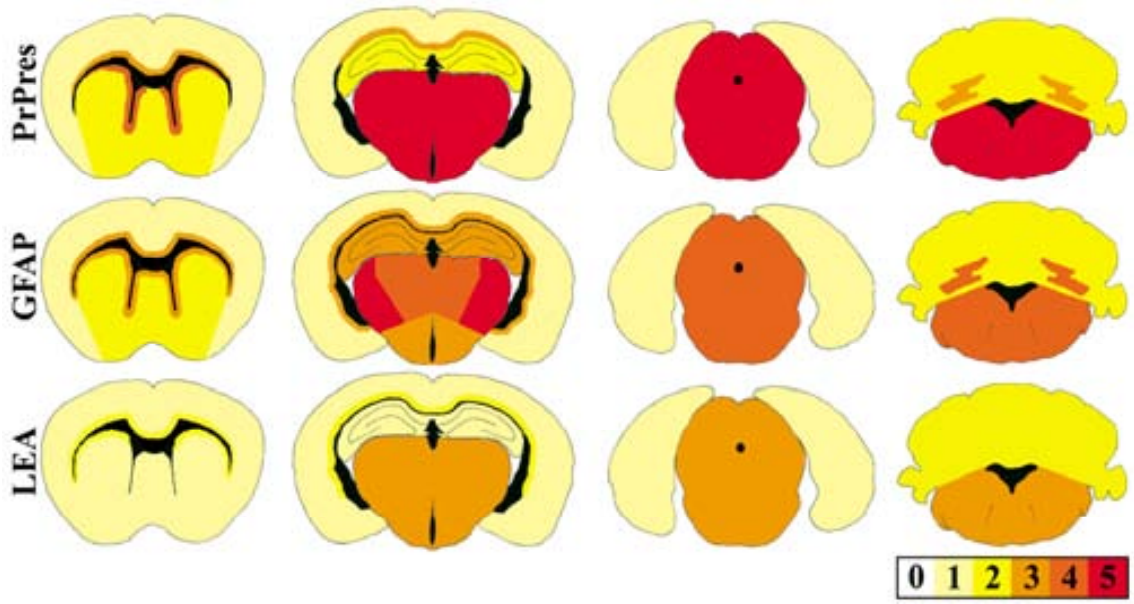

Figure 2: Schematic representation of the different brain sections studied. An overall evaluation of PrPres, GFAP and LEA staining at terminal stage of the disease in BSE-inoculated boTg110 mice.

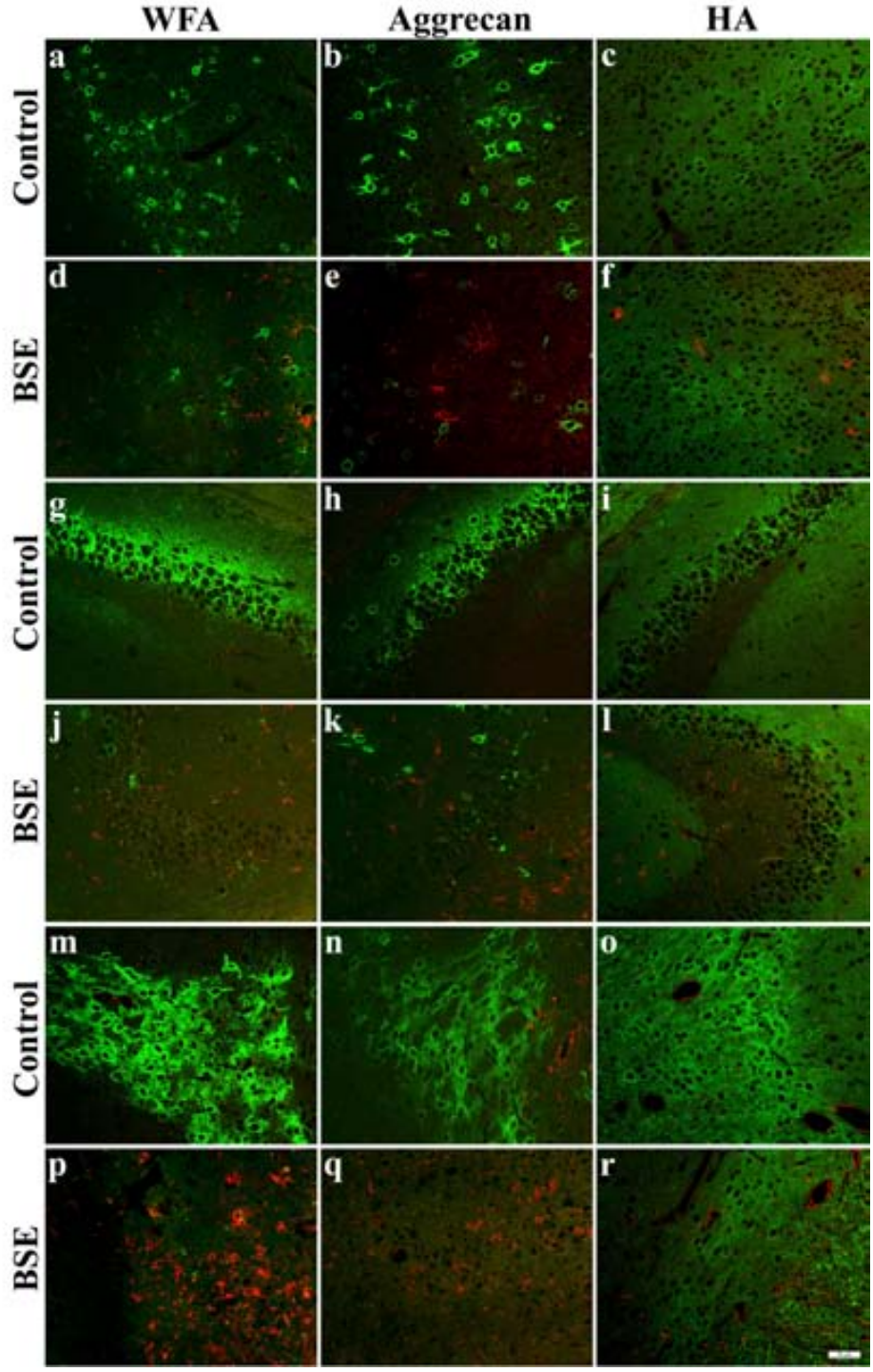

Figure 3: Double staining of GFAP (red) and WFA (green) (a, d, g, j, m, p), aggrecan (green) (b, e, h, k, n, q) and HA (green) (c, f, i, l, o, r) in neocortex (a, b, c, d, e, f), hippocampus (g, h, i, j, k, l) and reticular thalamic nuclei (m, n, o, p, q, r). Note the decrease of the intensity in the extracellular matrix markers (green) and the increase of GFAP (red) observed in terminal group of infected mice (d, e, f, j, k, l, p, q, r) when compared to the corresponding control mouse group (a, b, c, g, h, i, m, n, o). Scale bar 50 µm.

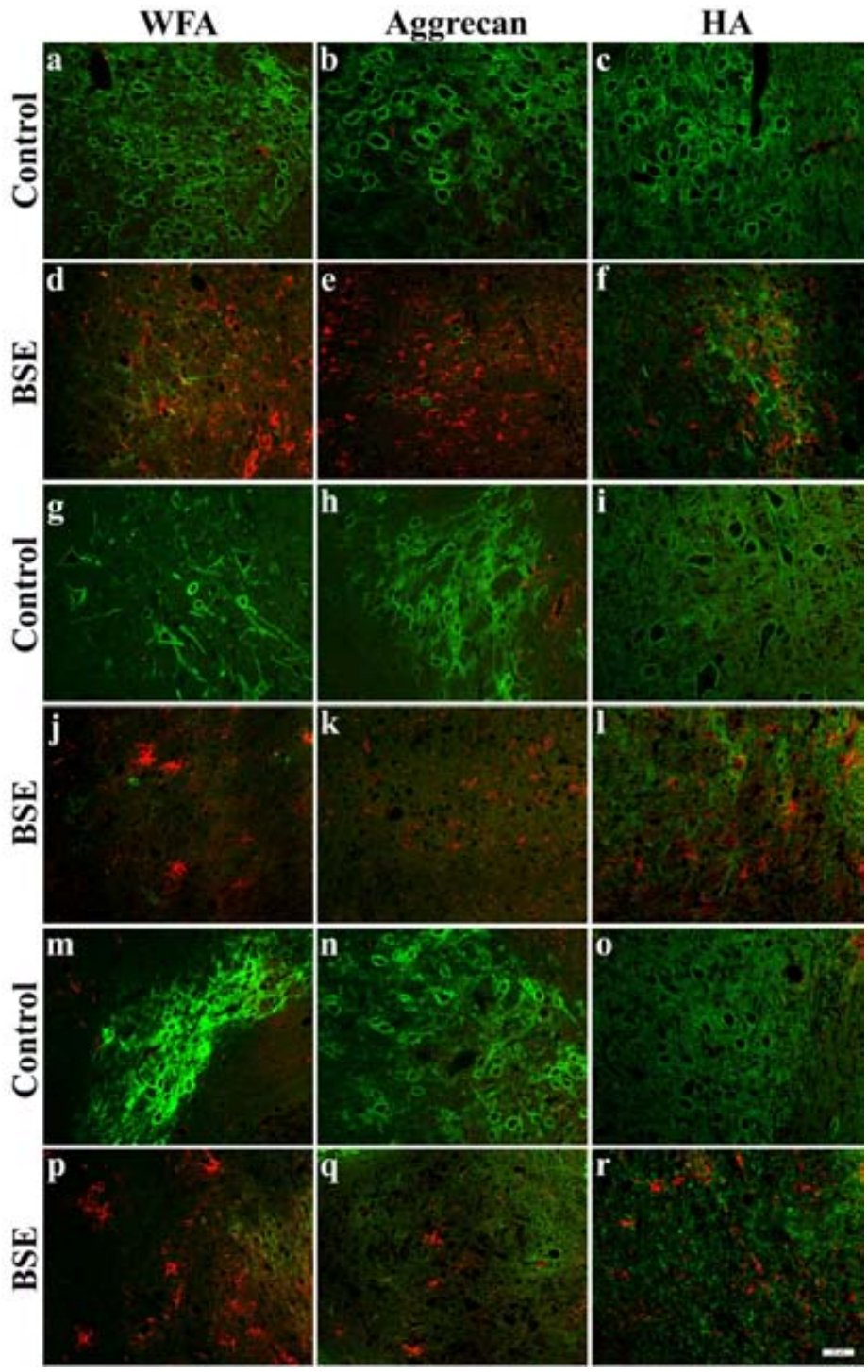

Figure 4: Double staining of GFAP (red) and WFA (green) (a, d, g, j, m, p), aggrecan (green) (b, e, h, k, n, q) and HA (green) (c, f, i, l, o, r) in mesencephalon (a, b, c, d, e, f), medulla oblongata (g, h, i, j, k, l) and deep cerebellar nuclei (m, n, o, p, q, r). Note the decrease of the intensity in the extracellular matrix markers (green) and the increase of GFAP (red) when control (a, b, c, g, h, i, m, n, o) and BSE-inoculated mice (d, e, f, j, k, l, p, q, r) of the terminal group are compared. Scale bar 50 µm.

REFERENCES

1. Prusiner S B. The prion diseases. Brain Pathol. (1998) 8: 499-513.
2. Hadlow W J, Eklund C M. Scrapie--a virus-induced chronic encephalopathy of sheep. Res Publ Assoc Res Nerv Ment Dis. (1968) 44: 281-306.
3. Barlow R M. Transmissible mink encephalopathy: pathogenesis and nature of the aetiological agent. J Clin Pathol Suppl (R Coll Pathol). (1972) 6: 102-9.
4. Williams E S, Young S. Chronic wasting disease of captive mule deer: a spongiform encephalopathy. J Wildl Dis. (1980) 16: 89-98.
5. Creutzfeldt H G. On a particular focal disease of the central nervous system (preliminary communication), 1920. Alzheimer Dis Assoc Disord. (1989) 3: 3-25.
6. Zigas V, Gajdusek D C. Kuru: clinical study of a new syndrome resembling paralysis agitans in natives of the Eastern Highlands of Australian New Guinea. Med J Aust. (1957) 44: 745-54.
7. Gajdusek D C, Zigas V. Degenerative disease of the central nervous system in New Guinea; the endemic occurrence of kuru in the native population. N Engl J Med. (1957) 257: 974-8.
8. Jakob A. Concerning a disorder of the central nervous system clinically resembling multiple sclerosis with remarkable anatomic findings (spastic pseudosclerosis). Report of a fourth case. Alzheimer Dis Assoc Disord. (1989) 3: 26-45.
9. Lugaresi E, Medori R, Montagna P, Baruzzi A, Cortelli P, Lugaresi A, Tinuper P, Zucconi M, Gambetti P. Fatal familial insomnia and dysautonomia with selective degeneration of thalamic nuclei. N Engl J Med. (1986) 315: 997-1003.
10. Scott M, Foster D, Mirenda C, Serban D, Coufal F, Walchli M, Torchia M, Groth D, Carlson G, DeArmond S J, et al. Transgenic mice expressing hamster prion protein produce species-specific scrapie infectivity and amyloid plaques. Cell. (1989) 59: 847-57.
11. Prusiner S B. Novel proteinaceous infectious particles cause scrapie. Science. (1982) 216: 136-44.
12. Legname G, Baskakov I V, Nguyen H O, Riesner D, Cohen F E, DeArmond S J, Prusiner S B. Synthetic mammalian prions. Science. (2004) 305: 673-6.
13. Celio M R, Blumcke I. Perineuronal nets--a specialized form of extracellular matrix in the adult nervous system. Brain Res Brain Res Rev. (1994) 19: 128-45.
14. Yamaguchi Y. Lecticans: organizers of the brain extracellular matrix. Cell Mol Life Sci. (2000) 57: 276-89.
15. Bruckner G, Szeoke S, Pavlica S, Grosche J, Kacza J. Axon initial segment ensheathed by extracellular matrix in perineuronal nets. Neuroscience. (2006) 138: 365-75.
16. Bruckner G, Brauer K, Hartig W, Wolff J R, Rickmann M J, Derouiche A, Delpech B, Girard N, Oertel W H, Reichenbach A. Perineuronal nets provide a polyanionic, glia-associated form of microenvironment around certain neurons in many parts of the rat brain. Glia. (1993) 8: 183-200.
17. Bruckner G, Hartig W, Kacza J, Seeger J, Welt K, Brauer K. Extracellular matrix organization in various regions of rat brain grey matter. J Neurocytol. (1996) 25: 333-46.
18. Hartig W, Derouiche A, Welt K, Brauer K, Grosche J, Mader M, Reichenbach A, Bruckner G. Cortical neurons immunoreactive for the potassium channel Kv3.1b subunit are predominantly surrounded by perineuronal nets presumed as a buffering system for cations. Brain Res. (1999) 842: 15-29.
19. Hockfield S, Kalb R G, Zaremba S, Fryer H. Expression of neural proteoglycans correlates with the acquisition of mature neuronal properties in the mammalian brain. Cold Spring Harb Symp Quant Biol. (1990) 55: 505-14.
20. Belichenko P V, Miklossy J, Belser B, Budka H, Celio M R. Early destruction of the extracellular matrix around parvalbumin-immunoreactive interneurons in Creutzfeldt-Jakob disease. Neurobiol Dis. (1999) 6: 269-79.
21. Guentchev M, Wanschitz J, Voigtlander T, Flicker H, Budka H. Selective neuronal vulnerability in human prion diseases. Fatal familial insomnia differs from other types of prion diseases. Am J Pathol. (1999) 155: 1453-7.

22. Guentchev M, Groschup M H, Kordek R, Liberski P P, Budka H. Severe, early and selective loss of a subpopulation of GABAergic inhibitory neurons in experimental transmissible spongiform encephalopathies. Brain Pathol. (1998) 8: 615-23.

23. Fryer H J, Kelly G M, Molinaro L, Hockfield S. The high molecular weight Cat-301 chondroitin sulfate proteoglycan from brain is related to the large aggregating proteoglycan from cartilage, aggrecan. J Biol Chem. (1992) 267: 9874-83.

24. Matthews R T, Kelly G M, Zerillo C A, Gray G, Tiemeyer M, Hockfield S. Aggrecan glycoforms contribute to the molecular heterogeneity of perineuronal nets. J Neurosci. (2002) 22: 7536-47.

25. Bignami A, Asher R, Perides G. Co-localization of hyaluronic acid and chondroitin sulfate proteoglycan in rat cerebral cortex. Brain Res. (1992) 579: 173-7.

26. Bignami A, Asher R. Some observations on the localization of hyaluronic acid in adult, newborn and embryonal rat brain. Int J Dev Neurosci. (1992) 10: 45-57.

27. Lundell A, Olin A I, Morgelin M, al-Karadaghi S, Aspberg A, Logan D T. Structural basis for interactions between tenascins and lectican C-type lectin domains: evidence for a crosslinking role for tenascins. Structure. (2004) 12: 1495-506.

28. Marella M, Chabry J. Neurons and astrocytes respond to prion infection by inducing microglia recruitment. J Neurosci. (2004) 24: 620-7.

29. Hafiz F B, Brown D R. A model for the mechanism of astrogliosis in prion disease. Mol Cell Neurosci. (2000) 16: 221-32.

30. Brown D R, Schmidt B, Kretzschmar H A. A prion protein fragment primes type 1 astrocytes to proliferation signals from microglia. Neurobiol Dis. (1998) 4: 410-22.

31. Gottschall P E, Deb S. Regulation of matrix metalloproteinase expressions in astrocytes, microglia and neurons. Neuroimmunomodulation. (1996) 3: 69-75.

32. Stern R. Devising a pathway for hyaluronan catabolism: are we there yet? Glycobiology. (2003) 13: 105R-15R.

33. Castilla J, Gutierrez Adan A, Brun A, Pintado B, Ramirez M A, Parra B, Doyle D, Rogers M, Salguero F J, Sanchez C, Sanchez-Vizcaino J M, Torres J M. Early detection of PrPres in BSE-infected bovine PrP transgenic mice. Arch Virol. (2003) 148: 677-91.

34. Castilla J, Brun A, Diaz-San Segundo F, Salguero F J, Gutierrez-Adan A, Pintado B, Ramirez M A, del Riego L, Torres J M. Vertical transmission of bovine spongiform encephalopathy prions evaluated in a transgenic mouse model. J Virol. (2005) 79: 8665-8.

35. Espinosa J C, Andreoletti O, Castilla J, Herva M E, Morales M, Alamillo E, San-Segundo F D, Lacroux C, Lugan S, Salguero F J, Langeveld J, Torres J M. Sheep-passaged bovine spongiform encephalopathy agent exhibits altered pathobiological properties in bovine-PrP transgenic mice. J Virol. (2007) 81: 835-43.

36. Scott M, Groth D, Foster D, Torchia M, Yang S L, DeArmond S J, Prusiner S B. Propagation of prions with artificial properties in transgenic mice expressing chimeric PrP genes. Cell. (1993) 73: 979-88.

37. Siso S, Ordonez M, Cordon I, Vidal E, Pumarola M. Distribution of PrP(res) in the brains of BSE-affected cows detected by active surveillance in Catalonia, Spain. Vet Rec. (2004) 155: 524-5.

38. Hartig W, Brauer K, Bruckner G. Wisteria floribunda agglutinin-labelled nets surround parvalbumin-containing neurons. Neuroreport. (1992) 3: 869-72.

39. Murakami T, Ohtsuka A, Su W D, Taguchi T, Oohashi T, Abe K, Ninomiya Y. The extracellular matrix in the mouse brain: its reactions to endo-alpha-N-acetylgalactosaminidase and certain other enzymes. Arch Histol Cytol. (1999) 62: 273-81.

40. Vidal E, Marquez M, Tortosa R, Costa C, Serafin A, Pumarola M. Immunohistochemical approach to the pathogenesis of bovine spongiform encephalopathy in its early stages. J Virol Methods. (2006) 134: 15-29.

41. Milev P, Maurel P, Chiba A, Mevissen M, Popp S, Yamaguchi Y, Margolis R K, Margolis R U. Differential regulation of expression of hyaluronan-binding proteoglycans in developing brain: aggrecan, versican, neurocan, and brevican. Biochem Biophys Res Commun. (1998) 247: 207-12.

42. Sherman L S, Struve J N, Rangwala R, Wallingford N M, Tuohy T M, Kuntz C t. Hyaluronate-based extracellular matrix: keeping glia in their place. Glia. (2002) 38: 93-102.

43. Belichenko P V, Miklossy J, Celio M R. HIV-I induced destruction of neocortical extracellular matrix components in AIDS victims. Neurobiol Dis. (1997) 4: 301-10.

44. Medina-Flores R, Wang G, Bissel S J, Murphey-Corb M, Wiley C A. Destruction of extracellular matrix proteoglycans is pervasive in simian retroviral neuroinfection. Neurobiol Dis. (2004) 16: 604-16.

45. Papakonstantinou E, Karakiulakis G, Roth M, Verghese-Nikolakaki S, Dawson M, Papadopoulos O, Sklaviadis T. Glycosaminoglycan analysis in brain stems from animals infected with the bovine spongiform encephalopathy agent. Arch Biochem Biophys. (1999) 370: 250-7.

46. Al'Qteishat A, Gaffney J, Krupinski J, Rubio F, West D, Kumar S, Kumar P, Mitsios N, Slevin M. Changes in hyaluronan production and metabolism following ischaemic stroke in man. Brain. (2006) 129: 2158-76.

47. Jeffrey M, Fraser J R, Halliday W G, Fowler N, Goodsir C M, Brown D A. Early unsuspected neuron and axon terminal loss in scrapie-infected mice revealed by morphometry and immunocytochemistry. Neuropathol Appl Neurobiol. (1995) 21: 41-9.

48. Bouzamondo-Bernstein E, Hopkins S D, Spilman P, Uyehara-Lock J, Deering C, Safar J, Prusiner S B, Ralston H J, 3rd, DeArmond S J. The neurodegeneration sequence in prion diseases: evidence from functional, morphological and ultrastructural studies of the GABAergic system. J Neuropathol Exp Neurol. (2004) 63: 882-99.

49. Jeffrey M, Halliday W G, Bell J, Johnston A R, MacLeod N K, Ingham C, Sayers A R, Brown D A, Fraser J R. Synapse loss associated with abnormal PrP precedes neuronal degeneration in the scrapie-infected murine hippocampus. Neuropathol Appl Neurobiol. (2000) 26: 41-54.

ANNEX TO STUDY 2

CENTRAL NERVOUS SYSTEM EXTRACELLULAR MATRIX CHANGES IN SCRAPIE-INFECTED MICE

Carme Costa, Enric Vidal, Martí Pumarola, Anna Bassols, Uwe Rauch.

Accepted as a poster in **Neuroprion 2007**.

CENTRAL NERVOUS SYSTEM EXTRACELLULAR MATRIX CHANGES IN SCRAPIE-INFECTED MICE

In this section, we report the results obtained in a preliminary study of several extracellular matrix components of the central nervous system in Scrapie-infected mice. This study was carried out during a 3-month-stage in Uwe Rauch's laboratory, at the Department of Experimental Pathology in the University Hospital of Lund University (Sweden). It was supported by the grant "Ajuts per a estades de curta durada fora de Catalunya de becaris predoctorals del programa de formació d'investigadors de la UAB per a l'any 2005".

ANTECEDENTS

The study was based on two previous works, where the loss of perineuronal nets (PNN) of the extracellular matrix (ECM) in human transmissible spongiform encephalopathies (TSEs) was described. Those studies were carried out in terminal human autopsy cases of Creutzfeldt-Jakob disease (1), and Gerstmann-Sträussler-Scheinker disease, Fatal Familial Insomnia and Kuru (2). The total loss of the PNN related to the deposition of resistant prion protein (PrPres) was described in both of them.

Due to the lack of antecedents in animal TSEs, our objective was to analyse which components of the ECM, especially of the PNN, were affected at terminal stage of Scrapie, using a murine model of the disease. For that purpose, Wisteria floribunda agglutinin (WFA) was used as a general marker of PNN, tenascin-R, brevican and neurocan were detected with specific antibodies, and a neurocan-GFP fusion protein was used as specific marker for hyaluronic acid (HA).

The changes observed in the ECM were correlated with the distribution of reactive astrocytes, as a reference of the degree of the lesion.

MATERIAL AND METHODS

Animals and general procedures

This work was developed in C57BL/6 mice obtained from a previous study published by our group (3). Briefly, C57BL/6 mice were infected intraperitoneally with the RML scrapie strain using a dose of 5 log LD50 (n=3); and control mice were inoculated intraperitoneally with 100 µl of 1% normal CD-1 mouse brain homogenate (mock) (n=2). All the mice were maintained under identical environmental conditions and received food and water ad libitum.

A neurological disease, manifesting as abnormal behavior, restlessness and progressive paraparesis, developed at about 215–230 days post-inoculation (dpi) in scrapie-infected mice. No neurological signs were seen in mock mice.

The mice were killed at 260 dpi, and they were intracardiacally perfused with 4% paraformaldehyde in phosphate buffer. Coronal slabs of their brains were embedded in paraffin, and sections, 5 µm thick, of the cerebrum, cerebellum and brain stem were obtained. Dewaxed sections were stained with haematoxylin and eosin, and processed for immunohistochemistry.

Histochemistry

Double fluorescence histochemical and immunohistochemical procedures were developed as it is described in the STUDY 2. The ECM and astrocyte markers are described in table 1. As a background control the primary antibody was omitted. No signal was observed in any of the control slides.

Marker	Recognize	Dilution
Wisteria floribunda lectin (Vector CNB 1355)	PNN	1:200
Rabbit polyclonal antibody anti-Neurocan (NC2)	Neurocan	1:300
Rabbit polyclonal antibody anti-Tenascin-R	Tenascin-R	1:300
Rabbit polyclonal antibody anti-Brevican	Brevican	1:300
Neurocan-GFP fusion protein (U. Rauch)	HA	1:5
Rabbit polyclonal antibody against glial fibrillary acidic protein (GFAP) (Sigma C-9205, clone G-A-5)	GFAP reactive astrocytes	1:200

Table 1: ECM and astrocyte markers. The antibodies against neurocan, tenascin-R and brevican were kindly provided by U. Rauch.

RESULTS

General neuropathological findings

The histopathological findings, PrPres deposition and glial cell reaction in the CNS of these animals were previously reported by Sisó S, 2002. (3) The main features are summarized in table 2.

	Spongiform degeneration	PrPres	Astrocytosis	Reactive microglia
Cerebral cortex	++	+++	+++	++
Hippocampus	+	+++	+++	++
Thalamus	+++	+++	+++	+++
Pons	+++	+++	+++	+++
Cerebellar cortex	+	+++	+++	+

Table 2: Main neuropathological findings in scrapie-infected mice. Semiquantitative representation of neuropathological findings: +++ marked, ++ moderate, + mild (3).

Extracellular matrix and GFAP double histochemistry

All the markers of the ECM were semiquantitatively assessed in the neocortex, hippocampus, cerebellar cortex, thalamus, mesencephalon and pons. Scrapie infected mice were compared with controls. The ECM changes were correlated with the presence of GFAP- immunostained astrocytes (table 3).

WFA staining showed a marked decrease of the PNNs around neurons in Scrapie infected mice, when compared with their controls. Loss of the PNNs was due to the loss of their components: tenascin-R and brevican, which showed a dramatic decrease too. Otherwise, HA stained with neurocan-GFP fusion protein showed a moderate decrease of the intensity in neuropil and in the PNN, and the preserved PNNs had a more diffuse HA staining. In contrast, neurocan immunostaining showed a generalized increase in the neuropil and in the PNNs (figures 1 and 2).

Changes in the PNNs, tenascin-R, brevican, HA and neurocan were mainly observed in the areas with a major increase of GFAP-immunoreactive astrocytes, as well as a marked PrPres deposition.

	PNN	Tenascin-R	Brevican	HA	Neurocan	GFAP
Neocortex	++	++	++	++	+++	++
Hippocampus	++	++	+	++	+++	++
Thalamus	+	+	+	+	+++	+++
Pons – Medulla Oblongata	+	+	+	+	+++	+++
Cerebellar cortex	++	++	++	++	+++	++

Table 3: Semiquantitative assessment of ECM components and astrocytosis in several brain areas. +++ marked, ++ moderate, + mild.

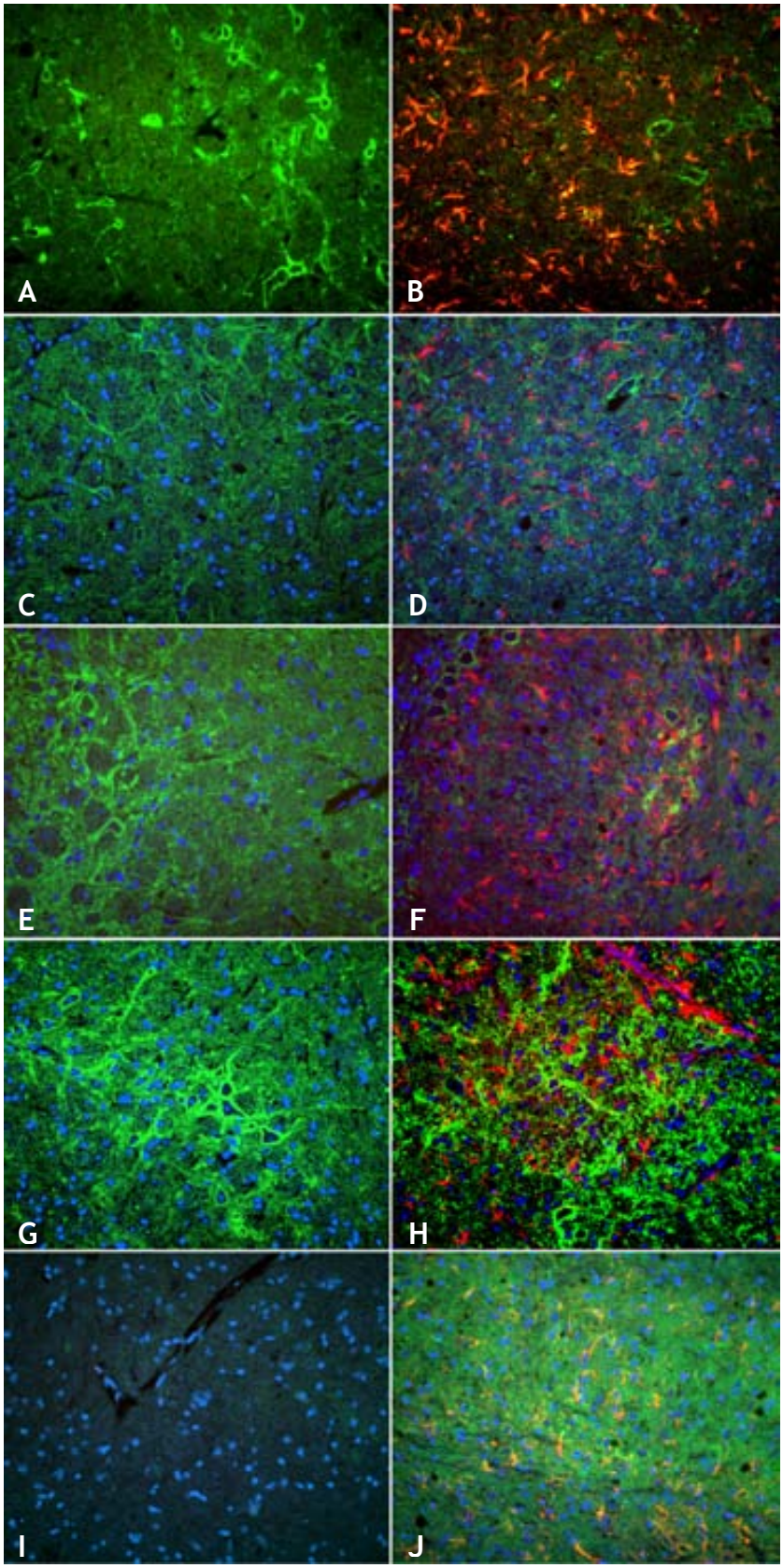

Figure 1: Histochemical staining in pons in control mice (A, C, E, G, I) and Scrapie- infected mice (B, D, F, H, J). PNN stained with WFA (green) (A, B), tenascin-R (green) (C, D), brevican (green) (E, F), HA (green) (G, H) and neurocan (green) (I, J). GFAP- immunostained astrocytes (red). Nuclei were counterstained with DAPI (blue).

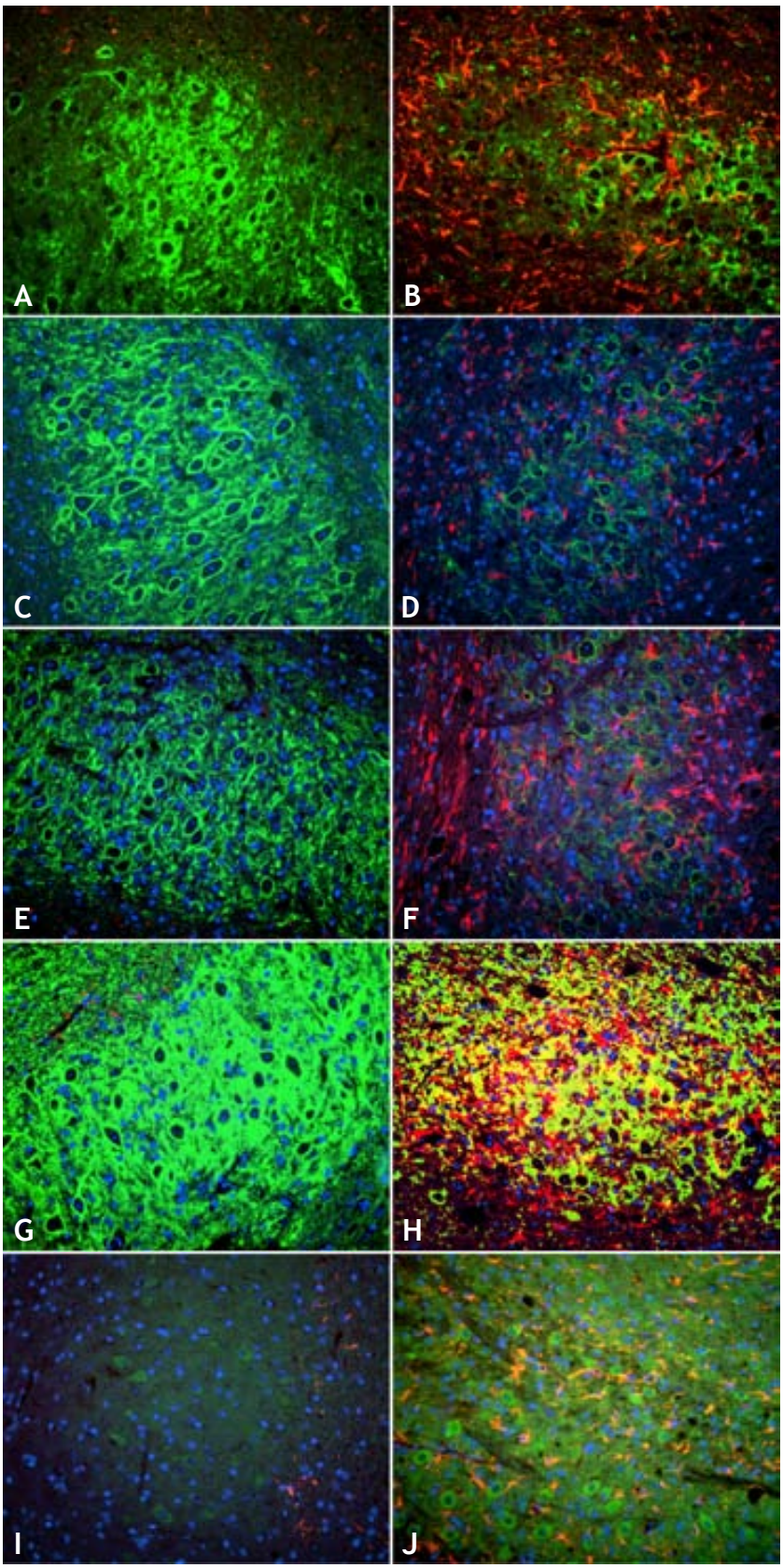

Figure 2: Histochemical staining in cerebellar nuclei in control mice (A, C, E, G, I) and Scrapie-infected mice (B, D, F, H, J). PNN stained with WFA (green) (A, B), tenascin-R (green) (C, D), brevican (green) (E, F), HA (green) (G, H) and neurocan (green) (I, J). GFAP-immunostained astrocytes (red). Nuclei were counterstained with DAPI (blue).

DISCUSSION

In these Scrapie-infected mice, a dramatic loss of PNNs at terminal stage of the disease has been observed. A similar finding has been reported at the terminal stage of several human TSEs (1, 2). We have also described that several PNN components undergo changes at this stage of the disease: a marked decrease in tenascin-R and brevican and mild alterations in HA have been observed. In contrast, a marked increase of neurocan has been reported.

Changes in the different components of the ECM were correlated with a marked presence of reactive astrocytes and PrPres deposition. This correlation suggests that loss of PNNs and their components may be produced by metalloprotease (MP) digestion. It is accepted that, upon activation by PrPres, glial cells produce MP (4, 5, 6), which in turn could degrade several ECM molecules (7, 8).

It is interesting to note that, in Scrapie-infected mice, ECM molecules that are lost are those characteristic of the mature brain, such as tenascin-R and brevican, whereas other components typical of the the immature brain, such as neurocan, are reexpressed.

A similar situation has been reported in several pathologies, as in multiple sclerosis (9, 10), ischemic lesions (11), epileptic seizures (12, 13, 14, 15), Alzheimer disease (16, 17) and gliomas (18, 19). In all of these diseases an important remodelation of the tissue takes place.

Our results suggest that a similar process could happen during the TSEs. The meaning of the ECM changes are not well-known, but they could be related to the repair process and neuronal plasticity as an attempt to reestablish the synaptic contacts (14, 20, 21). Nevertheless further studies are necessary to define completely this process.

REFERENCES

1. Belichenko P V, Miklossy J, Belser B, Budka H, Celio M R. Early destruction of the extracellular matrix around parvalbumin-immunoreactive interneurons in Creutzfeldt-Jakob disease. Neurobiol Dis. (1999) 6: 269-79.
2. Guentchev M, Wanschitz J, Voigtlander T, Flicker H, Budka H. Selective neuronal vulnerability in human prion diseases. Fatal familial insomnia differs from other types of prion diseases. Am J Pathol. (1999) 155: 1453-7.
3. Siso S, Puig B, Varea R, Vidal E, Acin C, Prinz M, Montrasio F, Badiola J, Aguzzi A, Pumarola M, Ferrer I. Abnormal synaptic protein expression and cell death in murine scrapie. Acta Neuropathol (Berl). (2002) 103: 615-26.
4. Brown D R, Schmidt B, Kretzschmar H A. A prion protein fragment primes type 1 astrocytes to proliferation signals from microglia. Neurobiol Dis. (1998) 4: 410-22.
5. Hafiz F B, Brown D R. A model for the mechanism of astrogliosis in prion disease. Mol Cell Neurosci. (2000) 16: 221-32.
6. Marella M, Chabry J. Neurons and astrocytes respond to prion infection by inducing microglia recruitment. J Neurosci. (2004) 24: 620-7.
7. Gottschall P E, Deb S. Regulation of matrix metalloproteinase expressions in astrocytes, microglia and neurons. Neuroimmunomodulation. (1996) 3: 69-75.
8. Stern R. Devising a pathway for hyaluronan catabolism: are we there yet? Glycobiology. (2003) 13: 105R-15R.
9. Sobel R A, Ahmed A S. White matter extracellular matrix chondroitin sulfate/dermatan sulfate proteoglycans in multiple sclerosis. J Neuropathol Exp Neurol. (2001) 60: 1198-207.
10. Gutowski N J, Newcombe J, Cuzner M L. Tenascin-R and C in multiple sclerosis lesions: relevance to extracellular matrix remodelling. Neuropathol Appl Neurobiol. (1999) 25: 207-14.
11. Lu A, Tang Y, Ran R, Clark J F, Aronow B J, Sharp F R. Genomics of the periinfarction cortex after focal cerebral ischemia. J Cereb Blood Flow Metab. (2003) 23: 786-810.
12. Kurazono S, Okamoto M, Sakiyama J, Mori S, Nakata Y, Fukuoka J, Amano S, Oohira A, Matsui H. Expression of brain specific chondroitin sulfate proteoglycans, neurocan and phosphacan, in the developing and adult hippocampus of Ihara's epileptic rats. Brain Res. (2001) 898: 36-48.
13. Okamoto M, Sakiyama J, Mori S, Kurazono S, Usui S, Hasegawa M, Oohira A. Kainic acid-induced convulsions cause prolonged changes in the chondroitin sulfate proteoglycans neurocan and phosphacan in the limbic structures. Exp Neurol. (2003) 184: 179-95.
14. Matsui F, Kawashima S, Shuo T, Yamauchi S, Tokita Y, Aono S, Keino H, Oohira A. Transient expression of juvenile-type neurocan by reactive astrocytes in adult rat brains injured by kainate-induced seizures as well as surgical incision. Neuroscience. (2002) 112: 773-81.
15. Nakic M, Mitrovic N, Sperk G, Schachner M. Kainic acid activates transient expression of tenascin-C in the adult rat hippocampus. J Neurosci Res. (1996) 44: 355-62.
16. Asher R A, Morgenstern D A, Fidler P S, Adcock K H, Oohira A, Braistead J E, Levine J M, Margolis R U, Rogers J H, Fawcett J W. Neurocan is upregulated in injured brain and in cytokine-treated astrocytes. J Neurosci. (2000) 20: 2427-38.
17. Deller T, Haas C A, Naumann T, Joester A, Faissner A, Frotscher M. Up-regulation of astrocyte-derived tenascin-C correlates with neurite outgrowth in the rat dentate gyrus after unilateral entorhinal cortex lesion. Neuroscience. (1997) 81: 829-46.
18. Zagzag D, Friedlander D R, Dosik J, Chikramane S, Chan W, Greco M A, Allen J C, Dorovini-Zis K, Grumet M. Tenascin-C expression by angiogenic vessels in human astrocytomas and by human brain endothelial cells in vitro. Cancer Res. (1996) 56: 182-9.
19. Delpech B, Maingonnat C, Girard N, Chauzy C, Maunoury R, Olivier A, Tayot J, Creissard P. Hyaluronan and hyaluronectin in the extracellular matrix of human brain tumour stroma. Eur J Cancer. (1993) 29A: 1012-7.
20. Lukoyanov N V, Brandao F, Cadete-Leite A, Madeira M D, Paula-Barbosa M M. Synaptic reorganization in the hippocampal formation of alcohol-fed rats may compensate for functional deficits related to neuronal loss. Alcohol. (2000) 20: 139-48.
21. Smith B N, Dudek F E. Short- and long-term changes in CA1 network excitability after kainate treatment in rats. J Neurophysiol. (2001) 85: 1-9.

STUDY 3

AQUAPORIN 1 AND AQUAPORIN 4 OVEREXPRESSION IN BOVINE SPONGIFORM ENCEPHALOPATHY IN A TRANSGENIC MURINE MODEL AND IN CATTLE FIELD CASES

Carme Costa, Raül Tortosa, Agustín Rodríguez, Isidre Ferrer, Juan Maria Torres, Anna Bassols, Martí Pumarola.

Brain Research (2007), DOI: 10.1016/j.brainres.2007.06.088.

ARTICLE IN PRESS
BRES-37088; No. of pages: 11; 4C: 3, 4, 6
BRAIN RESEARCH XX (2007) XXX–XXX

available at www.sciencedirect.com

www.elsevier.com/locate/brainres

BRAIN RESEARCH

Research Report

Aquaporin 1 and aquaporin 4 overexpression in bovine spongiform encephalopathy in a transgenic murine model and in cattle field cases

Carme Costa[a], *Raül Tortosa*[a], *Agustín Rodríguez*[d], *Isidre Ferrer*[d], *Juan Maria Torres*[e], *Anna Bassols*[c], *Martí Pumarola*[a,b,*]

[a]*Departamento de Medicina i Cirurgia Animals, Universitat Autònoma de Barcelona, 08193 Bellaterra (Cerdanyola del Vallès), Barcelona, Spain*
[b]*Laboratori Priocat, CReSA, Universitat Autònoma de Barcelona, 08193 Bellaterra (Cerdanyola del Vallès), Barcelona, Spain*
[c]*Departamento de Bioquímica i Biologia Molecular, Universitat Autònoma de Barcelona, 08193 Bellaterra (Cerdanyola del Vallès), Barcelona, Spain*
[d]*Institut de Neuropatologia, Servei Anatomia Patològica, IDIBELL-Hospital de Bellvitge, Universitat de Barcelona, 08907 Hospitalet de Llobregat, Barcelona, Spain*
[e]*Centro de Investigación en Sanidad Animal (CISA), INIA, 28130 Valdeolmos (Madrid), Spain*

ARTICLE INFO

Article history:
Accepted 20 June 2007

Keywords:
Transmissible spongiform encephalopathy
Prion disease
Aquaporin
Water channel
Prion protein
Bovine spongiform encephalopathy

ABSTRACT

Aquaporins (AQP) are a family of transmembrane proteins that act as water selective channels. AQP1 and AQP4 are widely expressed in the central nervous system where they play several roles. Overexpression of AQP has been reported in some human and animal transmissible spongiform encephalopathies, but information is scanty about their distribution in the central nervous system in bovine spongiform encephalopathy (BSE). Double immunohistochemistry for AQP1, AQP4 and GFAP was developed in a transgenic mouse line overexpressing the bovine cellular prion protein (BoTg110), intracerebrally infected with cattle BSE. Western blot for AQP1 and AQP4, and immunohistochemistry for both AQP and GFAP were carried out in cases of BSE-diagnosed cattle as part of surveillance plan in Catalonia (Spain). A marked increase in AQP1 and AQP4 was observed in mice at the terminal stage of the disease, when they had a wide range of clinical signs, whereas no increase could be observed in the early stage before the onset of the clinical signs. In cattle which did not show evidence of clinical signs, both AQP already showed a great increase. The AQP overexpression correlated with GFAP-immunoreactive astrocytes and PrPres deposition in both cases. The results of this study suggest that AQP overexpression in glial cells could lead to an imbalance in water and ion homeostasis which could contribute to triggering the typical histopathological changes of BSE.

* *Corresponding author*. Departamento Medicina i Cirurgia Animals, Facultat de Veterinària, Universitat Autònoma de Barcelona, 08193 Bellaterra (Cerdanyola del Vallès), Barcelona, Spain. Fax: +34 93 581 31 42.
E-mail address: marti.pumarola@uab.cat (M. Pumarola).

0006-8993/$ – see front matter © 2007 Elsevier B.V. All rights reserved.
doi:10.1016/j.brainres.2007.06.088

1. Introduction

Transmissible spongiform encephalopathies (TSE) or prion diseases are a group of fatal neurodegenerative disorders of sporadic, genetic or infectious origin (Prusiner, 1998). Bovine spongiform encephalopathy (BSE) belongs to this group, as well as scrapie in sheep and goat (Hadlow and Eklund, 1968) and Creutzfeldt–Jakob disease (CJD), Gerstmann–Sträussler–Scheinker disease, kuru and fatal familial insomnia in humans (Gajdusek and Zigas, 1957; Zigas and Gajdusek, 1957; Lugaresi et al., 1986; Creutzfeldt, 1989; Jakob, 1989).

According to the "protein-only" hypothesis (Prusiner, 1982), TSEs are caused by the conversion of the normal prion protein (PrPc) into an abnormally folded, β-sheet enriched and protease resistant isoform, PrPres, which is pathogenic (Prusiner, 1998). Its accumulation in the brain induces neuronal loss, glial cell proliferation and spongiform degeneration (Scott et al., 1989; Prusiner, 1998).

An alteration in water balance is suspected in CJD, because diffusion weighted images, obtained by magnetic resonance, show high signal intensity in selected brain areas, which are compatible with changes in viscosity in and around cells or changes in membrane constituents (Murata et al., 2002; Collie et al., 2003; Tsuboi et al., 2005; Ukisu et al., 2005). It has been suggested that aquaporins (AQP) might be, at least in part, responsible for the water disturbances in TSEs, since studies based on DNA microarray technology have shown up-regulation of AQP4 in scrapie experimentally infected mice and hamsters (Riemer et al., 2000, 2004; Xiang et al., 2004), as well as in the brains of CJD patients (Xiang et al., 2005). Otherwise, Western blot studies have shown an increase in AQP1 and AQP4 in CJD patients and in BSE-infected mice, localized in astrocytes by immunohistochemistry in CJD patients (Rodriguez et al., 2006), suggesting a possible relationship between the AQP increase and the spongiform degeneration found in TSEs.

Aquaporins (AQP) are a family of integral membrane proteins that act as water channels in many cell types (Wasson, 2006); 13 isoforms of AQP have been identified so far in mammals (Verkman, 2005). AQP1 was the first human AQP to be identified and functionally characterized (Preston et al., 1992). It has been found in several organs and tissues: red blood cells, vascular endothelial cells of the kidney, lung, eye and brain (Wasson, 2006). In the brain, it is found in the apical pole of choroidal plexus of epithelial cells (Nielsen et al., 1993) and ependimocytes (King and Agre, 1996; Nagy et al., 2002). It is involved in the regulation of cerebrospinal fluid secretion (Verkman, 2005) and glial cell migration (Zhang et al., 2002; Oshio et al., 2005).

AQP4 is found in brain, kidney, stomach, colon, eye, muscle and skin (Wasson, 2006). In the CNS, it is by far the predominant AQP (Jung et al., 1994; Venero et al., 2001; Verkman et al., 2006) and is mainly located in the end-feet membrane of astrocytes around blood vessels and basolateral membranes of ependymocytes (Amiry-Moghaddam et al., 2004). Several roles have been attributed to AQP4, revealed by phenotyping knockout mice (Amiry-Moghaddam et al., 2004; Verkman et al., 2006): water selective transport between blood and brain and between cerebrospinal fluid compartments, neural signal transduction through K^+ buffering (Amiry-Moghaddam et al., 2004; Verkman et al., 2006) and glial cell migration (Verkman et al., 2006).

Based on these observations, the present study has examined the expression of AQP1 and AQP4 in the brain of a transgenic mouse lain overexpressing the bovine PrPc, boTg110 (Castilla et al., 2003), infected with BSE, by immunohistochemistry; and in cattle BSE field cases, by Western blot and immunohistochemistry. The distribution of both AQP is described and compared with control animals during the progression of the disease, in terms of PrPres deposition and astrocyte activation.

2. Results

2.1. *BSE-infected mice boTg110*

2.1.1. *Histopathological study and PrPres immunohistochemistry*

Evident spongiform degeneration was observed in the terminal mice group but not in the 150 dpi group. Its distribution involved predominantly the pons, medulla oblongata, mesencephalon and cerebellar cortex and to a lesser extent the diencephalon (Fig. 1; Table 1). Gliosis was also present in these areas.

In BSE-inoculated BoTg110 mice, positive immunostaining against PrPres was first detected at 150 dpi with a mild punctated pattern in the neuropil around lateral ventricles of the diencephalon, mesencephalon, pons, medulla oblongata and deep cerebellar nuclei. In the terminal group, the PrPres deposition was much more intense in the periventricular areas of the diencephalon, brain stem and cerebellar nuclei, where not only were a punctated neuropil and plaque-like structures observed, but also intraneuronal and glial staining (Fig. 1). Moderate immunoreactivity was observed in the hippocampus and caudate nuclei, and mild punctated immunostaining was observed in the neocortex, mainly in the deepest cortical layers (Table 1). The PrPres deposits, however, were not directly associated with spongiotic areas. In control animals, no immunostaining against PrPres was observed at any time.

2.1.2. *AQP 1, AQP4 and GFAP double immunohistochemistry*

In control and BSE-infected mice at the early stage the disease, 150 dpi, AQP1 staining was restricted to the apical pole of choroid plexus and leptomeninges (Figs. 2a and b) whereas AQP4 was found in the end-feet of astrocytes in contact with the piamater, surrounding blood vessels and in the basal pole of ependimocytes (Figs. 2d and e), as it has been reported in a recent study, where the distribution of AQP4 is described in detail (Costa et al., 2007). Moreover, the GFAP immunostaining only showed mark in the external and internal glia limitans, and few fibrillary astrocytes were observed in white matter tracts.

In contrast, BSE-infected mice belonging to the terminal group, 300 dpi, when compared with their controls showed a marked increase in GFAP and more discrete increase in AQP1 immunostaining, which displayed a branching pattern in the neuropil and immunoreactivity associated with the membrane of hypertrophic astrocytes (Fig. 2c). Otherwise, AQP4 showed a marked increase in immunoreactivity, mainly associated to the membrane of GFAP reactive astrocytes; moreover, branching and punctated patterns were also observed in the neuropil (Fig. 2f).

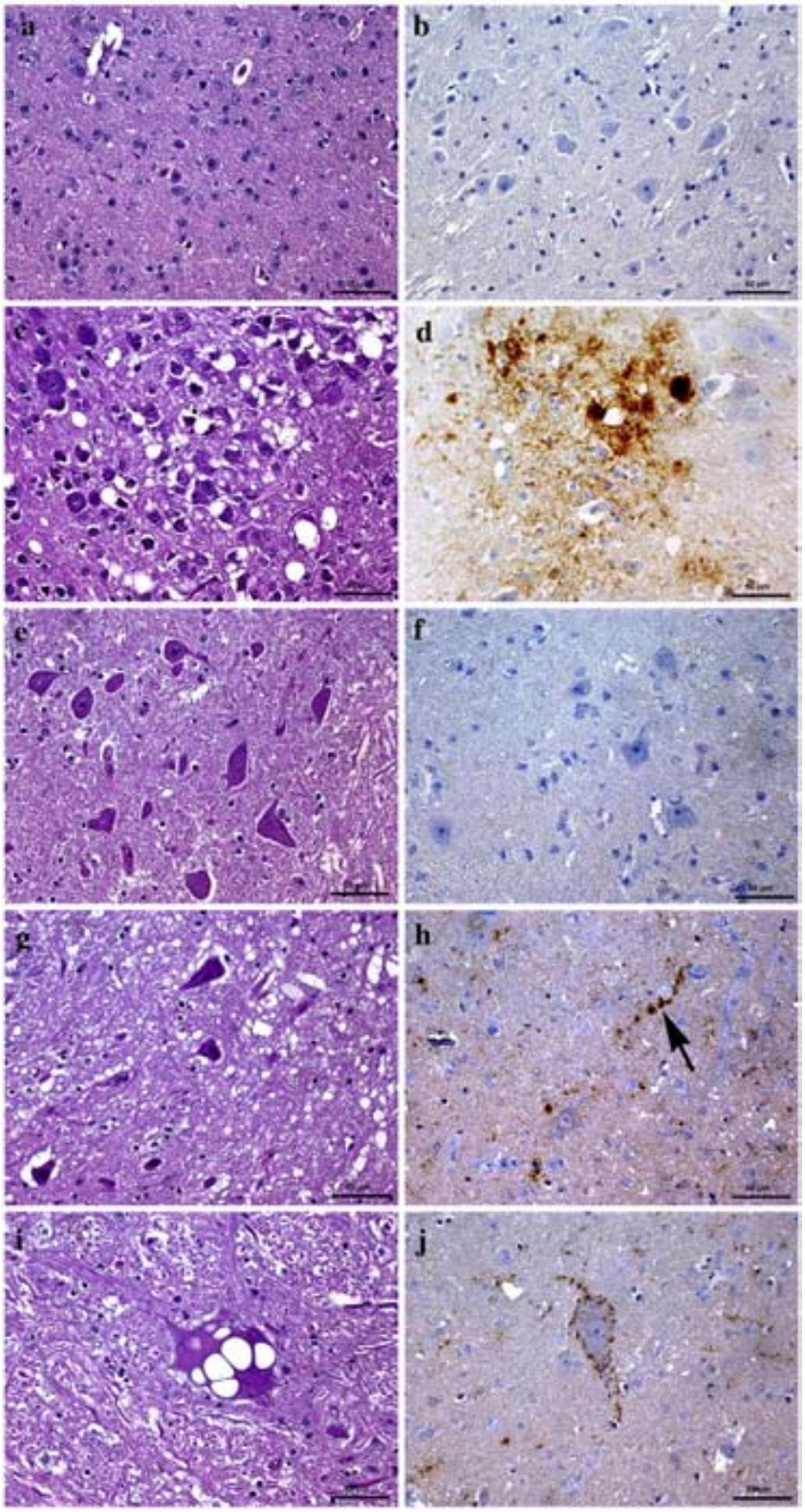

Fig. 1 – Hematoxylin–eosin (a, c, e, g, i) and PrPres immunohistochemistry (b, d, f, h, j), in mesencephalon of control mice (a, b), 300 dpi infected mice (c, d), control cattle (e, f) and BSE-affected cattle (g, h, i, j). 300 dpi infected mice showed a marked spongiosis in the neuropil (c) and plaque-like PrPres deposits (d). BSE-affected cattle showed spongiosis in the neuropil (g) and intraneuronal vaculation (i); PrPres immunostaining showed linear (arrow) (h), perineuronal and intraneuronal (j), and neuropil fine punctuate pattern (h, j). Scale bar=50 μm.

Table 1 – Summary of the main neuropathological findings in BSE-infected mice and cattle BSE field cases

	Mouse 150 dpi					Mouse 300 dpi					Cattle				
	SP	PrPres	GFAP	AQP1	AQP4	SP	PrPres	GFAP	AQP1	AQP4	SP	PrPres	GFAP	AQP1	AQP4
Neocortex	0	0	0	0	0	+	+	+	+	+	+	+	+	0	0
Hippocampus	0	0	0	0	0	+	++	+	+	+	+	+	+	+	+
Diencephalon	0	+	0	0	0	++	+++	+++	++	+++	++	++	++	++	++
Mesencephalon	0	+	0	0	0	+++	+++	+++	+++	+++	++	++	++	++	++
Pons – medulla oblongata	0	+	0	0	0	+++	+++	+++	+++	+++	++	++	++	++	++
Cerebellar cortex	0	0	0	0	0	+++	++	++	+	++	+	+	+	+	+
Spinal cord	0	+	0	0	0	+++	+++	+++	+++	+++	++	++	++	++	++

Semiquantitative representation of the clinical sings and the main neuropathological findings: +++ marked, ++ moderate, + mild, 0 no changes.
SP, spongiosis.

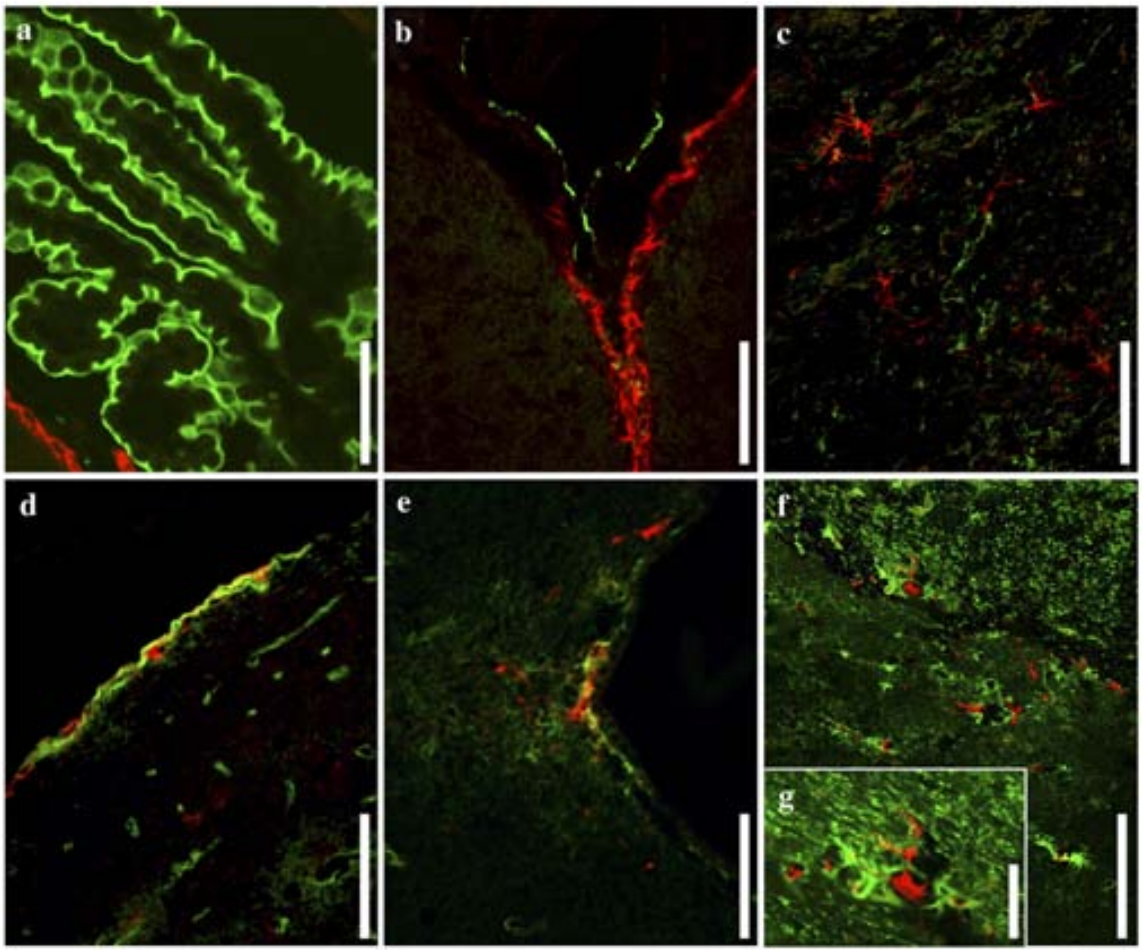

Fig. 2 – Double immunostaining of GFAP (red), AQP1 (green) (a, b, c) and AQP4 (green) (d, e, f, g) in mice. AQP1 in controls was found in apical pole of choroid plexus (a) and leptomeninges (b); in BSE-infected animals, at 300 dpi, (c) an increase of AQP1 and GFAP staining was observed in mesencephalon. AQP4 immunostaining in controls was detected at the astrocyte end-feet in contact with the piamater, surrounding blood vessels (d) and in the basal pole of ependimocytes (e); at terminal stage of the disease, 300 dpi, (f) AQP4 showed immunostaining in the membrane of GFAP reactive astrocytes in mesencephalon; detail of reactive astrocyte with the cytoplasm stained with GFAP and the membrane with AQP4 (g). Scale bar=50 μm (a, b, c, d, e, f) and 25 μm (g).

2.2. *Cattle BSE field cases*

2.2.1. *Histopathological study and PrPres immunohistochemistry*

The histopathological lesional pattern, immunohistochemical PrPres distribution and glial response are described in detail elsewhere (Vidal et al., 2006). Briefly, the most remarkable histopathological features were apparent spongiosis of the neuropil throughout the brain stem, with some vacuolated neurons (Fig. 1; Table 1). Gliosis was also present. Characteristic signs of neurodegeneration, such as pale, swollen or pyknotic neurons, were occasionally observed in the brain stem.

The major PrPres immunostaining was mainly observed in medulla oblongata, pons, mesencephalon and diencephalon, where punctated immunostaining was observed in the neuropil, perineuronally and even intraneuronally (Fig. 1). In the hippocampus, and cerebellar cortex mild punctated immunostaining was detected and the neocortex was the less affected area (Table 1).

2.2.2. *Aquaporin Western blot in BSE-affected cattle*

A Western blot study of AQP1 and AQP4 expression was carried out in mesencephalon of BSE-affected cattle with a high level of PrPres deposition in this area.

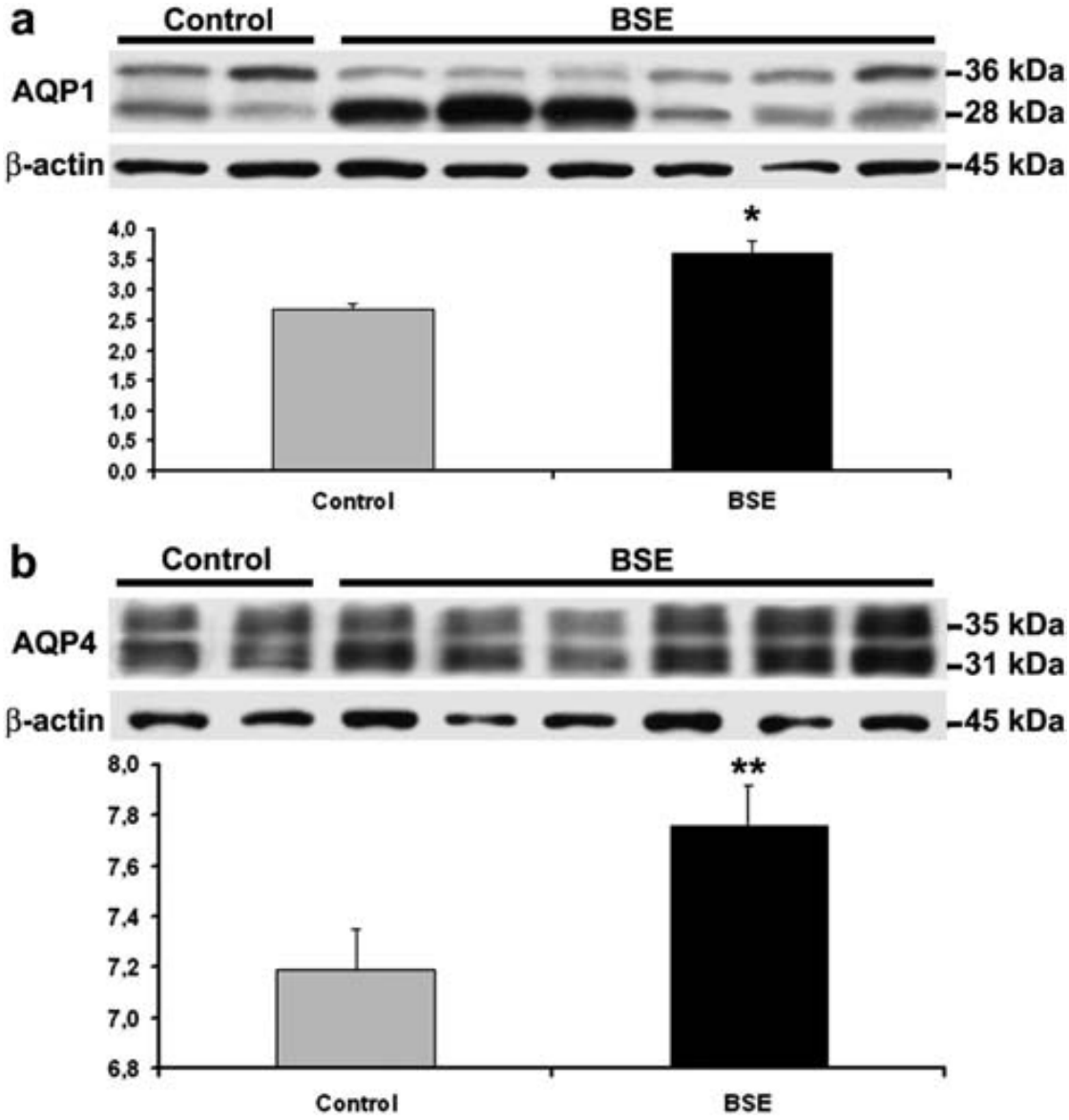

Fig. 3 – Western blot of AQP1 (a) and AQP4 (b) of mesencephalon from two controls and six BSE-affected cattle. AQP1 (a) showed two bands of 28 kDa and 36 kDa. The expression of AQP1 is increased in BSE-affected animals, especially the 28 kDa band. The densitometry of both bands normalized by β-actin (45 kDa) showed an increase of AQP1 expression in BSE cases when compared with controls, although the significance level was $^{*}P<0.1$. AQP4 (b) showed two bands of 31 kDa and 35 kDa; the expression of both AQP4 bands was increased in BSE-affected cattle. The densitometry of the two bands normalized by β-actin (45 kDa) showed a significant increase in AQP4 expression in BSE cases when compared with controls, $^{**}P<0.05$. Numbers in graph correspond to arbitrary units. Error bars = standard error.

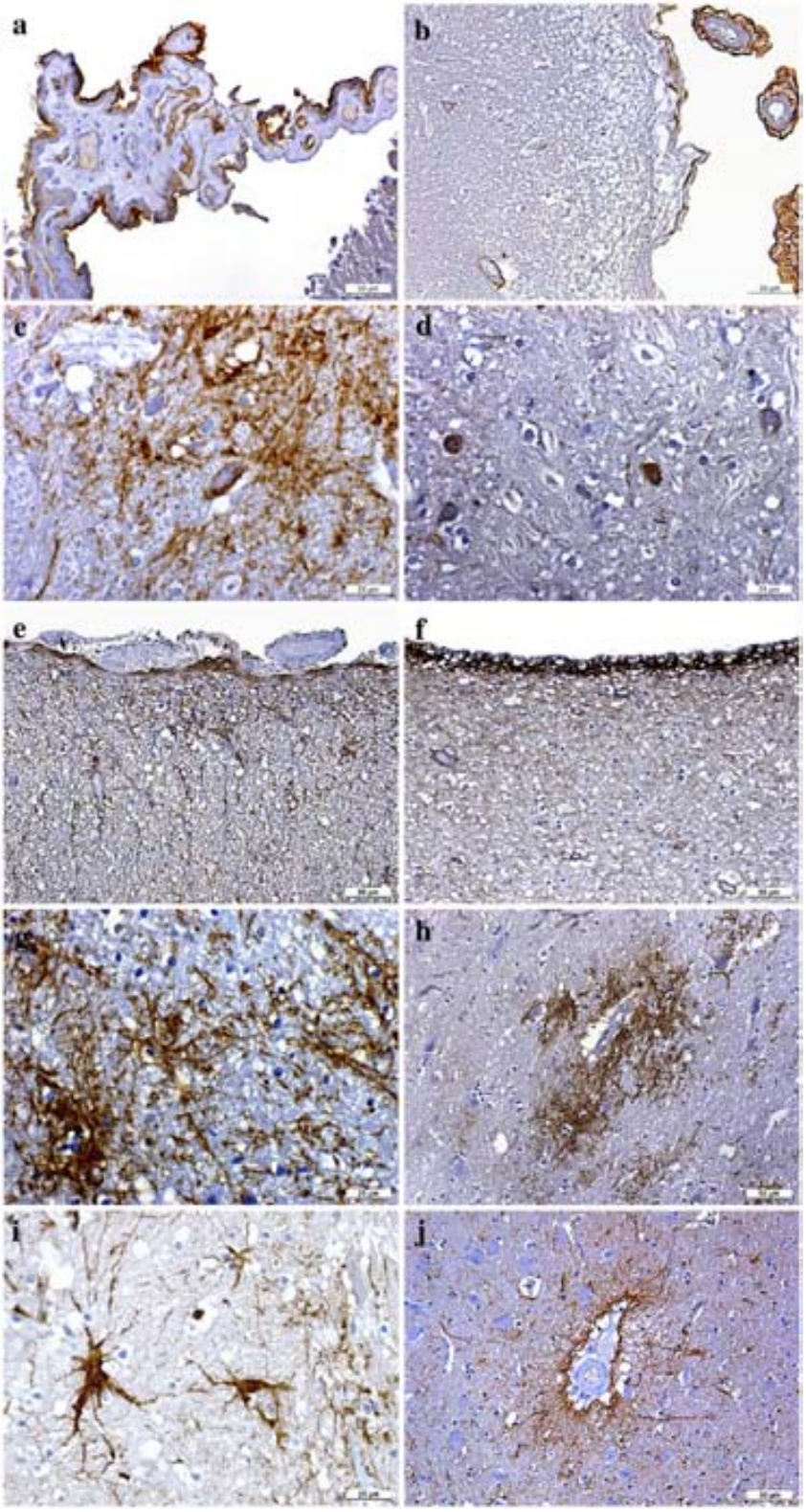

Fig. 4 – Immunostaining of AQP1 (a, b, c, d), AQP4 (e, f, g, h) and GFAP (i, j) in cattle. In controls, AQP1 was detected in apical pole of choroid plexus (a), and astrocyte end-feet lining the piamater and surrounding blood vessels (b); in the mesencephalon, BSE-affected animals showed a marked increase of AQP1 branching patter (c) and intracitoplasmatic staining of some glial cells (d). AQP4 was observed in astrocyte end-feet lining the piamater and surrounding blood vessels (e) and in the basal pole of ependimocytes (f); in the mesencephalon, BSE-affected animals showed an increase in AQP4 immunostaining appearing like astrocytes (g) and around blood vessels (h). GFAP immunostaining in BSE-affected cattle mesencephalon of reactive astrocytes in the neuropil (i) and around a blood vessel (j). Scale bars=50 μm (a, b, e, f, h, j) and 25 μm (c, d, g, i).

The anti-AQP1 antibody recognized two bands of 28 kDa and 36 kDa, both in controls and in BSE-affected animals. The 28 kDa band represented the non-glycosylated protein and the upper-band was considered to correspond to the glycosylated form of AQP1 (Spector et al., 2002). The anti-AQP4 antibody also recognized two bands of 31 kDa and 35 kDa in controls and BSE-affected cattle; these are considered to be two splice variants of the AQP4 gene (Jung et al., 1994).

The two bands of both AQP1 and AQP4 were densitometered together and normalized by β-actin; they showed a significant increase in AQP1 and AQP4 in BSE-affected cattle when compared with their controls.

The increase in AQP1 expression was variable between individuals, ranging from a slight to a marked increase, especially of the 28 kDa band. Similarly, not all BSE-affected animals showed the same increase in AQP4; some animals showed a marked increase of the two bands, whereas others had only a slight increase or no differences when compared with the controls (Figs. 3a and b).

2.2.3. *AQP1, AQP4 and GFAP immunohistochemistry in cattle*

To analyze the anatomical and cellular location of AQP1 and AQP4 in the whole CNS of BSE-affected cattle, an immunohistochemistry study was performed.

In the control cattle, AQP1 immunostaining was restricted to the apical pole of choroid plexus (Fig. 4a), leptomeninges and astrocyte end-feet, piamater lining and surrounding blood vessels (Fig. 4b); moreover, a very discrete branching pattern was observed dispersed in the neuropil, which was especially evident in the laminae I and II of the spinal cord.

AQP4, in control cattle, showed a more extensive immunoreactivity. It was observed in the astrocytes end-feet surrounding blood vessels, piamater lining (Fig. 4e) and basal pole of ependimocytes (Fig. 4f). A mild branching pattern was mainly seen in the white matter tracks, although it was also observed in the grey matter, especially surrounding large-sized neurons of the deep cerebellar nuclei and brain stem. A punctated pattern in the neuropil was especially evident in the granular cell layer of the cerebellar cortex and periventricular areas.

In BSE-affected cattle, AQP1 branching pattern became more abundant and more intense, occasionally with an appearance similar to that of astrocyte prolongations (Fig. 4c). Furthermore, AQP4 immunoreactivity showed a marked increase, with a branched staining pattern like that for astrocytes (Figs. 4g, h, i and j); the punctate pattern in the neuropil was more evident as well. Some glial cells also showed intracytoplasmatic immunostaining with AQP1 (Fig. 4d) and AQP4.

The most intense increase in immunostaining of the two AQP was observed in the spinal cord, medulla oblongata, pons, mesencephalon, diencephalon, striatum and piriform cortex. In the cerebellar cortex, the increased immunoreactivity was moderate whereas in the neocortex and hippocampus the changes observed were minimal (Table 1).

In general, in BSE-affected animals, a correlation between GFAP-immunoreactive astrocytes and AQP immunostaining was observed, which was stronger with AQP4 than with AQP1 (Table 1).

3. Discussion

The present study has shown that, both in the transgenic mouse boTg110 infected with BSE and in cattle BSE field cases, AQP1 and AQP4 were strongly expressed. In the mouse model, the increase in AQP1 and AQP4 was observed only in the terminal stage of the disease, when mice had a wide range of clinical signs, whereas it was not observed in the early stage before the onset of the clinical signs. In the case of cattle, the animals did not show evidence of clinical signs at the moment of the analysis. In both cases, AQP1 and AQP4 were found in the membrane of GFAP-immunoreactive astrocytes and they correlated with the gliosis.

Few precedents exist in the literature regarding AQP expression in TSEs. Recent studies based on microarray technology have shown that AQP4 is up-regulated in Scrapie experimentally infected mice and hamsters (Riemer et al., 2000, 2004; Xiang et al., 2004), and in human CJD patients (Xiang et al., 2005). The most recent report concerned human CJD cases, which showed increased expression of AQP1 and AQP4 in astrocytes by immunohistochemistry and Western blot (Rodriguez et al., 2006). The present study has shown that in transgenic boTg110 mice AQP1 and AQP4 are not found overexpressed in the membrane of reactive astrocytes until 300 dpi, when PrPres deposition is higher and glial cell activation stronger. In cattle, with a considerable amount of PrPres deposition and glial cell activation, an obvious increase of AQP1 and AQP4 in the astrocytes was also observed. Although both 300-dpi mice and cattle showed PrPres accumulation, presence of GFAP reactive astrocytes and overexpression of AQP1 and AQP4, mice showed a wide range of clinical signs whereas cattle did not. All these features indicate that cattle were in a less advanced stage of the disease than the 300-dpi infected mice, suggesting that the increase of AQP expression starts after glial cell activation, but earlier than the onset of clinical signs.

In contrast to other AQP, AQP1 and AQP4 have a well-known function as selective water channels (Preston et al., 1992; Hasegawa et al., 1994), and it is acknowledged that they play an important role in the control of water in the extracellular space of the brain under physiological and pathological conditions. Thus, the overexpression of AQP1 and AQP4 in BSE could lead to important changes and disturbances in the CNS homeostasis. In AQP4-knockout mice, it has been shown that lack of AQP4 decreases cerebral edema and improves survival rates in a model of acute water intoxication (Manley et al., 2000), reduces neurological after-effects in a model of acute ischemic stroke (Manley et al., 2000) and improves survival in a model of bacterial meningitis (Papadopoulos and Verkman, 2005), further supporting the importance of water flow in the pathogenesis of brain inflammation and infection. Taking into account all these references, it may be suggested that the AQP1 and AQP4 overexpression observed in BSE may alter water flow in the CNS and thereby have a negative effect on neural survival.

In addition, it is also known that AQP4 alters the ionic composition of the extracellular space (Nagelhus et al., 1998). The possible mechanism for involvement of AQP in rapid neural signal transduction is based on AQP4 coupling with

Kir4.1 K^+ channels in astroglia, impairing water re-uptake and thus modulating the function of excitable cells (Nagelhus et al., 2004). A failure to maintain water and K^+ homeostasis at sites of high neuronal activity would tend to cause cell depolarization and excessive neuronal discharge (Wen et al., 1999; Binder et al., 2004). In TSEs, it is likely that the increased expression of AQP4, if not balanced with Kir4.1 K^+ channels, leads to disturbances in K^+ uptake and to neuronal dysfunctions or even neuronal death.

Finally, the constitutive expression of AQP1 and AQP4 in GFAP and VIM reactive astrocytes has been correlated with astrocyte migration (Wang et al., 2004). Similarly, it has been described that PrP-activated microglia, which acquire an ameboid shape (Marella and Chabry, 2004), express AQP1 and AQP4 in order to increase their migration speed (Tomas-Camardiel et al., 2004).

A general mechanism to explain how AQP influence cell migration has been suggested. It is supposed that the rapid increase in osmolarity produced by actin depolymerization drives the entry of water through the AQP located in the membrane of the leading end of migrating cells. Thus, the osmotic influx of water across the membrane would expand that part of the cell, and would be followed by actin polymerization to stabilize the membrane protrusion (Oster and Perelson, 1987). Therefore, in vivo modifications of the cell cytoskeleton are always associated with changes in cell morphology, which may affect neuronal excitability by changing the volume of the extracellular space (Hawrylak et al., 1998).

It has been proposed that the overexpression of AQP1 and AQP4 may play a role in the formation of the spongiform change typical of the TSEs (Rodriguez et al., 2006). Consistent with the roles for AQP1 and AQP4 cited above, it is likely that the excess of water channels facilitates the creation of tubulovesicular structures that could lead to formation of vacuoles and spongiform changes. Ultrastructural studies have shown the formation of tubulovesicular structures in the CNS in several TSEs, and it has been suggested that these tubulovesicular structures give rise to vacuoles and spongiosis (Landis et al., 1981; Kim and Manuelidis, 1986; Miyakawa et al., 1986; Liberski et al., 2005), although their histogenesis remains uncertain.

In conclusion, overexpression of AQP1 and AQP4 is correlated with the presence of reactive astrocytes which, as a consequence, would migrate more easily. Other potential consequences of AQP overexpression would be the unbalance of water and K^+ ions, leading to changes in cell compartmentalization, thus facilitating the formation of the BSE typical spongiform lesions or even neuronal loss.

With Western blot, cattle AQP1 appears as two bands, a 28 kDa band representing the non-glycosylated protein and one broad band over 36 kDa representing the mature glycosylated protein (Spector et al., 2002). In BSE-affected cattle, the 28 kDa band showed a greater increase than the 36 kDa band, although it was not observed in all the animals. These results suggest that the increase in AQP1 takes place at the protein level, and that post-translational modification by glycosylation cannot keep pace with this increase. In contrast, AQP4 shows two bands of 31 kDa and 35 kDa, corresponding with different isoforms as a result of alternative splicing (Jung et al., 1994), and the two bands exhibit a similar increase of expression.

A certain degree of variability between BSE-affected cattle has been observed in Western blot of AQP. This fact was not unexpected since they are naturally infected animals, although all of them had similar levels of PrPres deposition and glial activation. Otherwise, in the immunohistochemical study, the differences between animals in AQP1 and AQP4 were much more discreet; this is probably due to the individual assessment of every CNS region, as well as to the differences in the sensibility of the two techniques.

In summary, the results presented in this work indicate that, at the beginning of the disease, PrPres is deposited and glial cells are activated by PrPres. After that, these cells overexpress AQP1 and AQP4. The time point at which AQP starts to be overexpressed is not exactly known, but in cattle the overexpression appears earlier than detectable clinical signs. Thus, we might suggest that the overexpression of AQP in glial cells is an adaptive response that facilitates glial cell migration after activation, but as a consequence this could lead to an imbalance in water and ion homeostasis and produce neuronal dysfunctions, formation of vacuoles which may originate the spongiform lesion, and even neuronal death. In other words, AQP overexpression may be a factor that contributes to triggering the typical histopathological changes of BSE.

4. Experimental procedures

4.1. *Animals and general procedures*

4.1.1. *Mice*

The study was developed in the transgenic mouse line boTg110 which was established as previously described (Castilla et al., 2003). These mice express bovine cellular prion protein (PrPc) under the murine *prnp* promoter in a murine PrP0/0 background. Bovine PrPc expression levels in this mouse line are 8-fold higher than the PrPc levels found in cattle brain homogenates. The characteristics of these transgenic mice, their susceptibility to different prion strains and the incubation time following BSE inoculation, as well as the behavioral and neuropathological findings in inoculated mice, have been described in detail elsewhere (Castilla et al., 2003).

For BSE infection, boTg110 mice (6–7 weeks old) were inoculated in the right parietal lobe using a 25 gauge disposable hypodermic needle with 20 μl of 10% brain homogenate (TSE/08/59 inocula). The TSE/08/59 inocula was obtained from a pool of the brainstem of 49 BSE-infected cattle and supplied by Veterinary Laboratory Agency (New Haw, Addlestone, Surrey, UK). The procedure was carried out at CISA-INIA (Madrid, Spain).

All mice were maintained under identical environmental conditions and received food and water *ad libitum*. To evaluate the clinical signs appearing after inoculation, mice were observed daily and their neurological status was assessed twice a week. The presence of three signs of neurological dysfunction, using 10 different items (Scott et al., 1989, 1993), was necessary for a mouse to score positive for prion disease.

A brain PrPres deposition kinetic in these mice was previously reported (Castilla et al., 2003). From this kinetic, two different stages in the progression of the disease were used for the present study: one group of mice was sacrificed early in the incubation period, at 150 days post inoculation

(dpi) ($n=4$), when the first deposits of PrPres are detected but before the onset of clinical signs. The second group, terminally ill mice with evident clinical signs, was sacrificed between 290 and 320 dpi ($n=8$). Uninoculated age-matched control animals were also included: 150 dpi ($n=4$) and 285–350 dpi ($n=6$).

Mice were culled following the recommendations and approval of the ethics committee. Necropsy was carried out; brains were immediately removed from the skull and fixed by immersion in 10% buffered formalin. The brains were cut in coronal sections at the level of the optic chiasm, piriform cortex and medulla oblongata. Samples were dehydrated by increasing alcohol concentrations, and embedded in xylene and paraffin. Four-micrometer sections were obtained and hematoxylin–eosin stained for morphological evaluation, while further sections were mounted in 3-trietoxysilil-propylamine-coated glass slides for immunohistochemical studies.

4.1.2. *Cattle*

For the present study, six brains of cattle diagnosed with BSE and two healthy control specimens were used. These brains, obtained from the active TSE surveillance program in Catalonia, were positive for PrPres in the screening test (Prionics-Check Western Blotting) and confirmed as such by histopathology and immunohistochemistry.

None of the cases studied, according to official veterinary reports, showed any detectable clinical sign at the ante-mortem inspection. All the animals were female cattle belonging to the Friesian breed and their ages ranged from 4 to 8 years. Post-mortem delay was approximately 24–48 h at 4 °C. The brain was sectioned sagitally into halves: one half was dissected and kept frozen at −74 °C for biochemical studies, while the other half was immersed in 10% phosphate-buffered formalin for 15 days. After fixation, 4 mm-thick tissue sections of spinal cord, medulla oblongata, pons, mesencephalon, thalamus, striatum, cerebellar cortex, occipital cortex, parietal cortex, temporal cortex, frontal cortex, hippocampus, piriform lobe and olfactory bulbs were blocked and immersed in 98% formic acid for 1 h to reduce prion infectivity before being embedded in paraffin wax. Four micrometer-thick sections were then obtained for routine hematoxylin and eosin staining, and immunohistochemical procedures.

4.2. *Immunohistochemistry*

4.2.1. *Prion protein*

Immunohistochemistry against PrPres in cattle and mouse CNS was performed as previously described (Siso et al., 2004). Briefly, sections were immersed in formic acid and boiled at low pH in a pressure cooker with endogenous peroxidases blocked. After pre-treatment with proteinase K, the sections were incubated overnight with the anti-PrP mAb 6H4 as the primary antibody (1:2000, kindly provided by Prionics AG) and, finally, developed using DAKO EnVision system and 3,3′diaminobenzidine as chromogen.

4.2.2. *Double immunohistochemistry of AQP 1, AQP4 and GFAP in mice*

Sections were deparaffinized and rehydrated. Non-specific protein binding was blocked with 2% bovine albumin in PBS for 1 h at room temperature. All sections were incubated overnight at 4 °C with mouse anti-glial fibrillary acidic protein marked with Cy3 (GFAP) (Sigma, Madrid, Spain), diluted 1:200 and at the same time with rabbit anti-aquaporin-1 polyclonal antibody (Chemicon International Inc., Madrid, Spain), diluted 1:100, or rabbit anti-aquaporin-4 polyclonal antibody (Chemicon International Inc., Madrid, Spain), diluted 1:200, in blocking solution. Then the sections were incubated with the secondary goat anti-rabbit biotinylated IgG antibody (Dakocytomation, Barcelona, Spain) diluted 1:200 in blocking solution at room temperature. Streptavidin-FITC (Sigma, Madrid, Spain) was applied to all sections for 1 h, diluted at 1:200.

As a background control, the primary antibody incubation was omitted. No signal was observed in any of the control slides.

4.2.3. *Immunohistochemistry of AQP1, AQP4 and GFAP in cattle*

The immunohistochemistry was carried out as described above in mice, with the following differences: endogenous peroxidase activity was blocked by incubating the sections for 20 min in 2% hydrogen peroxide, 70% methanol and PBS; the anti-GFAP antibody used was rabbit-anti-GFAP (Dakocytomation, Barcelona, Spain), diluted 1:500; avidin–biotin–peroxidase complex (ImmunoPure ABC Peroxidase Staining Kits, Pierce, Madrid, Spain) was applied after the secondary antibodies, diluted 1:100 in PBS, for 1 h at room temperature; and, finally, the peroxidase reaction was visualized with 2.5 μg/ml of 3,3′-diaminobenzidine and 0.05% hydrogen peroxide. Sections were counterstained with hematoxylin.

As a background control, the primary antibody incubation was omitted. No signal was observed in any of the control slides.

4.3. *Western blot*

4.3.1. *Gel electrophoresis and Western blot*

For Western blot studies, about 0.1 g of cattle mesencephalon was homogenized in a glass tissue grinder in 10 volumes (w/v) of cold buffer containing TBS, 0.5% NP-40, 0.5% deoxycholic acid sodium salt, 0.1 mM phenylmethylsulfonylfluoride, 10 μg/ml aprotinin, 10 μg/ml leupeptin and 10 μg/ml pepstatin, pH 7.4, to inhibit endogenous phosphatases. After centrifugation at 5000×*g* for 5 min, protein concentration of total homogenate was determined with the BCA Protein Assay Kit (Pierce, Barcelona). Thirty micrograms of protein was mixed with loading buffer containing 0.125 M Tris (pH 6.8), 20% glycerol, 10% of mercaptoethanol, 4% SDS and 0.002% bromophenol blue, and then heated at 96°C for 5 min. Sodium dodecylsulfate-polyacrylamide gel electrophoresis (12% SDS-PAGE) was carried out using a Mini-Protean system (Bio-Rad, Madrid) with molecular weight standards (Calidoscope, Bio-Rad, Madrid). Proteins were then transferred to nitrocellulose membranes using an electrophoretic transfer semi-dry system (Bio-Rad, Madrid). The membranes were washed with TTBS containing 10 mM Tris–HCl, pH 7.4, 140 mM NaCl and 0.1% Tween-20. Non-specific blocking was performed by incubating the membranes in TTBS containing 5% skimmed milk for 1 h. Membranes were incubated with the primary antibodies at 4 °C overnight. The rabbit anti-aquaporin 1 polyclonal antibody (Chemicon, Madrid) was used at a dilution of 1:500 in the TBST-5% skimmed milk. The rabbit anti-aquaporin 4 polyclonal antibody (Chemicon, Madrid) was used at a dilution of 1:500. After rinsing, the

membranes were incubated with the secondary goat anti-rabbit biotinylated IgG antibody (Dakocytomation, Barcelona) at a dilution of 1:5000 for 1 h at room temperature. The membranes were then washed and developed with the chemiluminescence ECL system (Amersham, Barcelona) followed by exposure of the membranes to autoradiographic films. The monoclonal anti-β-actin antibody (Sigma, Madrid, Spain) was used at a dilution of 1:5000 as a control for protein loading.

4.3.2. *Densitometry and statistical analysis*

Protein expression levels were determined by densitometry of the bands using Total Laboratory v2.01 software. This software detects the bands obtained by Western blot and gives individual values which are dependent on the light quantification of the corresponding band. Measurements are expressed as arbitrary units. The results were normalized for β-actin. The numerical data obtained from BSE and the corresponding controls were statistically analyzed using R 2.0.0. software from the non-parametric *U* Mann–Whitney test. Asterisks indicate the following *P* values: $^{*}P<0.1$ (90% confidence level) and $^{**}P<0.05$ (95% confidence level).

Acknowledgments

The authors wish to acknowledge the support of Dr. Enric Vidal and the excellent technical assistance of Maria Sierra Espinar and Marta Valle of the Priocat Laboratory, CReSA. We thank Tom Yohannan for editorial help and Josep Costa for statistical support. This study has been financially supported by the Spanish *Ministerio de Ciencia y Tecnología* (Grant ref. EET2002-05168-C04). C.C. was supported by a fellowship from the *Universitat Autònoma de Barcelona*, R.T. was supported by a fellowship attached to the grant EET2002-05168-C04-01 (to M.P.) from the *Ministerio de Ciencia y Tecnología* and AR was supported by a grant from the "Fundació IDIBELL". We also thank the Animal Tissue Bank of Catalunya for providing cattle samples from Priocat-CReSA.

REFERENCES

Amiry-Moghaddam, M., Frydenlund, D.S., Ottersen, O.P., 2004. Anchoring of aquaporin-4 in brain: molecular mechanisms and implications for the physiology and pathophysiology of water transport. Neuroscience 129, 999–1010.

Binder, D.K., Oshio, K., Ma, T., Verkman, A.S., Manley, G.T., 2004. Increased seizure threshold in mice lacking aquaporin-4 water channels. NeuroReport 15, 259–262.

Castilla, J., Gutierrez Adan, A., Brun, A., Pintado, B., Ramirez, M.A., Parra, B., Doyle, D., Rogers, M., Salguero, F.J., Sanchez, C., Sanchez-Vizcaino, J.M., Torres, J.M., 2003. Early detection of PrPres in BSE-infected bovine PrP transgenic mice. Arch. Virol. 148, 677–691.

Collie, D.A., Summers, D.M., Sellar, R.J., Ironside, J.W., Cooper, S., Zeidler, M., Knight, R., Will, R.G., 2003. Diagnosing variant Creutzfeldt–Jakob disease with the pulvinar sign: MR imaging findings in 86 neuropathologically confirmed cases. AJNR Am. J. Neuroradiol. 24, 1560–1569.

Costa, C., Tortosa, R., Domenech, A., Vidal, E., Pumarola, M., Bassols, A., 2007. Mapping of aggrecan, hyaluronic acid, heparan sulphate proteoglycans and aquaporin 4 in the central nervous system of the mouse. J. Chem. Neuroanat. 33, 111–123.

Creutzfeldt, H.G., 1989. On a particular focal disease of the central nervous system (preliminary communication), 1920 Alzheimer Dis. Assoc. Disord. 3, 3–25.

Gajdusek, D.C., Zigas, V., 1957. Degenerative disease of the central nervous system in New Guinea; the endemic occurrence of Kuru in the native population. N. Engl. J. Med. 257, 974–978.

Hadlow, W.J., Eklund, C.M., 1968. Scrapie—a virus-induced chronic encephalopathy of sheep. Res. Publ. - Assoc. Res. Nerv. Ment. Dis. 44, 281–306.

Hasegawa, H., Ma, T., Skach, W., Matthay, M.A., Verkman, A.S., 1994. Molecular cloning of a mercurial-insensitive water channel expressed in selected water-transporting tissues. J. Biol. Chem. 269, 5497–5500.

Hawrylak, N., Fleming, J.C., Salm, A.K., 1998. Dehydration and rehydration selectively and reversibly alter glial fibrillary acidic protein immunoreactivity in the rat supraoptic nucleus and subjacent glial limitans. Glia 22, 260–271.

Jakob, A., 1989. Concerning a disorder of the central nervous system clinically resembling multiple sclerosis with remarkable anatomic findings (spastic pseudosclerosis). Report of a fourth case. Alzheimer Dis. Assoc. Disord. 3, 26–45.

Jung, J.S., Bhat, R.V., Preston, G.M., Guggino, W.B., Baraban, J.M., Agre, P., 1994. Molecular characterization of an aquaporin cDNA from brain: candidate osmoreceptor and regulator of water balance. Proc. Natl. Acad. Sci. U. S. A. 91, 13052–13056.

Kim, J.H., Manuelidis, E.E., 1986. Serial ultrastructural study of experimental Creutzfeldt–Jacob disease in guinea pigs. Acta Neuropathol. (Berl) 69, 81–90.

King, L.S., Agre, P., 1996. Pathophysiology of the aquaporin water channels. Annu. Rev. Physiol. 58, 619–648.

Landis, D.M., Williams, R.S., Masters, C.L., 1981. Golgi and electronmicroscopic studies of spongiform encephalopathy. Neurology 31, 538–549.

Liberski, P.P., Streichenberger, N., Giraud, P., Soutrenon, M., Meyronnet, D., Sikorska, B., Kopp, N., 2005. Ultrastructural pathology of prion diseases revisited: brain biopsy studies. Neuropathol. Appl. Neurobiol. 31, 88–96.

Lugaresi, E., Medori, R., Montagna, P., Baruzzi, A., Cortelli, P., Lugaresi, A., Tinuper, P., Zucconi, M., Gambetti, P., 1986. Fatal familial insomnia and dysautonomia with selective degeneration of thalamic nuclei. N. Engl. J. Med. 315, 997–1003.

Manley, G.T., Fujimura, M., Ma, T., Noshita, N., Filiz, F., Bollen, A.W., Chan, P., Verkman, A.S., 2000. Aquaporin-4 deletion in mice reduces brain edema after acute water intoxication and ischemic stroke. Nat. Med. 6, 159–163.

Marella, M., Chabry, J., 2004. Neurons and astrocytes respond to prion infection by inducing microglia recruitment. J. Neurosci. 24, 620–627.

Miyakawa, T., Katsuragi, S., Koga, Y., Moriyama, S., 1986. Status spongiosus in Creutzfeldt–Jakob disease. Clin. Neuropathol. 5, 146–152.

Murata, T., Shiga, Y., Higano, S., Takahashi, S., Mugikura, S., 2002. Conspicuity and evolution of lesions in Creutzfeldt–Jakob disease at diffusion-weighted imaging. AJNR Am. J. Neuroradiol. 23, 1164–1172.

Nagelhus, E.A., Veruki, M.L., Torp, R., Haug, F.M., Laake, J.H., Nielsen, S., Agre, P., Ottersen, O.P., 1998. Aquaporin-4 water channel protein in the rat retina and optic nerve: polarized expression in muller cells and fibrous astrocytes. J. Neurosci. 18, 2506–2519.

Nagelhus, E.A., Mathiisen, T.M., Ottersen, O.P., 2004. Aquaporin-4 in the central nervous system: cellular and subcellular distribution and coexpression with Kir4.1. Neuroscience 129, 905–913.

Nagy, G., Szekeres, G., Kvell, K., Berki, T., Nemeth, P., 2002. Development and characterisation of a monoclonal antibody family against aquaporin 1 (Aqp1) and aquaporin 4 (Aqp4). Pathol. Oncol. Res. 8, 115–124.

Nielsen, S., Smith, B.L., Christensen, E.I., Agre, P., 1993. Distribution of the aquaporin chip in secretory and resorptive epithelia and capillary endothelia. Proc. Natl. Acad. Sci. U. S. A. 90, 7275–7279.

Oshio, K., Watanabe, H., Song, Y., Verkman, A.S., Manley, G.T., 2005. Reduced cerebrospinal fluid production and intracranial pressure in mice lacking choroid plexus water channel aquaporin-1. FASEB J. 19, 76–78.

Oster, G.F., Perelson, A.S., 1987. The physics of cell motility. J. Cell Sci., Suppl. 8, 35–54.

Papadopoulos, M.C., Verkman, A.S., 2005. Aquaporin-4 gene disruption in mice reduces brain swelling and mortality in pneumococcal meningitis. J. Biol. Chem. 280, 13906–13912.

Preston, G.M., Carroll, T.P., Guggino, W.B., Agre, P., 1992. Appearance of water channels in *Xenopus* oocytes expressing red cell Chip28 protein. Science 256, 385–387.

Prusiner, S.B., 1982. Novel proteinaceous infectious particles cause scrapie. Science 216, 136–144.

Prusiner, S.B., 1998. The prion diseases. Brain Pathol. 8, 499–513.

Riemer, C., Queck, I., Simon, D., Kurth, R., Baier, M., 2000. Identification of upregulated genes in scrapie-infected brain tissue. J. Virol. 74, 10245–10248.

Riemer, C., Neidhold, S., Burwinkel, M., Schwarz, A., Schultz, J., Kratzschmar, J., Monning, U., Baier, M., 2004. Gene expression profiling of scrapie-infected brain tissue. Biochem. Biophys. Res. Commun. 323, 556–564.

Rodriguez, A., Perez-Gracia, E., Espinosa, J.C., Pumarola, M., Torres, J.M., Ferrer, I., 2006. Increased expression of water channel aquaporin 1 and aquaporin 4 in Creutzfeldt–Jakob disease and in bovine spongiform encephalopathy-infected bovine-PrP transgenic mice. Acta Neuropathol. (Berl) 112, 573–585.

Scott, M., Foster, D., Mirenda, C., Serban, D., Coufal, F., Walchli, M., Torchia, M., Groth, D., Carlson, G., DeArmond, S.J., et al., 1989. Transgenic mice expressing hamster prion protein produce species-specific scrapie infectivity and amyloid plaques. Cell 59, 847–857.

Scott, M., Groth, D., Foster, D., Torchia, M., Yang, S.L., DeArmond, S.J., Prusiner, S.B., 1993. Propagation of prions with artificial properties in transgenic mice expressing chimeric PrP genes. Cell 73, 979–988.

Siso, S., Ordonez, M., Cordon, I., Vidal, E., Pumarola, M., 2004. Distribution of PrP(Res) in the brains of BSE-affected cows detected by active surveillance in Catalonia, Spain. Vet. Rec. 155, 524–525.

Spector, D.A., Wade, J.B., Dillow, R., Steplock, D.A., Weinman, E.J., 2002. Expression, localization, and regulation of aquaporin-1 to -3 in rat urothelia. Am. J. Physiol., Renal Fluid Electrolyte Physiol. 282, F1034–F1042.

Tomas-Camardiel, M., Venero, J.L., de Pablos, R.M., Rite, I., Machado, A., Cano, J., 2004. In vivo expression of aquaporin-4 by reactive microglia. J. Neurochem. 91, 891–899.

Tsuboi, Y., Baba, Y., Doh-ura, K., Imamura, A., Fujioka, S., Yamada, T., 2005. Diffusion-weighted MRI in familial Creutzfeldt–Jakob disease with the codon 200 mutation in the prion protein gene. J. Neurol. Sci. 232, 45–49.

Ukisu, R., Kushihashi, T., Kitanosono, T., Fujisawa, H., Takenaka, H., Ohgiya, Y., Gokan, T., Munechika, H., 2005. Serial diffusion-weighted MRI of Creutzfeldt–Jakob disease. AJR Am. J. Roentgenol. 184, 560–566.

Venero, J.L., Vizuete, M.L., Machado, A., Cano, J., 2001. Aquaporins in the central nervous system. Prog. Neurobiol. 63, 321–336.

Verkman, A.S., 2005. More than just water channels: unexpected cellular roles of aquaporins. J. Cell Sci. 118, 3225–3232.

Verkman, A.S., Binder, D.K., Bloch, O., Auguste, K., Papadopoulos, M.C., 2006. Three distinct roles of aquaporin-4 in brain function revealed by knockout mice. Biochim. Biophys. Acta 1758, 1085–1093.

Vidal, E., Marquez, M., Tortosa, R., Costa, C., Serafin, A., Pumarola, M., 2006. Immunohistochemical approach to the pathogenesis of bovine spongiform encephalopathy in its early stages. J. Virol. Methods 134, 15–29.

Wang, K., Bekar, L.K., Furber, K., Walz, W., 2004. Vimentin-expressing proximal reactive astrocytes correlate with migration rather than proliferation following focal brain injury. Brain Res. 1024, 193–202.

Wasson, K., 2006. Phenotypes of aquaporin mutants in genetically altered mice. Comp. Med. 56, 96–104.

Wen, H., Nagelhus, E.A., Amiry-Moghaddam, M., Agre, P., Ottersen, O.P., Nielsen, S., 1999. Ontogeny of water transport in rat brain: postnatal expression of the aquaporin-4 water channel. Eur. J. Neurosci. 11, 935–945.

Xiang, W., Windl, O., Wunsch, G., Dugas, M., Kohlmann, A., Dierkes, N., Westner, I.M., Kretzschmar, H.A., 2004. Identification of differentially expressed genes in scrapie-infected mouse brains by using global gene expression technology. J. Virol. 78, 11051–11060.

Xiang, W., Windl, O., Westner, I.M., Neumann, M., Zerr, I., Lederer, R.M., Kretzschmar, H.A., 2005. Cerebral gene expression profiles in sporadic Creutzfeldt–Jakob disease. Ann. Neurol. 58, 242–257.

Zhang, D., Vetrivel, L., Verkman, A.S., 2002. Aquaporin deletion in mice reduces intraocular pressure and aqueous fluid production. J. Gen. Physiol. 119, 561–569.

Zigas, V., Gajdusek, D.C., 1957. Kuru: clinical study of a new syndrome resembling paralysis agitans in natives of the eastern highlands of Australian New Guinea. Med. J. Aust. 44, 745–754.

DISCUSSION

Conducting a histochemical study of the ECM components of the mouse CNS and applying this knowledge to study the pathogeny of a disease such as BSE, by using a transgenic mouse model, has turned out to be an exciting as well as complex challenge.

First, it was necessary to analyze the composition and structure of the ECM of healthy adult mice CNS; the first surprise came here. Despite the fact that on a biochemical level a large number of proteins that make up the ECM are very well known, at the histological level, there are no good descriptions of its normal anatomic distribution in the CNS. The published works focus on very specific areas of the CNS and on certain species (see table 1). For this reason, we first studied this distribution in control mice. Then, there was another surprise: in the commercial catalogues there were hardly any antibodies to mark the ECM elements of the CNS for hitochemical techniques. Moreover, there are even less options if you want to work with mouse paraffin-embedded tissue. Optimizing several markers, whether bought or given, for histochemcial techniques in the CNS of mouse set in parrafin became arduous work, full of fruitless attempts. Nevertheless, there were a few small successes which finally gave rise to the three projects that make up this thesis.

	Species	Studied areas	References
PNN	Mouse	Whole brain	(135)
		Hippocampus	(132)
	Rat	Neocortex and some GABAergic nuclei	(24, 68, 137)
	Guinea pig	Neocortex	(138)
	Short tailed-oposum	Whole brain	(139)
	Human	Whole brain	(140, 141)
	Rhesus monkey	Basal forebrain	(140)
Aggrecan	Mouse	Hippocampus and superior colliculus	(3, 132)
	Rat	Neocortex	(12)
	Guinea pig	Neocortex	(138)
	Gerbil	Cochlear, olivary nuclei and trapezoid body	(142)
	Cat	Lateral geniculate nuclei	(143)
HA	Mouse	Whole brain	(132, 135)
	Rat	Neocortex	(53, 54)
	Frog	Whole brain	(244)
HSPG	Mouse	Mesencephalon	(146)
	Rat	Whole brain	(144, 145)
AQP4	Mouse	Astrocyte end-feet of the external glial limitans	(128, 150, 152)
		Spinal cord	(148, 149)
		Neocortex	(118, 153, 154)

Table 1: Most important works that describe the normal distribution of the PNNs, aggrecan, the HA, the HSPG and the AQP4 in the CNS, or in any of its areas in different animal species.

The first technique used was a histochemical affinity technique with a Wisteria floribunda (WFA) lectin; this made it possible to generally mark all of the neuropile CS and the PNN. This lectin specifically recognizes the N-acetylgalactosamine, a disaccharide that is found in the GAG chains of the CSPG (133), and thus it specifically recognizes the PNNs (134, 137). Another histochemical affinity technique with a

hyaluronan binding protein allowed us to mark the HA, which is the most abundant ECM element of the CNS (52).

We also optimized various immunohistochemical techniques: rabbit anti-aggrecan polyclonal antibody to specifically mark the aggrecan, which is the most abundant lectican in the adult CNS (10) and one of the most important components of the PNNs (12); also, anti-Δ-heparan sulphate monoclonal antibody (3G10), another antibody to generally identify any HSPG because it recognizes the unsaturated uronate residue generated by enzymatic digestion with heparitinase of the HSPG chains (245).

Later on we added two more antibodies for the immunohistochemical study of water channels: AQP1 and AQP4. Due to the hydrodynamic properties and maintenance of the homeostasis of the extracellular space of the ECM, it seemed that the AQPs, due to their function, could also be related.

1.- MAP OF THE ECM, HSPG AND AQP4 IN THE MOUSE CNS: STUDY 1

1.1.- The heterogeneity

As we knew better the distribution of more ECM elements and the water channels, some of its characteristics became apparent. The first, and the most interesting, was how heterogeneous the distribution was of all those markers in the CNS, in the neuropile as well as perineuronally.

The distribution of the PNNs observed with WFA coincided with that published by other authors (see table 1). As far as the aggrecan, for which there was no description of its normal distribution in mouse CNS, we observed that it was practically identical to that of the PNNs, with a similar distribution to the one previously described by other authors (see table 1). Moreover, we observed its presence in new areas, such as: piriform cortex, cerebellar cortex, lateral globus pallidus, reticular thalamic nucleus, inferior colliculus, substantia nigra and spinal cord, where it had never been descibed in mouse.

This distribution which coincided between the PNN and aggrecan is not odd, but rather the contrary. The aggrecan is a CSPG, and therefore contains CS lateral chains that have N-acetylgalactosamine; this is the same sugar that the WFA identifies. In any case, what was marked from the WFA is a bit more extensive and more intense that of the aggrecan, most likely because the WFA identifies other CSPG such as versican, neurocan, brevican or phosphacan, which are also part of the PNNs (8, 9).

The HA showed a very wide and heterogeneous distribution, in the PNNs as well as in the neuropile, as it was expected of the GAG which is considered to be the main ECM element (52). The distribution observed coincided with the descriptions by other authors on mice and other animals (see table 1).

The HSPG, which also lacked a detailed description of their distribution in the mice CNS (see table 1), showed a very wide distribution perineuronally as well as in the neuropile, rather similar to what had been described in rats (144, 145). Moreover,

the presence of HSPG in other areas which had not been described before was also observed, as for example: surrounding the Golgi neurons or in the laminae I and II of the spinal cord dorsal horn. The advantage of the antibody used was that it made possible to mark all the HSPGs in a general way (245); at the same time this was a disadvantage because we could not tell them apart.

The AQP4 also showed as wide and heterogeneous distribution as the other ECM elements studied; sometimes their distributions coincide, but other times they don't. The works published to date describe its distribution in very specific areas (see table 1). Furthermore, we were able to determine that the AQP4 is found in the neuropile of many other areas that have not been described to date, such as: the piriform cortex, lacunosum moleculare of the hippocampal formation, dorsal part of the lateral septal nucleus, superficial grey layer of the superior colliculus, reticular part of the substantia nigra, lateral lemniscus, pontine nuclei, rostral periolivary region, periaqueductal grey, raphe nuclei and the interpeduncular nuclei.

As other authors have already indicated, the heterogeneity suggests that each one of these elements have a very specific physiological role in maintaining the properties of the extracellular microenvironment of a certain region (2, 59, 68, 132, 246).

1.2.- Similarities and differences: functional implications

When we compare the distribution of the ECM elements, HSPG and AQP4, it is inevitable to find very marked similarities and differences in their distribution.

For example, in many regions rich in AQP4 an intense mark of HSPGs is also observed. This suggests the possibility that the AQP4 forms some kind of complex such as the dystroglycan complex (128), which contributes to the polarization of the AQP4 in the astrocyte end-feet, and of what makes up part of an HSPG: the agrin (128). But when the AQP4 is not located in the astrocyte end-feet, it also showed a distribution which coincided with the HSPG, as has been observed in: laminae I and II of the spinal cord, granular layer of the cerebellar cortex, periaqueductal grey and dorsal part of the lateral septal nuclei. More detailed studies need to be conducted with specific markers to identify certain HSPGs, in order to verify if any HSPG colocalizes with the AQP4; if this is the case, it would also have to be known if this is also an agrin or another HSPG.

Several authors have tried to correlate the distribution of the ECM components with specific neuronal populations. In studies carried out on the mouse CNS (137), it has been proven that the distribution of the PNN and the subset of GABAergic neurons containing parvalbumins is very similar, despite the fact that these do not fully coincide (138). On the other hand, in rats it has also been proven that a part of the subset of GABAergic neurons is surrounded by PNNs rich in HSPGs (145) and that the ECM in aminergic nuclei is usually scarce (246).

In this study it was also observed that the PNN marked with WFA and their components: aggrecan and HA, as well as the HSPG have a similar distribution to that of the subset of GABAergic neurons as for example in the neocortex or reticular

thalamic nuclei, in spite of the fact that double immunostaining were not done. We were also able to confirm that in aminergic nuclei, like the solitary tract nucleus, prepositus nucleus and the locus coeruleus (247), these elements are not observed or are very scarce, as has already been indicated (246).

Despite not being able to establish a precise relationship between the ECM components and specific neuronal populations, the heterogeneity of the ECM distribution suggests a function that is linked to the functional needs of the surrounding neurons. A study published by Hartig, et. al (1999) (68) suggests that the PNNs, due to having anionic sites, could link cations such as Na^+ and K^+. Therefore, when an action potential is generated and there are modifications to the concentrations of these ions, they would act as a buffer and favour their rapid distribution through the extracellular space.

It is believed that the ECM components, such as the HA and the CSPG are quite hydrophilic, and thus contribute to maintaining the hydrodynamic properties of the extracellular space (59, 68, 132).

The AQP4 also plays a very important role in metabolizing the water in the CNS (109, 128, 148, 150, 152). In this study, we have verified that in many areas such as: neocortex layer I, dorsal part of the lateral septal nucleus, lacunosum molecular layer of the hippocampus, hypothalamus, superficial grey layer of the superior colliculus, periaqueductal grey, interpenduncular nucleus, raphe nuclei, in the granular layer of the cerebellar cortex, and laminae I and II of the dorsal horn of the spinal cord, where there is a lack of ECM elements, such as the aggrecan or the HA, there is a high expression of AQP4. Thus, reinforcing the hypothesis that states that in the regions where ECM is scarce, the space between cells is less, and the AQP4 could facilitate the diffusion of the water and ions; in the regions with ECM, which is very rich in very hydrophilic molecules, the water can easily circulate through the extracellular space (148). Nevertheless, it was also verified that in some areas such as layer I of the piriform cortex, lateral globus pallidus, substantia nigra, pontine nuclei, olive nuclei and the ventral cochlear nuclei, the ECM components and AQP4 are expressed at the same time, so that in these areas, perhaps as a response to functional needs, these two mechanisms could work together in maintaining homeostasis.

2.- THE ECM AND THE AQPS IN THE BSE PATHOGENY: STUDIES 2 AND 3

2.1.- Few precedents

When we began the study of the ECM in the mouse line boTg110 infected with BSE, we did it based on two prior studies which, with histochemical techniques, described the loss of the PNNs in human TSEs: Creutzfeldt-Jacob disease (230), Gerstmann-Sträussler-Scheinker disease, Fatal Familial Insomnia and Kuru (231). These studies were conducted on tissue from the autopsies of terminally ill patients affected by these diseases. Both considered that in the course of the TSEs, the PNNs disappeared

and in their place the PrPres were deposited; then the retraction of the synapsis, and finally neuronal death occurred (230, 231).

As far as the AQPs, there also are not many precedents that relate them to the pathogeny of the TSEs. Studies based on microarray technology had observed that the AQP4 is over expressed in mice and hamsters infected with Scrapie (236, 237, 238) and in Creutzfeldt-Jacob disease patients (239). Another more recent study has demonstrated an increase in the expression of the AQP1 and AQP4, with immunohistochemical and western blot techniques, in Creutzfeldt-Jacob disease patients, as well as by means of western blot in this same line of transgenic mice infected with BSE (240).

2.2.- The boTg110 mice infected by BSE

The ECM studies cited avobe had been developed in humans, for that reason they only showed the terminal stage of the disease, and there was not information about the relationship between the ECM and the PrPres deposition and glial activation. And in AQPs, the same lack of information was also found. For that reason, the studies 2 and 3 of this thesis were developed in the transgenic mouse line boTg110, which had already been characterized by its response to intracranial infection with the BSE1 inoculum (241). Based on this, two different study points were chosen throughout the disease:

- 150 days post-inoculation (dpi): an initial stage of the disease, in which the PrPres begins to be detectable in the brain of these animals with immunohistochemical and western blot techniques. Therefore, it can already be confirmed that the infection has occurred even though no clinical sign is yet observed (241).

- 300 dpi: the terminal stage of the disease, in which the animals show obvious PrPres deposits and a very noticeable clinical signs (241).

In studies 2 and 3, in the initial stage of the disease (150 dpi), we observed that the PNNs and some of their components such as the aggrecan and the HA did not show any change with respect to their controls. Variations in the expression of the AQP1 and AQP4 were also not observed.

On the other hand, in the final stage of the disease (300 dpi) there was an obvious loss of PNNs, which implied a loss of aggrecan and the disorganization of the HA. Likewise, the expression of AQP1 and AQP4 increased considerably in the astrocytes membrane.

The situation of the mouse ECM in the initial stage of the disease was similar to what was observed in natural cases of BSE: deposits of PrPres were found without clinical symptoms, and on the other hand the PNNs were well-preserved, even around the neurons with significant vacuolization (248). The mice in the terminal stage showed a comparable situation to the one described in the human TSEs, where a very significant loss of PNNs was observed in subjects that had died due to the advanced stage of the TSE they were afflicted with (230, 231). Moreover, the

immunohistochemical study of the distribution of the PrPres deposits, the microglia and the astrocytes showed that in the areas with greater PrPres deposition, the glial activation was more evident, showing a greater loss of the PNNs and their components.

The increase of the expression of the AQP1 and AQP4 in the final stage of the disease also coincided with a clear PrPres deposition and significant glial activation, thus being comparable to the observations described in humans affected by Creutzfeldt-Jacob disease and mice infected with BSE (240).

2.3.- Study of the BSE field cases

In study 3, AQP1 and AQP4 were studied for the purpose of comparing the transgenic mouse model with field cases of the disease. Cattle diagnosed with BSE from the TSE active surveillance programme of Catalonia were also added. These animals still had not showed any detectable clinical signs at the time of sacrifice, but did have a clear PrPres deposition and obvious glial activation. As they were BSE field cases, neither the time, form nor dosage with which the infection had occurred was known. For this reason, individuals were chosen that showed similar histopathological lesions, and similar PrPres deposition and glial activation levels.

The results obtained with western blot showed that overexpression of AQP1 was mainly observed at 28kDa band (a non-glycosylated form) whereas at 36kDa band (a glycosylated form) (249) the increase was much more discrete. This suggests that post-transcriptional modification due glycosylation can not be produced. On the other hand, AQP4 also showed two bands of 31kDa and 35kDa which corresponded with two different isoforms generated by alternative splicing (127). In this case, both showed very similar increase of expression.

Nevertheless, the increase of expression of AQPs showed a rather clear variability between the individuals analyzed by western blot. We observed that in the animals with a greater increase of AQP1, the increase of AQP4 was very discrete and vice versa, suggesting that perhaps both AQPs could work together, in spite of the fact that in order to confirm it, the sample size, which is quite small (n = 6 BSE cases), would have to be wider.

On the other hand, the immunohistochemical study did not reflect this variability. This could be due to the fact that through immunohistochemistry, an individual assessment of each area is completed and the differences observed are very small, whereas with western blot, a very large area, the entire mesencephalon, is assessed and thus there are more differences and they are more obvious.

With immunohistochemistry and western blot techniques we have also seen how the increase of AQP1 and AQP4 occurs in the natural form of BSE. This happens relatively early in the course of the disease because these animals, unlike the mice in the terminal disease stage, still did not show detectable clinical signs, but did show significant glial activations and PrPres deposition.

2.4.- The ECM in the BSE pathogeny: study 2

In studies developed in cell cultures, it was proven that the presence of PrPres or parts of this can activate neurons and astrocytes (250, 251) and favour the recruitment of microglia (208). In study 2, we observed a correlation between the presence of PrPres, activated astrocytes and microglia, and the loss of PNN. When the glia is activated produces metalloproteases (90), enzymes that have the capacity to degrade the ECM proteins, such as the aggrecan, which has been proven in human and primate chronic encephalitis (252, 253). In in vitro studies, it has also been seen how the astrocytes produce mostly MMP-2, while the microglia produce MMP-9 (90, 254), two enzymes that play a key role in the activation of the ECM degradation cascade (94, 98). Therefore, this could explain why the ECM, specifically the PNNs and aggrecan, disappear at the terminal stages of the disease.

We also observed the disorganization of HA in the terminal stage of the disease. This may be due to two factors: first, the loss of proteins with those that interact according to the HTL model (6), in such a way that the structure of the PNNs is lost and its appearance becomes anarchic. Secondly, as occurs with the proteins such as the aggrecan, the HA could be degraded by the activated glia, as has already been proven in other processes like tumoral invasion, wound healing or stroke lesions, where the glia is activated and secretes hyaluronidases, the enzymes that degrade the HA (56). The fragments that are generated have different properties according to their size, including the capacity to activate more glial cells (55). It is possible that one of these phenomena, or both, also occurs during BSE.

From a functional point of view, the alterations in the ECM proteins and HA can upset the PNN structural balance, and thus change their properties and, therefore, the association with water and ions (6). At the same time, the microenvironment the neurons need around them would be modified, thus altering their functionality; the synapsis could retract or even the neurons could die (230, 231).

The opposite situation, where the PNNs disappear as a consequence of the loss of the neurons, must also be taken into consideration; nevertheless, it is believed that this process occurs in acute situations (255). In chronic situations such as the TSEs, the most likely is that the activated glial cells destroy the MEC progressively before the neuron disappears (230, 252, 253).

Therefore, we could summarize the situation in the following way: in BSE, the PrPres accumulates from the beginning of the disease before the PNNs disappear. In more advanced stages of the disease, as the PrPres accumulates, the level of glial activation increases; then enzymes are produced that progressively digest the aggrecan and HA and, as a result, the PNNs disappear. This alteration of the ECM would imply alterations in the microenvironment surrounding the neurons and this could end up causing dysfunctions and finally, neuronal death.

We have observed how the PNN and the aggrecan disappeared in these mice affected by BSE in the terminal phase. In the study presented in the annexe for study 2, conducted on mice affected by Scrapie, we have shown that in the terminal stage of

the disease, the PNN and some of their components such as the brevican and tenascin-R also disappeared; however the expression of neurocan increased. This phenomenon, where the typical components of the mature brain stop expressing themselves and the components which are more typical of the developing encephalon such as neurocan are expressed, has been described in several diseases where remodelation of the nervous tissue occurs: multiple sclerosis (256, 257), ischemic lesions (258), epileptic seizures (21, 22, 259, 260), Alzheimer disease (261, 262) and gliomas (263, 264). In the course of the TSEs, a similar remodelation process may occur. It could be an attempt of the nervous tissue to repair the loss neuronal processes and recover the plasticity to re-establish the synaptic contacts (22, 265, 266), although this is an area that still must be studied in depth.

2.5.- The AQPs in the BSE pathogeny: study 3

The AQP1 as well as the AQP4 act as water channels (103, 125) and it is believed that they play a very significant role in controlling and circulating the water in the extracellular space of the CNS. Therefore, it would be likely that their overexpression would influence or even cause significant changes in the homeostasis of the CNS water. In fact, the opposite situation, where there are no AQPs, has been studied in AQP4 knock-out mice. In an acute water intoxication model, its absence reduces the formation of cerebral oedemas and improves survival, in acute ischemic stroke models, it reduces the neurological damage and in a murine bacterial meningitis model, it improves survival (267), proving the importance of the flow of water in the CNS inflammation pathogeny. These references could suggest that the overexpression of AQP1 and AQP4 may also alter the flow of water in the CNS and negatively influence neuronal survival. But, despite this, the role the AQPs play in the in vivo pathological processes is still not well-enough understood.

It has been proven that AQP1 and AQP4 are constitutively expressed in reactive astrocytes (112), independently of the cause. This has been linked to the migration capacity of astrocytes (268) and it has also been seen that the same thing can happen with the microglia when it is activated (208, 269). This allows for the cell migration speed to increase and a mechanism has been proposed to explain it, where the phenomenon of cytoskeleton polymerization also intervene (104, 131). Moreover, it must be taken into consideration that the modifications of the cytoskeleton always involve changes to the cell morphology, which also affect the volume of extracellular space, and as a result, the change in volume can include changes in cell excitability (270).

AQP4 can indirectly influence the ionic composition of the extracellular space (271), given that it is located in the astrocyte membrane along with the K^+ channel Kir4.1. Despite it still not being possible to determine how this relationship works, it seems that in accordance with the amount of water the AQPs intake, the amount of K^+ the Kir4.1 canal intake can vary, which means it can influence the rapid transduction of signals and the excitable cells function (129, 130). It is possible that the inability to maintain the homeostasis, of water and K^+, in areas with high neuronal activity ends up causing excessive neuronal discharge (272, 273).

It has also been suggested that the overexpression of AQP1 and AQP4 may intervene in the formation of the vacuoles in the TSEs (240). Although it is still not known through which mechanism the vacuoles and spongiotic changes, which are typical of the TSEs, are formed, in electronic microscopic studies, it has been observed that tubulovesicular structures which could end up converging and giving rise to the vacuoles which are typical of the disease (274, 275, 276, 277). Therefore, it is possible that the overexpression of AQPs and their consequences influence their formation.

The results of the study 3 indicate that the PrPres which activates the glial cells is deposited at the beginning of the disease. Then, the glia begins to overexpress AQP1 and 4. Even though we don't know exactly when, it most likely happens before clinical signs appear. As has been proven in many other inflammatory phenomena of the encephalon, the AQPs are expressed adaptatively in the glial cells in order to facilitate their migration after activation, and therefore, the result may be an alteration in the balance of the water and ion homeostasis, which alter the normal cellular compartmentalization and contribute to the formation of vacuoles.

3.- THE PrPres, GLIAL CELLS, MEC AND AQPS

As far as we have been able to observe in studies 2 and 3, it seems that during the course of the BSE, PrPres deposits begin to form before the PNN disappear and while the glia progressively activates.

As the glia activates, the AQP1 and AQP4 begin to be expressed in its membrane, most likely adaptively in order to facilitate its migration. As a result, this can alter the water concentrations in the extracellular space and produce some kind of neuronal malfunction (figure 1). This phenomenon begins forming early in the course of the disease before any obvious clinical signs appear as indicated by the results observed in cattle.

The activated glia also produces enzymes that degrade the ECM and can end up causing the disappearance of the PNN, aggrecan and the alterations observed in the HA. Given the hydrophilic and anionic properties of these elements, its absence can also influence the ion and water concentrations in the extracellular space as well as neural functionality (figure 1). Furthermore, the ECM changes could also lead the retraccion of dendrites and the loss of synaptic contacts.

Therefore, we propose a model where the ECM and AQP modifications in the course of the BSE are due to glial activation, as none of the changes appear before this is obvious. And these alterations can end up modifying the quantities of water and ions in the extracellular space, and therefore the microenvironment surrounding the neurons and as a result, produce neuronal dysfunctions and end up causing neuronal death.

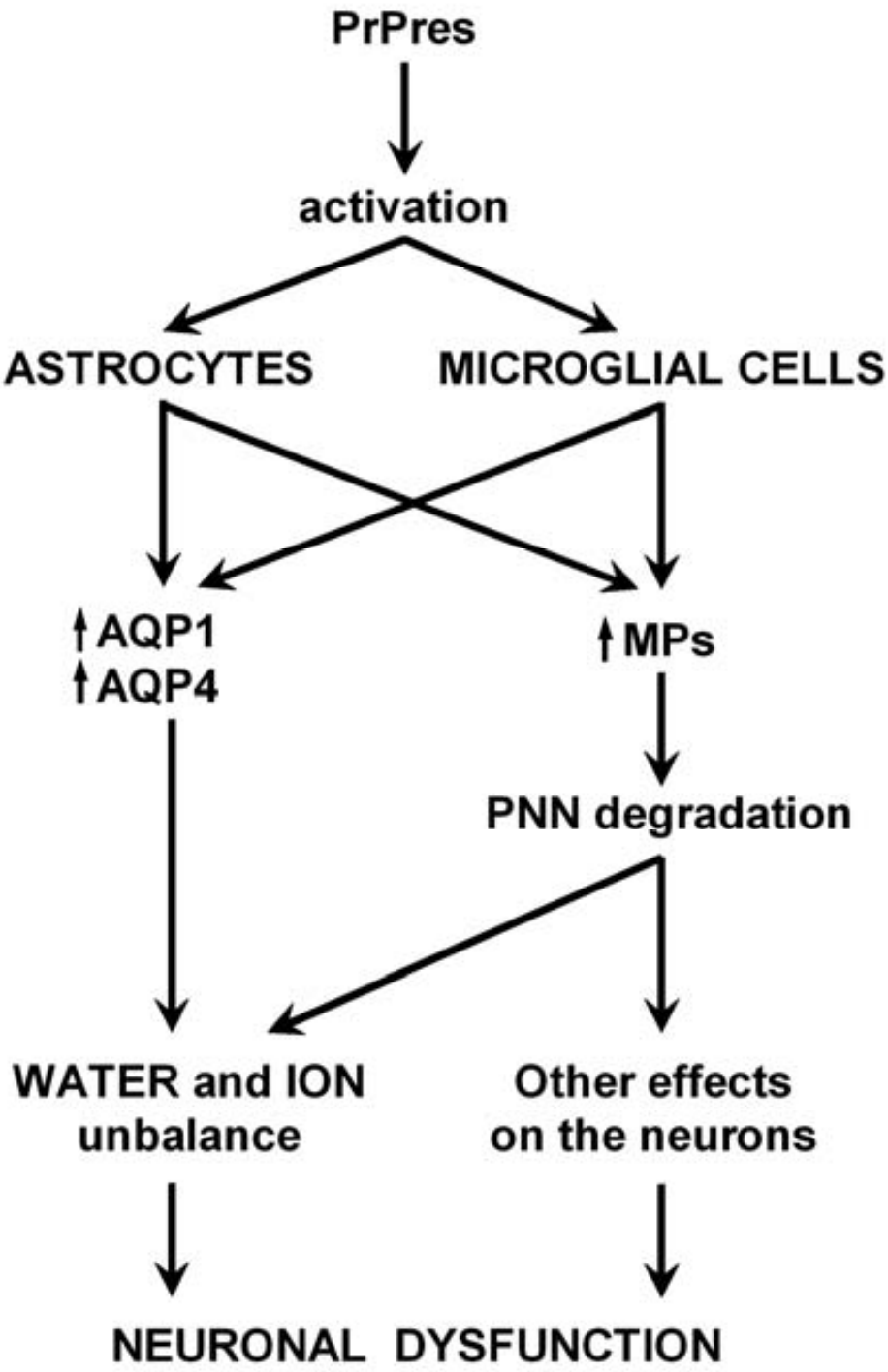

Figure 1: Proposed model for the influence of ECM, AQP1 and AQP4 on BSE pathogeny.

CONCLUSIONS

1.- The PNN, aggrecan, HA and HSPG, have a very extensive and heterogeneous distribution in the CNS. The aggrecan have a distribution which is practically identical to that of the PNN marked with WFA. The HA also coincides with this PNN distribution, but it also has a very extensive distribution in the neuropile. The HSPG distribution partially coincides with the PNN distribution, as is also very extensive in the neuropile.

2.- The PNN, aggrecan, HA and HSPG are mostly found in GABAergic nuclei, however these elements are very scarce or inexistent in aminergic nuclei. Therefore, the distribution of the ECM elements could be linked to the functional needs of the types of surrounding neurons.

3.- The AQP4 has a very heterogeneous distribution, which is not only limited to the astrocyte end-feet that form the external and internal glial limitans, but is also located in the neuropile of several areas of the CNS.

4.- The distribution of AQP4 and HSPG widely coincides, suggesting the possibility that both elements may be organized by forming some kind of complex.

5.- The areas with a very scarce staining of WFA, aggrecan and HA show an extensive expression of AQP4, and vice versa, suggesting that in an ECM which is very rich in hydrophilic molecules, water can easily circulate through the extracellular space, whereas in regions where the ECM is scarce, the water diffusion mechanism would mainly be through the AQP4. Nevertheless, in some areas, all of the elements are expressed at the same time, suggesting that they may work together.

6.- In the boTg110 transgenic mouse at the initial stages of the BSE, PrPres deposition is observed, but there are no alterations to the PNN, aggrecan or HA.

7.- In the boTg110 transgenic mouse at the terminal stages of the BSE, the loss of the PNN and aggrecan as well as alterations to the HA are observed. In C57BL/6 mice, in the final stages of Scrapie, the PNN, tenascin-R and brevican disappear, and alterations in the HA are observed, while the neurocan increases. These changes are related to the presence of activated astrocytes and PrPres deposits. The ECM alterations observed in BSE and Scrapie could alter the homeostasis of the extracellular space and synapsis and, as result, produce neuronal dysfunctions.

8.- In the terminal stages of BSE, in the boTg100 transgenic mouse, and in field cases of BSE, the expression of AQP1 and AQP4 in the astrocyte membrane increases, especially in the areas with the most glial activation and PrPres presence. This increase in expression occurs after the accumulation of PrPres and prior to the appearance of clinical signs. The overexpression of AQP1 and AQP4 could lead to ionic and water unbalances in the extracellular space and as result, in neuronal dysfunctions.

9.- The boTg110 transgenic mouse has behaved similarly to BSE field cases, thus proving that it can be a useful model for the study of BSE through intracranial infection.

BIBLIOGRAPHY

1. Gartner L P, Hiatt J L. Histología: texto y atlas. McGraw-Hill Interamericana. 1st ed. (1997).
2. Bruckner G, Brauer K, Hartig W, Wolff J R, Rickmann M J, Derouiche A, Delpech B, Girard N, Oertel W H, Reichenbach A. Perineuronal nets provide a polyanionic, glia-associated form of microenvironment around certain neurons in many parts of the rat brain. Glia. (1993) 8: 183-200.
3. Bruckner G, Szeoke S, Pavlica S, Grosche J, Kacza J. Axon initial segment ensheathed by extracellular matrix in perineuronal nets. Neuroscience. (2006) 138: 365-75.
4. Celio M R, Blumcke I. Perineuronal nets--a specialized form of extracellular matrix in the adult nervous system. Brain Res Brain Res Rev. (1994) 19: 128-45.
5. Celio M R, Spreafico R, De Biasi S, Vitellaro-Zuccarello L. Perineuronal nets: past and present. Trends Neurosci. (1998) 21: 510-5.
6. Yamaguchi Y. Lecticans: organizers of the brain extracellular matrix. Cell Mol Life Sci. (2000) 57: 276-89.
7. Bandtlow C E, Zimmermann D R. Proteoglycans in the developing brain: new conceptual insights for old proteins. Physiol Rev. (2000) 80: 1267-90.
8. Carulli D, Rhodes K E, Brown D J, Bonnert T P, Pollack S J, Oliver K, Strata P, Fawcett J W. Composition of perineuronal nets in the adult rat cerebellum and the cellular origin of their components. J Comp Neurol. (2006) 494: 559-77.
9. Deepa S S, Carulli D, Galtrey C, Rhodes K, Fukuda J, Mikami T, Sugahara K, Fawcett J W. Composition of perineuronal net extracellular matrix in rat brain: a different disaccharide composition for the net-associated proteoglycans. J Biol Chem. (2006) 281: 17789-800.
10. Milev P, Maurel P, Chiba A, Mevissen M, Popp S, Yamaguchi Y, Margolis R K, Margolis R U. Differential regulation of expression of hyaluronan-binding proteoglycans in developing brain: aggrecan, versican, neurocan, and brevican. Biochem Biophys Res Commun. (1998) 247: 207-12.
11. Fryer H J, Kelly G M, Molinaro L, Hockfield S. The high molecular weight Cat-301 chondroitin sulfate proteoglycan from brain is related to the large aggregating proteoglycan from cartilage, aggrecan. J Biol Chem. (1992) 267: 9874-83.
12. Matthews R T, Kelly G M, Zerillo C A, Gray G, Tiemeyer M, Hockfield S. Aggrecan glycoforms contribute to the molecular heterogeneity of perineuronal nets. J Neurosci. (2002) 22: 7536-47.
13. Bode-Lesniewska B, Dours-Zimmermann M T, Odermatt B F, Briner J, Heitz P U, Zimmermann D R. Distribution of the large aggregating proteoglycan versican in adult human tissues. J Histochem Cytochem. (1996) 44: 303-12.
14. Asher R A, Morgenstern D A, Shearer M C, Adcock K H, Pesheva P, Fawcett J W. Versican is upregulated in CNS injury and is a product of oligodendrocyte lineage cells. J Neurosci. (2002) 22: 2225-36.
15. Schmalfeldt M, Dours-Zimmermann M T, Winterhalter K H, Zimmermann D R. Versican V2 is a major extracellular matrix component of the mature bovine brain. J Biol Chem. (1998) 273: 15758-64.
16. Ogawa T, Hagihara K, Suzuki M, Yamaguchi Y. Brevican in the developing hippocampal fimbria: differential expression in myelinating oligodendrocytes and adult astrocytes suggests a dual role for brevican in central nervous system fiber tract development. J Comp Neurol. (2001) 432: 285-95.
17. Hagihara K, Miura R, Kosaki R, Berglund E, Ranscht B, Yamaguchi Y. Immunohistochemical evidence for the brevican-tenascin-R interaction: colocalization in perineuronal nets suggests a physiological role for the interaction in the adult rat brain. J Comp Neurol. (1999) 410: 256-64.
18. Yamada H, Fredette B, Shitara K, Hagihara K, Miura R, Ranscht B, Stallcup W B, Yamaguchi Y. The brain chondroitin sulfate proteoglycan brevican associates with astrocytes ensheathing cerebellar glomeruli and inhibits neurite outgrowth from granule neurons. J Neurosci. (1997) 17: 7784-95.
19. Gary S C, Zerillo C A, Chiang V L, Gaw J U, Gray G, Hockfield S. cDNA cloning, chromosomal localization, and expression analysis of human BEHAB/brevican, a brain specific proteoglycan regulated during cortical development and in glioma. Gene. (2000) 256: 139-47.
20. Meyer-Puttlitz B, Milev P, Junker E, Zimmer I, Margolis R U, Margolis R K. Chondroitin sulfate and chondroitin/keratan sulfate proteoglycans of nervous tissue: developmental changes of neurocan and phosphacan. J Neurochem. (1995) 65: 2327-37.

21. Okamoto M, Sakiyama J, Mori S, Kurazono S, Usui S, Hasegawa M, Oohira A. Kainic acid-induced convulsions cause prolonged changes in the chondroitin sulfate proteoglycans neurocan and phosphacan in the limbic structures. Exp Neurol. (2003) 184: 179-95.

22. Matsui F, Kawashima S, Shuo T, Yamauchi S, Tokita Y, Aono S, Keino H, Oohira A. Transient expression of juvenile-type neurocan by reactive astrocytes in adult rat brains injured by kainate-induced seizures as well as surgical incision. Neuroscience. (2002) 112: 773-81.

23. Matsui F, Nishizuka M, Yasuda Y, Aono S, Watanabe E, Oohira A. Occurrence of a N-terminal proteolytic fragment of neurocan, not a C-terminal half, in a perineuronal net in the adult rat cerebrum. Brain Res. (1998) 790: 45-51.

24. Haunso A, Celio M R, Margolis R K, Menoud P A. Phosphacan immunoreactivity is associated with perineuronal nets around parvalbumin-expressing neurones. Brain Res. (1999) 834: 219-22.

25. Dobbertin A, Rhodes K E, Garwood J, Properzi F, Heck N, Rogers J H, Fawcett J W, Faissner A. Regulation of RPTPbeta/phosphacan expression and glycosaminoglycan epitopes in injured brain and cytokine-treated glia. Mol Cell Neurosci. (2003) 24: 951-71.

26. Meyer-Puttlitz B, Junker E, Margolis R U, Margolis R K. Chondroitin sulfate proteoglycans in the developing central nervous system. II. Immunocytochemical localization of neurocan and phosphacan. J Comp Neurol. (1996) 366: 44-54.

27. Jones L L, Yamaguchi Y, Stallcup W B, Tuszynski M H. NG2 is a major chondroitin sulfate proteoglycan produced after spinal cord injury and is expressed by macrophages and oligodendrocyte progenitors. J Neurosci. (2002) 22: 2792-803.

28. Shoshan Y, Nishiyama A, Chang A, Mork S, Barnett G H, Cowell J K, Trapp B D, Staugaitis S M. Expression of oligodendrocyte progenitor cell antigens by gliomas: implications for the histogenesis of brain tumors. Proc Natl Acad Sci U S A. (1999) 96: 10361-6.

29. Properzi F, Fawcett J W. Proteoglycans and brain repair. News Physiol Sci. (2004) 19: 33-8.

30. Schwartz N B, Domowicz M. Proteoglycans in brain development. Glycoconj J. (2004) 21: 329-41.

31. Yamaguchi Y. Heparan sulfate proteoglycans in the nervous system: their diverse roles in neurogenesis, axon guidance, and synaptogenesis. Semin Cell Dev Biol. (2001) 12: 99-106.

32. Winkler S, Stahl R C, Carey D J, Bansal R. Syndecan-3 and perlecan are differentially expressed by progenitors and mature oligodendrocytes and accumulate in the extracellular matrix. J Neurosci Res. (2002) 69: 477-87.

33. Yamaguchi Y. Glycobiology of the synapse: the role of glycans in the formation, maturation, and modulation of synapses. Biochim Biophys Acta. (2002) 1573: 369-76.

34. Ethell I M, Yamaguchi Y. Cell surface heparan sulfate proteoglycan syndecan-2 induces the maturation of dendritic spines in rat hippocampal neurons. J Cell Biol. (1999) 144: 575-86.

35. Ruegg M A, Tsim K W, Horton S E, Kroger S, Escher G, Gensch E M, McMahan U J. The agrin gene codes for a family of basal lamina proteins that differ in function and distribution. Neuron. (1992) 8: 691-9.

36. O'Connor L T, Lauterborn J C, Gall C M, Smith M A. Localization and alternative splicing of agrin mRNA in adult rat brain: transcripts encoding isoforms that aggregate acetylcholine receptors are not restricted to cholinergic regions. J Neurosci. (1994) 14: 1141-52.

37. Aviezer D, Hecht D, Safran M, Eisinger M, David G, Yayon A. Perlecan, basal lamina proteoglycan, promotes basic fibroblast growth factor-receptor binding, mitogenesis, and angiogenesis. Cell. (1994) 79: 1005-13.

38. Shee W L, Ong W Y, Lim T M. Distribution of perlecan in mouse hippocampus following intracerebroventricular kainate injections. Brain Res. (1998) 799: 292-300.

39. Joseph S J, Ford M D, Barth C, Portbury S, Bartlett P F, Nurcombe V, Greferath U. A proteoglycan that activates fibroblast growth factors during early neuronal development is a perlecan variant. Development. (1996) 122: 3443-52.

40. Bernfield M, Gotte M, Park P W, Reizes O, Fitzgerald M L, Lincecum J, Zako M. Functions of cell surface heparan sulfate proteoglycans. Annu Rev Biochem. (1999) 68: 729-77.

41. Joester A, Faissner A. The structure and function of tenascins in the nervous system. Matrix Biol. (2001) 20: 13-22.

42. Deckner M, Lindholm T, Cullheim S, Risling M. Differential expression of tenascin-C, tenascin-R, tenascin/J1, and tenascin-X in spinal cord scar tissue and in the olfactory system. Exp Neurol. (2000) 166: 350-62.

43. Kawano H, Ohyama K, Kawamura K, Nagatsu I. Migration of dopaminergic neurons in the embryonic mesencephalon of mice. Brain Res Dev Brain Res. (1995) 86: 101-13.

44. Gonzalez M L, Silver J. Axon-glia interactions regulate ECM patterning in the postnatal rat olfactory bulb. J Neurosci. (1994) 14: 6121-31.

45. Laywell E D, Dorries U, Bartsch U, Faissner A, Schachner M, Steindler D A. Enhanced expression of the developmentally regulated extracellular matrix molecule tenascin following adult brain injury. Proc Natl Acad Sci U S A. (1992) 89: 2634-8.

46. Gladson C L. The extracellular matrix of gliomas: modulation of cell function. J Neuropathol Exp Neurol. (1999) 58: 1029-40.

47. Norenberg U, Hubert M, Rathjen F G. Structural and functional characterization of tenascin-R (restrictin), an extracellular matrix glycoprotein of glial cells and neurons. Int J Dev Neurosci. (1996) 14: 217-31.

48. Carnemolla B, Leprini A, Borsi L, Querze G, Urbini S, Zardi L. Human tenascin-R. Complete primary structure, pre-mRNA alternative splicing and gene localization on chromosome 1q23-q24. J Biol Chem. (1996) 271: 8157-60.

49. Probstmeier R, Stichel C C, Muller H W, Asou H, Pesheva P. Chondroitin sulfates expressed on oligodendrocyte-derived tenascin-R are involved in neural cell recognition. Functional implications during CNS development and regeneration. J Neurosci Res. (2000) 60: 21-36.

50. Wintergerst E S, Rathjen F G, Schwaller B, Eggli P, Celio M R. Tenascin-R associates extracellularly with parvalbumin immunoreactive neurones but is synthesised by another neuronal population in the adult rat cerebral cortex. J Neurocytol. (2001) 30: 293-301.

51. Tammi M I, Day A J, Turley E A. Hyaluronan and homeostasis: a balancing act. J Biol Chem. (2002) 277: 4581-4.

52. Sherman L S, Struve J N, Rangwala R, Wallingford N M, Tuohy T M, Kuntz C t. Hyaluronate-based extracellular matrix: keeping glia in their place. Glia. (2002) 38: 93-102.

53. Bignami A, Asher R, Perides G. Co-localization of hyaluronic acid and chondroitin sulfate proteoglycan in rat cerebral cortex. Brain Res. (1992) 579: 173-7.

54. Bignami A, Asher R. Some observations on the localization of hyaluronic acid in adult, newborn and embryonal rat brain. Int J Dev Neurosci. (1992) 10: 45-57.

55. Stern R. Devising a pathway for hyaluronan catabolism: are we there yet? Glycobiology. (2003) 13: 105R-15R.

56. Al'Qteishat A, Gaffney J, Krupinski J, Rubio F, West D, Kumar S, Kumar P, Mitsios N, Slevin M. Changes in hyaluronan production and metabolism following ischaemic stroke in man. Brain. (2006) 129: 2158-76.

57. Csoka T B, Frost G I, Stern R. Hyaluronidases in tissue invasion. Invasion Metastasis. (1997) 17: 297-311.

58. Lundell A, Olin A I, Morgelin M, al-Karadaghi S, Aspberg A, Logan D T. Structural basis for interactions between tenascins and lectican C-type lectin domains: evidence for a crosslinking role for tenascins. Structure. (2004) 12: 1495-506.

59. Bruckner G, Hartig W, Kacza J, Seeger J, Welt K, Brauer K. Extracellular matrix organization in various regions of rat brain grey matter. J Neurocytol. (1996) 25: 333-46.

60. Engel M, Maurel P, Margolis R U, Margolis R K. Chondroitin sulfate proteoglycans in the developing central nervous system. I. cellular sites of synthesis of neurocan and phosphacan. J Comp Neurol. (1996) 366: 34-43.

61. Oohashi T, Hirakawa S, Bekku Y, Rauch U, Zimmermann D R, Su W D, Ohtsuka A, Murakami T, Ninomiya Y. Bral1, a brain-specific link protein, colocalizing with the versican V2 isoform at the nodes of Ranvier in developing and adult mouse central nervous systems. Mol Cell Neurosci. (2002) 19: 43-57.

62. Toole B P. Hyaluronan in morphogenesis. Semin Cell Dev Biol. (2001) 12: 79-87.

63. Kujawa M J, Pechak D G, Fiszman M Y, Caplan A I. Hyaluronic acid bonded to cell culture surfaces inhibits the program of myogenesis. Dev Biol. (1986) 113: 10-6.

64. Kinnunen A, Niemi M, Kinnunen T, Kaksonen M, Nolo R, Rauvala H. Heparan sulphate and HB-GAM (heparin-binding growth-associated molecule) in the development of the thalamocortical pathway of rat brain. Eur J Neurosci. (1999) 11: 491-502.

65. Kinnunen A, Kinnunen T, Kaksonen M, Nolo R, Panula P, Rauvala H. N-syndecan and HB-GAM (heparin-binding growth-associated molecule) associate with early axonal tracts in the rat brain. Eur J Neurosci. (1998) 10: 635-48.

66. Hockfield S, Kalb R G, Zaremba S, Fryer H. Expression of neural proteoglycans correlates with the acquisition of mature neuronal properties in the mammalian brain. Cold Spring Harb Symp Quant Biol. (1990) 55: 505-14.

67. Rhodes K E, Fawcett J W. Chondroitin sulphate proteoglycans: preventing plasticity or protecting the CNS? J Anat. (2004) 204: 33-48.

68. Hartig W, Derouiche A, Welt K, Brauer K, Grosche J, Mader M, Reichenbach A, Bruckner G. Cortical neurons immunoreactive for the potassium channel Kv3.1b subunit are predominantly surrounded by perineuronal nets presumed as a buffering system for cations. Brain Res. (1999) 842: 15-29.

69. Brakebusch C, Seidenbecher C I, Asztely F, Rauch U, Matthies H, Meyer H, Krug M, Bockers T M, Zhou X, Kreutz M R, Montag D, Gundelfinger E D, Fassler R. Brevican-deficient mice display impaired hippocampal CA1 long-term potentiation but show no obvious deficits in learning and memory. Mol Cell Biol. (2002) 22: 7417-27.

70. Bruckner G, Bringmann A, Hartig W, Koppe G, Delpech B, Brauer K. Acute and long-lasting changes in extracellular-matrix chondroitin-sulphate proteoglycans induced by injection of chondroitinase ABC in the adult rat brain. Exp Brain Res. (1998) 121: 300-10.

71. Fox K, Caterson B. Neuroscience. Freeing the bain from the perineuronal net. Science. (2002) 298: 1187-9.

72. Moon L D, Asher R A, Fawcett J W. Limited growth of severed CNS axons after treatment of adult rat brain with hyaluronidase. J Neurosci Res. (2003) 71: 23-37.

73. Pizzorusso T, Medini P, Berardi N, Chierzi S, Fawcett J W, Maffei L. Reactivation of ocular dominance plasticity in the adult visual cortex. Science. (2002) 298: 1248-51.

74. Murakami T, Ohtsuka A. Perisynaptic barrier of proteoglycans in the mature brain and spinal cord. Arch Histol Cytol. (2003) 66: 195-207.

75. Morawski M, Bruckner M K, Riederer P, Bruckner G, Arendt T. Perineuronal nets potentially protect against oxidative stress. Exp Neurol. (2004) 188: 309-15.

76. Crichton R R, Wilmet S, Legssyer R, Ward R J. Molecular and cellular mechanisms of iron homeostasis and toxicity in mammalian cells. J Inorg Biochem. (2002) 91: 9-18.

77. Bruckner G, Hausen D, Hartig W, Drlicek M, Arendt T, Brauer K. Cortical areas abundant in extracellular matrix chondroitin sulphate proteoglycans are less affected by cytoskeletal changes in Alzheimer's disease. Neuroscience. (1999) 92: 791-805.

78. Porta E A. Pigments in aging: an overview. Ann N Y Acad Sci. (2002) 959: 57-65.

79. Forsberg E, Hirsch E, Frohlich L, Meyer M, Ekblom P, Aszodi A, Werner S, Fassler R. Skin wounds and severed nerves heal normally in mice lacking tenascin-C. Proc Natl Acad Sci U S A. (1996) 93: 6594-9.

80. Weber P, Bartsch U, Rasband M N, Czaniera R, Lang Y, Bluethmann H, Margolis R U, Levinson S R, Shrager P, Montag D, Schachner M. Mice deficient for tenascin-R display alterations of the extracellular matrix and decreased axonal conduction velocities in the CNS. J Neurosci. (1999) 19: 4245-62.

81. Rauch U, Zhou X H, Roos G. Extracellular matrix alterations in brains lacking four of its components. Biochem Biophys Res Commun. (2005) 328: 608-17.

82. Mjaatvedt C H, Yamamura H, Capehart A A, Turner D, Markwald R R. The Cspg2 gene, disrupted in the hdf mutant, is required for right cardiac chamber and endocardial cushion formation. Dev Biol. (1998) 202: 56-66.

83. Watanabe H, Kimata K, Line S, Strong D, Gao L Y, Kozak C A, Yamada Y. Mouse cartilage matrix deficiency (cmd) caused by a 7 bp deletion in the aggrecan gene. Nat Genet. (1994) 7: 154-7.

84. Asher R A, Morgenstern D A, Moon L D, Fawcett J W. Chondroitin sulphate proteoglycans: inhibitory components of the glial scar. Prog Brain Res. (2001) 132: 611-9.

85. Bradbury E J, Moon L D, Popat R J, King V R, Bennett G S, Patel P N, Fawcett J W, McMahon S B. Chondroitinase ABC promotes functional recovery after spinal cord injury. Nature. (2002) 416: 636-40.

86. Moon L D, Asher R A, Rhodes K E, Fawcett J W. Regeneration of CNS axons back to their target following treatment of adult rat brain with chondroitinase ABC. Nat Neurosci. (2001) 4: 465-6.

87. Noble P W. Hyaluronan and its catabolic products in tissue injury and repair. Matrix Biol. (2002) 21: 25-9.

88. Termeer C, Sleeman J P, Simon J C. Hyaluronan--magic glue for the regulation of the immune response? Trends Immunol. (2003) 24: 112-4.

89. Termeer C C, Hennies J, Voith U, Ahrens T, Weiss J M, Prehm P, Simon J C. Oligosaccharides of hyaluronan are potent activators of dendritic cells. J Immunol. (2000) 165: 1863-70.

90. Gottschall P E, Deb S. Regulation of matrix metalloproteinase expressions in astrocytes, microglia and neurons. Neuroimmunomodulation. (1996) 3: 69-75.

91. Gottschall P E, Yu X. Cytokines regulate gelatinase A and B (matrix metalloproteinase 2 and 9) activity in cultured rat astrocytes. J Neurochem. (1995) 64: 1513-20.

92. Oh L Y, Larsen P H, Krekoski C A, Edwards D R, Donovan F, Werb Z, Yong V W. Matrix metalloproteinase-9/gelatinase B is required for process outgrowth by oligodendrocytes. J Neurosci. (1999) 19: 8464-75.

93. Rosenberg G A. Matrix metalloproteinases in neuroinflammation. Glia. (2002) 39: 279-91.

94. Yong V W, Krekoski C A, Forsyth P A, Bell R, Edwards D R. Matrix metalloproteinases and diseases of the CNS. Trends Neurosci. (1998) 21: 75-80.

95. Chang C, Werb Z. The many faces of metalloproteases: cell growth, invasion, angiogenesis and metastasis. Trends Cell Biol. (2001) 11: S37-43.

96. Huovila A P, Turner A J, Pelto-Huikko M, Karkkainen I, Ortiz R M. Shedding light on ADAM metalloproteinases. Trends Biochem Sci. (2005) 30: 413-22.

97. Apte S S. A disintegrin-like and metalloprotease (reprolysin type) with thrombospondin type 1 motifs: the ADAMTS family. Int J Biochem Cell Biol. (2004) 36: 981-5.

98. Crocker S J, Pagenstecher A, Campbell I L. The TIMPs tango with MMPs and more in the central nervous system. J Neurosci Res. (2004) 75: 1-11.

99. Lo E H, Wang X, Cuzner M L. Extracellular proteolysis in brain injury and inflammation: role for plasminogen activators and matrix metalloproteinases. J Neurosci Res. (2002) 69: 1-9.

100. Csoka A B, Frost G I, Stern R. The six hyaluronidase-like genes in the human and mouse genomes. Matrix Biol. (2001) 20: 499-508.

101. Wasson K. Phenotypes of aquaporin mutants in genetically altered mice. Comp Med. (2006) 56: 96-104.

102. Preston G M, Agre P. Isolation of the cDNA for erythrocyte integral membrane protein of 28 kilodaltons: member of an ancient channel family. Proc Natl Acad Sci U S A. (1991) 88: 11110-4.

103. Preston G M, Carroll T P, Guggino W B, Agre P. Appearance of water channels in Xenopus oocytes expressing red cell CHIP28 protein. Science. (1992) 256: 385-7.

104. Verkman A S. More than just water channels: unexpected cellular roles of aquaporins. J Cell Sci. (2005) 118: 3225-32.

105. Fujiyoshi Y, Mitsuoka K, de Groot B L, Philippsen A, Grubmuller H, Agre P, Engel A. Structure and function of water channels. Curr Opin Struct Biol. (2002) 12: 509-15.

106. Stroud R M, Nollert P, Miercke L. The glycerol facilitator GlpF its aquaporin family of channels, and their selectivity. Adv Protein Chem. (2003) 63: 291-316.

107. Verbavatz J M, Ma T, Gobin R, Verkman A S. Absence of orthogonal arrays in kidney, brain and muscle from transgenic knockout mice lacking water channel aquaporin-4. J Cell Sci. (1997) 110 (Pt 22): 2855-60.

108. Verbavatz J M, Brown D, Sabolic I, Valenti G, Ausiello D A, Van Hoek A N, Ma T, Verkman A S. Tetrameric assembly of CHIP28 water channels in liposomes and cell membranes: a freeze-fracture study. J Cell Biol. (1993) 123: 605-18.

109. Badaut J, Lasbennes F, Magistretti P J, Regli L. Aquaporins in brain: distribution, physiology, and pathophysiology. J Cereb Blood Flow Metab. (2002) 22: 367-78.

110. Badaut J, Hirt L, Granziera C, Bogousslavsky J, Magistretti P J, Regli L. Astrocyte-specific expression of aquaporin-9 in mouse brain is increased after transient focal cerebral ischemia. J Cereb Blood Flow Metab. (2001) 21: 477-82.

111. Nielsen S, Nagelhus E A, Amiry-Moghaddam M, Bourque C, Agre P, Ottersen O P. Specialized membrane domains for water transport in glial cells: high-resolution immunogold cytochemistry of aquaporin-4 in rat brain. J Neurosci. (1997) 17: 171-80.

112. Venero J L, Vizuete M L, Ilundain A A, Machado A, Echevarria M, Cano J. Detailed localization of aquaporin-4 messenger RNA in the CNS: preferential expression in periventricular organs. Neuroscience. (1999) 94: 239-50.

113. Yamamoto N, Yoneda K, Asai K, Sobue K, Tada T, Fujita Y, Katsuya H, Fujita M, Aihara N, Mase M, Yamada K, Miura Y, Kato T. Alterations in the expression of the AQP family in cultured rat astrocytes during hypoxia and reoxygenation. Brain Res Mol Brain Res. (2001) 90: 26-38.

114. Denker B M, Smith B L, Kuhajda F P, Agre P. Identification, purification, and partial characterization of a novel Mr 28,000 integral membrane protein from erythrocytes and renal tubules. J Biol Chem. (1988) 263: 15634-42.

115. Herrera M, Hong N J, Garvin J L. Aquaporin-1 transports NO across cell membranes. Hypertension. (2006) 48: 157-64.

116. Nielsen S, Smith B L, Christensen E I, Agre P. Distribution of the aquaporin CHIP in secretory and resorptive epithelia and capillary endothelia. Proc Natl Acad Sci U S A. (1993) 90: 7275-9.

117. King L S, Agre P. Pathophysiology of the aquaporin water channels. Annu Rev Physiol. (1996) 58: 619-48.

118. Nagy G, Szekeres G, Kvell K, Berki T, Nemeth P. Development and characterisation of a monoclonal antibody family against aquaporin 1 (AQP1) and aquaporin 4 (AQP4). Pathol Oncol Res. (2002) 8: 115-24.

119. Shields S D, Mazario J, Skinner K, Basbaum A I. Anatomical and functional analysis of aquaporin 1, a water channel in primary afferent neurons. Pain. (2007)

120. Oshio K, Song Y, Verkman A S, Manley G T. Aquaporin-1 deletion reduces osmotic water permeability and cerebrospinal fluid production. Acta Neurochir Suppl. (2003) 86: 525-8.

121. Oshio K, Watanabe H, Song Y, Verkman A S, Manley G T. Reduced cerebrospinal fluid production and intracranial pressure in mice lacking choroid plexus water channel Aquaporin-1. Faseb J. (2005) 19: 76-8.

122. Saadoun S, Papadopoulos M C, Watanabe H, Yan D, Manley G T, Verkman A S. Involvement of aquaporin-4 in astroglial cell migration and glial scar formation. J Cell Sci. (2005)

123. Verkman A S, Binder D K, Bloch O, Auguste K, Papadopoulos M C. Three distinct roles of aquaporin-4 in brain function revealed by knockout mice. Biochim Biophys Acta. (2006) 1758: 1085-93.

124. King L S, Yasui M, Agre P. Aquaporins in health and disease. Mol Med Today. (2000) 6: 60-5.

125. Hasegawa H, Ma T, Skach W, Matthay M A, Verkman A S. Molecular cloning of a mercurial-insensitive water channel expressed in selected water-transporting tissues. J Biol Chem. (1994) 269: 5497-500.

126. Venero J L, Vizuete M L, Machado A, Cano J. Aquaporins in the central nervous system. Prog Neurobiol. (2001) 63: 321-36.

127. Jung J S, Bhat R V, Preston G M, Guggino W B, Baraban J M, Agre P. Molecular characterization of an aquaporin cDNA from brain: candidate osmoreceptor and regulator of water balance. Proc Natl Acad Sci U S A. (1994) 91: 13052-6.

128. Amiry-Moghaddam M, Frydenlund D S, Ottersen O P. Anchoring of aquaporin-4 in brain: molecular mechanisms and implications for the physiology and pathophysiology of water transport. Neuroscience. (2004) 129: 999-1010.

129. Nagelhus E A, Mathiisen T M, Ottersen O P. Aquaporin-4 in the central nervous system: cellular and subcellular distribution and coexpression with KIR4.1. Neuroscience. (2004) 129: 905-13.

130. Nagelhus E A, Horio Y, Inanobe A, Fujita A, Haug F M, Nielsen S, Kurachi Y, Ottersen O P. Immunogold evidence suggests that coupling of K+ siphoning and water transport in rat retinal Muller cells is mediated by a coenrichment of Kir4.1 and AQP4 in specific membrane domains. Glia. (1999) 26: 47-54.

131. Oster G F, Perelson A S. The physics of cell motility. J Cell Sci Suppl. (1987) 8: 35-54.

132. Bruckner G, Grosche J, Hartlage-Rubsamen M, Schmidt S, Schachner M. Region and lamina-specific distribution of extracellular matrix proteoglycans, hyaluronan and tenascin-R in the mouse hippocampal formation. J Chem Neuroanat. (2003) 26: 37-50.

133. Murakami T, Ohtsuka A, Su W D, Taguchi T, Oohashi T, Abe K, Ninomiya Y. The extracellular matrix in the mouse brain: its reactions to endo-alpha-N-acetylgalactosaminidase and certain other enzymes. Arch Histol Cytol. (1999) 62: 273-81.

134. Seeger G, Brauer K, Hartig W, Bruckner G. Mapping of perineuronal nets in the rat brain stained by colloidal iron hydroxide histochemistry and lectin cytochemistry. Neuroscience. (1994) 58: 371-88.

135. Bruckner G, Grosche J, Schmidt S, Hartig W, Margolis R U, Delpech B, Seidenbecher C I, Czaniera R, Schachner M. Postnatal development of perineuronal nets in wild-type mice and in a mutant deficient in tenascin-R. J Comp Neurol. (2000) 428: 616-29.

136. Fernaud-Espinosa I, Nieto-Sampedro M, Bovolenta P. Developmental distribution of glycosaminoglycans in embryonic rat brain: relationship to axonal tract formation. J Neurobiol. (1996) 30: 410-24.

137. Hartig W, Brauer K, Bruckner G. Wisteria floribunda agglutinin-labelled nets surround parvalbumin-containing neurons. Neuroreport. (1992) 3: 869-72.

138. Ojima H, Sakai M, Ohyama J. Molecular heterogeneity of Vicia villosa-recognized perineuronal nets surrounding pyramidal and nonpyramidal neurons in the guinea pig cerebral cortex. Brain Res. (1998) 786: 274-80.

139. Bruckner G, Hartig W, Seeger J, Rubsamen R, Reimer K, Brauer K. Cortical perineuronal nets in the gray short-tailed opossum (Monodelphis domestica): a distribution pattern contrasting with that shown in placental mammals. Anat Embryol (Berl). (1998) 197: 249-62.

140. Adams I, Brauer K, Arelin C, Hartig W, Fine A, Mader M, Arendt T, Bruckner G. Perineuronal nets in the rhesus monkey and human basal forebrain including basal ganglia. Neuroscience. (2001) 108: 285-98.

141. Bertolotto A, Rocca G, Canavese G, Migheli A, Schiffer D. Chondroitin sulfate proteoglycan surrounds a subset of human and rat CNS neurons. J Neurosci Res. (1991) 29: 225-34.

142. Lurie D I, Pasic T R, Hockfield S J, Rubel E W. Development of Cat-301 immunoreactivity in auditory brainstem nuclei of the gerbil. J Comp Neurol. (1997) 380: 319-34.

143. Kalb R G, Hockfield S. Large diameter primary afferent input is required for expression of the Cat-301 proteoglycan on the surface of motor neurons. Neuroscience. (1990) 34: 391-401.

144. Fuxe K, Chadi G, Tinner B, Agnati L F, Pettersson R, David G. On the regional distribution of heparan sulfate proteoglycan immunoreactivity in the rat brain. Brain Res. (1994) 636: 131-8.

145. Fuxe K, Tinner B, Staines W, David G, Agnati L F. Regional distribution of neural cell adhesion molecule immunoreactivity in the adult rat telencephalon and diencephalon. Partial colocalization with heparan sulfate proteoglycan immunoreactivity. Brain Res. (1997) 746: 25-33.

146. McBride P A, Wilson M I, Eikelenboom P, Tunstall A, Bruce M E. Heparan sulfate proteoglycan is associated with amyloid plaques and neuroanatomically targeted PrP pathology throughout the incubation period of scrapie-infected mice. Exp Neurol. (1998) 149: 447-54.

147. Bloch O, Auguste K I, Manley G T, Verkman A S. Accelerated progression of kaolin-induced hydrocephalus in aquaporin-4-deficient mice. J Cereb Blood Flow Metab. (2006)

148. Vitellaro-Zuccarello L, Mazzetti S, Bosisio P, Monti C, De Biasi S. Distribution of Aquaporin 4 in rodent spinal cord: relationship with astrocyte markers and chondroitin sulfate proteoglycans. Glia. (2005) 51: 148-59.

149. Oshio K, Binder D K, Yang B, Schecter S, Verkman A S, Manley G T. Expression of aquaporin water channels in mouse spinal cord. Neuroscience. (2004) 127: 685-93.

150. Amiry-Moghaddam M, Otsuka T, Hurn P D, Traystman R J, Haug F M, Froehner S C, Adams M E, Neely J D, Agre P, Ottersen O P, Bhardwaj A. An alpha-syntrophin-dependent pool of AQP4 in astroglial end-feet confers bidirectional water flow between blood and brain. Proc Natl Acad Sci U S A. (2003) 100: 2106-11.

151. Inoue M, Wakayama Y, Liu J W, Murahashi M, Shibuya S, Oniki H. Ultrastructural localization of aquaporin 4 and alpha1-syntrophin in the vascular feet of brain astrocytes. Tohoku J Exp Med. (2002) 197: 87-93.

152. Bragg A D, Amiry-Moghaddam M, Ottersen O P, Adams M E, Froehner S C. Assembly of a perivascular astrocyte protein scaffold at the mammalian blood-brain barrier is dependent on alpha-syntrophin. Glia. (2006) 53: 879-90.

153. Frigeri A, Nicchia G P, Nico B, Quondamatteo F, Herken R, Roncali L, Svelto M. Aquaporin-4 deficiency in skeletal muscle and brain of dystrophic mdx mice. Faseb J. (2001) 15: 90-8.

154. Manley G T, Binder D K, Papadopoulos M C, Verkman A S. New insights into water transport and edema in the central nervous system from phenotype analysis of aquaporin-4 null mice. Neuroscience. (2004) 129: 983-91.

155. Summers B A, Cumming J F, de Lahunta A. Veterinary Neuropathology. Mosby-Year Book. 1st ed. (1995).

156. Graham D I, Lantos P L. Greenfield's Neuropathology. Arnol. 6th ed. ed. (1997).

157. Siso S, Hanzlicek D, Fluehmann G, Kathmann I, Tomek A, Papa V, Vandevelde M. Neurodegenerative diseases in domestic animals: a comparative review. Vet J. (2006) 171: 20-38.

158. Creutzfeldt H G. On a particular focal disease of the central nervous system (preliminary communication), 1920. Alzheimer Dis Assoc Disord. (1989) 3: 3-25.

159. Jakob A. Concerning a disorder of the central nervous system clinically resembling multiple sclerosis with remarkable anatomic findings (spastic pseudosclerosis). Report of a fourth case. Alzheimer Dis Assoc Disord. (1989) 3: 26-45.

160. Gajdusek D C, Zigas V. Degenerative disease of the central nervous system in New Guinea; the endemic occurrence of kuru in the native population. N Engl J Med. (1957) 257: 974-8.

161. Zigas V, Gajdusek D C. Kuru: clinical study of a new syndrome resembling paralysis agitans in natives of the Eastern Highlands of Australian New Guinea. Med J Aust. (1957) 44: 745-54.

162. Lugaresi E, Medori R, Montagna P, Baruzzi A, Cortelli P, Lugaresi A, Tinuper P, Zucconi M, Gambetti P. Fatal familial insomnia and dysautonomia with selective degeneration of thalamic nuclei. N Engl J Med. (1986) 315: 997-1003.

163. Hadlow W J, Eklund C M. Scrapie--a virus-induced chronic encephalopathy of sheep. Res Publ Assoc Res Nerv Ment Dis. (1968) 44: 281-306.

164. Barlow R M. Transmissible mink encephalopathy: pathogenesis and nature of the aetiological agent. J Clin Pathol Suppl (R Coll Pathol). (1972) 6: 102-9.

165. Williams E S, Young S. Chronic wasting disease of captive mule deer: a spongiform encephalopathy. J Wildl Dis. (1980) 16: 89-98.

166. Wells G A, Scott A C, Johnson C T, Gunning R F, Hancock R D, Jeffrey M, Dawson M, Bradley R. A novel progressive spongiform encephalopathy in cattle. Vet Rec. (1987) 121: 419-20.

167. Wyatt J M, Pearson G R, Smerdon T N, Gruffydd-Jones T J, Wells G A, Wilesmith J W. Naturally occurring scrapie-like spongiform encephalopathy in five domestic cats. Vet Rec. (1991) 129: 233-6.

168. Bruce M E, Will R G, Ironside J W, McConnell I, Drummond D, Suttie A, McCardle L, Chree A, Hope J, Birkett C, Cousens S, Fraser H, Bostock C J. Transmissions to mice indicate that 'new variant' CJD is caused by the BSE agent. Nature. (1997) 389: 498-501.

169. Prusiner S B. Molecular biology of prion diseases. Science. (1991) 252: 1515-22.

170. Bolton D C, McKinley M P, Prusiner S B. Identification of a protein that purifies with the scrapie prion. Science. (1982) 218: 1309-11.

171. Prusiner S B. Novel proteinaceous infectious particles cause scrapie. Science. (1982) 216: 136-44.

172. Legname G, Baskakov I V, Nguyen H O, Riesner D, Cohen F E, DeArmond S J, Prusiner S B. Synthetic mammalian prions. Science. (2004) 305: 673-6.

173. Manuelidis L. A 25 nm virion is the likely cause of transmissible spongiform encephalopathies. J Cell Biochem. (2007) 100: 897-915.

174. Manuelidis L, Yu Z X, Barquero N, Mullins B. Cells infected with scrapie and Creutzfeldt-Jakob disease agents produce intracellular 25-nm virus-like particles. Proc Natl Acad Sci U S A. (2007) 104: 1965-70.

175. Riek R, Hornemann S, Wider G, Glockshuber R, Wuthrich K. NMR characterization of the full-length recombinant murine prion protein, mPrP(23-231). FEBS Lett. (1997) 413: 282-8.

176. Riek R, Hornemann S, Wider G, Billeter M, Glockshuber R, Wuthrich K. NMR structure of the mouse prion protein domain PrP(121-321). Nature. (1996) 382: 180-2.

177. Prusiner S B. The prion diseases. Brain Pathol. (1998) 8: 499-513.

178. Stahl N, Baldwin M A, Hecker R, Pan K M, Burlingame A L, Prusiner S B. Glycosylinositol phospholipid anchors of the scrapie and cellular prion proteins contain sialic acid. Biochemistry. (1992) 31: 5043-53.

179. McBride P A, Eikelenboom P, Kraal G, Fraser H, Bruce M E. PrP protein is associated with follicular dendritic cells of spleens and lymph nodes in uninfected and scrapie-infected mice. J Pathol. (1992) 168: 413-8.

180. Kretzschmar H A, Prusiner S B, Stowring L E, DeArmond S J. Scrapie prion proteins are synthesized in neurons. Am J Pathol. (1986) 122: 1-5.

181. Moser M, Colello R J, Pott U, Oesch B. Developmental expression of the prion protein gene in glial cells. Neuron. (1995) 14: 509-17.

182. Lasmezas C I. Putative functions of PrP(C). Br Med Bull. (2003) 66: 61-70.

183. Herms J, Tings T, Gall S, Madlung A, Giese A, Siebert H, Schurmann P, Windl O, Brose N, Kretzschmar H. Evidence of presynaptic location and function of the prion protein. J Neurosci. (1999) 19: 8866-75.

184. Mironov A, Jr., Latawiec D, Wille H, Bouzamondo-Bernstein E, Legname G, Williamson R A, Burton D, DeArmond S J, Prusiner S B, Peters P J. Cytosolic prion protein in neurons. J Neurosci. (2003) 23: 7183-93.

185. Pan T, Wong B S, Liu T, Li R, Petersen R B, Sy M S. Cell-surface prion protein interacts with glycosaminoglycans. Biochem J. (2002) 368: 81-90.

186. Warner R G, Hundt C, Weiss S, Turnbull J E. Identification of the heparan sulfate binding sites in the cellular prion protein. J Biol Chem. (2002) 277: 18421-30.

187. Graner E, Mercadante A F, Zanata S M, Forlenza O V, Cabral A L, Veiga S S, Juliano M A, Roesler R, Walz R, Minetti A, Izquierdo I, Martins V R, Brentani R R. Cellular prion protein binds laminin and mediates neuritogenesis. Brain Res Mol Brain Res. (2000) 76: 85-92.

188. Collinge J, Whittington M A, Sidle K C, Smith C J, Palmer M S, Clarke A R, Jefferys J G. Prion protein is necessary for normal synaptic function. Nature. (1994) 370: 295-7.

189. Wong B S, Pan T, Liu T, Li R, Gambetti P, Sy M S. Differential contribution of superoxide dismutase activity by prion protein in vivo. Biochem Biophys Res Commun. (2000) 273: 136-9.

190. Zou W Q, Cashman N R. Acidic pH and detergents enhance in vitro conversion of human brain PrPC to a PrPSc-like form. J Biol Chem. (2002) 277: 43942-7.

191. Torrent J, Alvarez-Martinez M T, Harricane M C, Heitz F, Liautard J P, Balny C, Lange R. High pressure induces scrapie-like prion protein misfolding and amyloid fibril formation. Biochemistry. (2004) 43: 7162-70.

192. Chien P, Weissman J S, DePace A H. Emerging principles of conformation-based prion inheritance. Annu Rev Biochem. (2004) 73: 617-56.

193. Scott M, Foster D, Mirenda C, Serban D, Coufal F, Walchli M, Torchia M, Groth D, Carlson G, DeArmond S J, et al. Transgenic mice expressing hamster prion protein produce species-specific scrapie infectivity and amyloid plaques. Cell. (1989) 59: 847-57.

194. Houston E F, Gravenor M B. Clinical signs in sheep experimentally infected with scrapie and BSE. Vet Rec. (2003) 152: 333-4.

195. Eloit M, Adjou K, Coulpier M, Fontaine J J, Hamel R, Lilin T, Messiaen S, Andreoletti O, Baron T, Bencsik A, Biacabe A G, Beringue V, Laude H, Le Dur A, Vilotte J L, Comoy E, Deslys J P, Grassi J, Simon S, Lantier F, Sarradin P. BSE agent signatures in a goat. Vet Rec. (2005) 156: 523-4.

196. Wells G A, Wilesmith J W. The neuropathology and epidemiology of bovine spongiform encephalopathy. Brain Pathol. (1995) 5: 91-103.

197. Mabbott N A, Bruce M E. The immunobiology of TSE diseases. J Gen Virol. (2001) 82: 2307-18.

198. Beekes M, McBride P A. Early accumulation of pathological PrP in the enteric nervous system and gut-associated lymphoid tissue of hamsters orally infected with scrapie. Neurosci Lett. (2000) 278: 181-4.

199. Beekes M, McBride P A, Baldauf E. Cerebral targeting indicates vagal spread of infection in hamsters fed with scrapie. J Gen Virol. (1998) 79 (Pt 3): 601-7.

200. van Keulen L J, Vromans M E, van Zijderveld F G. Early and late pathogenesis of natural scrapie infection in sheep. Apmis. (2002) 110: 23-32.

201. Heggebo R, Gonzalez L, Press C M, Gunnes G, Espenes A, Jeffrey M. Disease-associated PrP in the enteric nervous system of scrapie-affected Suffolk sheep. J Gen Virol. (2003) 84: 1327-38.

202. Hunter N, Foster J, Chong A, McCutcheon S, Parnham D, Eaton S, MacKenzie C, Houston F. Transmission of prion diseases by blood transfusion. J Gen Virol. (2002) 83: 2897-905.

203. Diedrich J F, Bendheim P E, Kim Y S, Carp R I, Haase A T. Scrapie-associated prion protein accumulates in astrocytes during scrapie infection. Proc Natl Acad Sci U S A. (1991) 88: 375-9.

204. Georgsson G, Gisladottir E, Arnadottir S. Quantitative assessment of the astrocytic response in natural scrapie of sheep. J Comp Pathol. (1993) 108: 229-40.

205. Brown D R. Microglia and prion disease. Microsc Res Tech. (2001) 54: 71-80.

206. Siso S, Puig B, Varea R, Vidal E, Acin C, Prinz M, Montrasio F, Badiola J, Aguzzi A, Pumarola M, Ferrer I. Abnormal synaptic protein expression and cell death in murine scrapie. Acta Neuropathol (Berl). (2002) 103: 615-26.

207. Jeffrey M, Goodsir C M, Bruce M, McBride P A, Scott J R, Halliday W G. Correlative light and electron microscopy studies of PrP localisation in 87V scrapie. Brain Res. (1994) 656: 329-43.

208. Marella M, Chabry J. Neurons and astrocytes respond to prion infection by inducing microglia recruitment. J Neurosci. (2004) 24: 620-7.

209. El Hachimi K H, Chaunu M P, Brown P, Foncin J F. Modifications of oligodendroglial cells in spongiform encephalopathies. Exp Neurol. (1998) 154: 23-30.

210. Sponne I, Fifre A, Koziel V, Kriem B, Oster T, Olivier J L, Pillot T. Oligodendrocytes are susceptible to apoptotic cell death induced by prion protein-derived peptides. Glia. (2004) 47: 1-8.

211. Prinz M, Montrasio F, Furukawa H, van der Haar M E, Schwarz P, Rulicke T, Giger O T, Hausler K G, Perez D, Glatzel M, Aguzzi A. Intrinsic resistance of oligodendrocytes to prion infection. J Neurosci. (2004) 24: 5974-81.

212. Wood J L, McGill I S, Done S H, Bradley R. Neuropathology of scrapie: a study of the distribution patterns of brain lesions in 222 cases of natural scrapie in sheep, 1982-1991. Vet Rec. (1997) 140: 167-74.

213. Jeffrey M, Halliday W G. Numbers of neurons in vacuolated and non-vacuolated neuroanatomical nuclei in bovine spongiform encephalopathy-affected brains. J Comp Pathol. (1994) 110: 287-93.

214. Jeffrey M, Goodbrand I A, Goodsir C M. Pathology of the transmissible spongiform encephalopathies with special emphasis on ultrastructure. Micron. (1995) 26: 277-98.

215. Giese A, Groschup M H, Hess B, Kretzschmar H A. Neuronal cell death in scrapie-infected mice is due to apoptosis. Brain Pathol. (1995) 5: 213-21.

216. Lucassen P J, Williams A, Chung W C, Fraser H. Detection of apoptosis in murine scrapie. Neurosci Lett. (1995) 198: 185-8.

217. Williams A, Lucassen P J, Ritchie D, Bruce M. PrP deposition, microglial activation, and neuronal apoptosis in murine scrapie. Exp Neurol. (1997) 144: 433-8.

218. Kretzschmar H A, Giese A, Brown D R, Herms J, Keller B, Schmidt B, Groschup M. Cell death in prion disease. J Neural Transm Suppl. (1997) 50: 191-210.

219. Theil D, Fatzer R, Meyer R, Schobesberger M, Zurbriggen A, Vandevelde M. Nuclear DNA fragmentation and immune reactivity in bovine spongiform encephalopathy. J Comp Pathol. (1999) 121: 357-67.

220. Fairbairn D W, Carnahan K G, Thwaits R N, Grigsby R V, Holyoak G R, O'Neill K L. Detection of apoptosis induced DNA cleavage in scrapie-infected sheep brain. FEMS Microbiol Lett. (1994) 115: 341-6.

221. Pillot T, Drouet B, Pincon-Raymond M, Vandekerckhove J, Rosseneu M, Chambaz J. A nonfibrillar form of the fusogenic prion protein fragment [118-135] induces apoptotic cell death in rat cortical neurons. J Neurochem. (2000) 75: 2298-308.

222. Ferrer I. Nuclear DNA fragmentation in Creutzfeldt-Jakob disease: does a mere positive in situ nuclear end-labeling indicate apoptosis? Acta Neuropathol (Berl). (1999) 97: 5-12.

223. Brown D, Belichenko P, Sales J, Jeffrey M, Fraser J R. Early loss of dendritic spines in murine scrapie revealed by confocal analysis. Neuroreport. (2001) 12: 179-83.

224. Bouzamondo-Bernstein E, Hopkins S D, Spilman P, Uyehara-Lock J, Deering C, Safar J, Prusiner S B, Ralston H J, 3rd, DeArmond S J. The neurodegeneration sequence in prion diseases: evidence from functional, morphological and ultrastructural studies of the GABAergic system. J Neuropathol Exp Neurol. (2004) 63: 882-99.

225. Jeffrey M, Halliday W G, Bell J, Johnston A R, MacLeod N K, Ingham C, Sayers A R, Brown D A, Fraser J R. Synapse loss associated with abnormal PrP precedes neuronal degeneration in the scrapie-infected murine hippocampus. Neuropathol Appl Neurobiol. (2000) 26: 41-54.

226. Gonzalez-Iglesias R, Pajares M A, Ocal C, Espinosa J C, Oesch B, Gasset M. Prion protein interaction with glycosaminoglycan occurs with the formation of oligomeric complexes stabilized by Cu(II) bridges. J Mol Biol. (2002) 319: 527-40.

227. Hijazi N, Kariv-Inbal Z, Gasset M, Gabizon R. PrPSc incorporation to cells requires endogenous GAGs expression. J Biol Chem. (2005)

228. Papakonstantinou E, Karakiulakis G, Roth M, Verghese-Nikolakaki S, Dawson M, Papadopoulos O, Sklaviadis T. Glycosaminoglycan analysis in brain stems from animals infected with the bovine spongiform encephalopathy agent. Arch Biochem Biophys. (1999) 370: 250-7.

229. Guentchev M, Groschup M H, Kordek R, Liberski P P, Budka H. Severe, early and selective loss of a subpopulation of GABAergic inhibitory neurons in experimental transmissible spongiform encephalopathies. Brain Pathol. (1998) 8: 615-23.

230. Belichenko P V, Miklossy J, Belser B, Budka H, Celio M R. Early destruction of the extracellular matrix around parvalbumin-immunoreactive interneurons in Creutzfeldt-Jakob disease. Neurobiol Dis. (1999) 6: 269-79.

231. Guentchev M, Wanschitz J, Voigtlander T, Flicker H, Budka H. Selective neuronal vulnerability in human prion diseases. Fatal familial insomnia differs from other types of prion diseases. Am J Pathol. (1999) 155: 1453-7.

232. Collie D A, Summers D M, Sellar R J, Ironside J W, Cooper S, Zeidler M, Knight R, Will R G. Diagnosing variant Creutzfeldt-Jakob disease with the pulvinar sign: MR imaging findings in 86 neuropathologically confirmed cases. AJNR Am J Neuroradiol. (2003) 24: 1560-9.

233. Murata T, Shiga Y, Higano S, Takahashi S, Mugikura S. Conspicuity and evolution of lesions in Creutzfeldt-Jakob disease at diffusion-weighted imaging. AJNR Am J Neuroradiol. (2002) 23: 1164-72.

234. Tsuboi Y, Baba Y, Doh-ura K, Imamura A, Fujioka S, Yamada T. Diffusion-weighted MRI in familial Creutzfeldt-Jakob disease with the codon 200 mutation in the prion protein gene. J Neurol Sci. (2005) 232: 45-9.

235. Ukisu R, Kushihashi T, Kitanosono T, Fujisawa H, Takenaka H, Ohgiya Y, Gokan T, Munechika H. Serial diffusion-weighted MRI of Creutzfeldt-Jakob disease. AJR Am J Roentgenol. (2005) 184: 560-6.

236. Xiang W, Windl O, Wunsch G, Dugas M, Kohlmann A, Dierkes N, Westner I M, Kretzschmar H A. Identification of differentially expressed genes in scrapie-infected mouse brains by using global gene expression technology. J Virol. (2004) 78: 11051-60.

237. Riemer C, Queck I, Simon D, Kurth R, Baier M. Identification of upregulated genes in scrapie-infected brain tissue. J Virol. (2000) 74: 10245-8.

238. Riemer C, Neidhold S, Burwinkel M, Schwarz A, Schultz J, Kratzschmar J, Monning U, Baier M. Gene expression profiling of scrapie-infected brain tissue. Biochem Biophys Res Commun. (2004) 323: 556-64.

239. Xiang W, Windl O, Westner I M, Neumann M, Zerr I, Lederer R M, Kretzschmar H A. Cerebral gene expression profiles in sporadic Creutzfeldt-Jakob disease. Ann Neurol. (2005) 58: 242-57.

240. Rodriguez A, Perez-Gracia E, Espinosa J C, Pumarola M, Torres J M, Ferrer I. Increased expression of water channel aquaporin 1 and aquaporin 4 in Creutzfeldt-Jakob disease and in bovine spongiform encephalopathy-infected bovine-PrP transgenic mice. Acta Neuropathol (Berl). (2006) 112: 573-85.

241. Castilla J, Gutierrez Adan A, Brun A, Pintado B, Ramirez M A, Parra B, Doyle D, Rogers M, Salguero F J, Sanchez C, Sanchez-Vizcaino J M, Torres J M. Early detection of PrPres in BSE-infected bovine PrP transgenic mice. Arch Virol. (2003) 148: 677-91.

242. Espinosa J C, Andreoletti O, Castilla J, Herva M E, Morales M, Alamillo E, San-Segundo F D, Lacroux C, Lugan S, Salguero F J, Langeveld J, Torres J M. Sheep-passaged bovine spongiform encephalopathy agent exhibits altered pathobiological properties in bovine-PrP transgenic mice. J Virol. (2007) 81: 835-43.

243. Castilla J, Brun A, Diaz-San Segundo F, Salguero F J, Gutierrez-Adan A, Pintado B, Ramirez M A, del Riego L, Torres J M. Vertical transmission of bovine spongiform encephalopathy prions evaluated in a transgenic mouse model. J Virol. (2005) 79: 8665-8.

244. Szigeti Z M, Matesz C, Szekely G, Felszeghy S, Bacskai T, Halasi G, Meszar Z, Modis L. Distribution of hyaluronan in the central nervous system of the frog. J Comp Neurol. (2006) 496: 819-31.

245. David G, Bai X M, Van der Schueren B, Cassiman J J, Van den Berghe H. Developmental changes in heparan sulfate expression: in situ detection with mAbs. J Cell Biol. (1992) 119: 961-75.

246. Hobohm C, Hartig W, Brauer K, Bruckner G. Low expression of extracellular matrix components in rat brain stem regions containing modulatory aminergic neurons. J Chem Neuroanat. (1998) 15: 135-42.

247. King A S. Physiological and Clinical Anatomy of the Domestic Mammals. Oxford Science Publications. Oxford University Press. 1st ed. (1987). 1:

248. Vidal E, Marquez M, Tortosa R, Costa C, Serafin A, Pumarola M. Immunohistochemical approach to the pathogenesis of bovine spongiform encephalopathy in its early stages. J Virol Methods. (2006) 134: 15-29.

249. Spector D A, Wade J B, Dillow R, Steplock D A, Weinman E J. Expression, localization, and regulation of aquaporin-1 to -3 in rat urothelia. Am J Physiol Renal Physiol. (2002) 282: F1034-42.

250. Brown D R, Schmidt B, Kretzschmar H A. A prion protein fragment primes type 1 astrocytes to proliferation signals from microglia. Neurobiol Dis. (1998) 4: 410-22.

251. Hafiz F B, Brown D R. A model for the mechanism of astrogliosis in prion disease. Mol Cell Neurosci. (2000) 16: 221-32.

252. Belichenko P V, Miklossy J, Celio M R. HIV-I induced destruction of neocortical extracellular matrix components in AIDS victims. Neurobiol Dis. (1997) 4: 301-10.

253. Medina-Flores R, Wang G, Bissel S J, Murphey-Corb M, Wiley C A. Destruction of extracellular matrix proteoglycans is pervasive in simian retroviral neuroinfection. Neurobiol Dis. (2004) 16: 604-16.

254. Deb S, Wenjun Zhang J, Gottschall P E. Beta-amyloid induces the production of active, matrix-degrading proteases in cultured rat astrocytes. Brain Res. (2003) 970: 205-13.

255. Hobohm C, Gunther A, Grosche J, Rossner S, Schneider D, Bruckner G. Decomposition and long-lasting downregulation of extracellular matrix in perineuronal nets induced by focal cerebral ischemia in rats. J Neurosci Res. (2005) 80: 539-48.

256. Gutowski N J, Newcombe J, Cuzner M L. Tenascin-R and C in multiple sclerosis lesions: relevance to extracellular matrix remodelling. Neuropathol Appl Neurobiol. (1999) 25: 207-14.

257. Sobel R A, Ahmed A S. White matter extracellular matrix chondroitin sulfate/dermatan sulfate proteoglycans in multiple sclerosis. J Neuropathol Exp Neurol. (2001) 60: 1198-207.

258. Lu A, Tang Y, Ran R, Clark J F, Aronow B J, Sharp F R. Genomics of the periinfarction cortex after focal cerebral ischemia. J Cereb Blood Flow Metab. (2003) 23: 786-810.

259. Kurazono S, Okamoto M, Sakiyama J, Mori S, Nakata Y, Fukuoka J, Amano S, Oohira A, Matsui H. Expression of brain specific chondroitin sulfate proteoglycans, neurocan and phosphacan, in the developing and adult hippocampus of Ihara's epileptic rats. Brain Res. (2001) 898: 36-48.

260. Nakic M, Mitrovic N, Sperk G, Schachner M. Kainic acid activates transient expression of tenascin-C in the adult rat hippocampus. J Neurosci Res. (1996) 44: 355-62.

261. Asher R A, Morgenstern D A, Fidler P S, Adcock K H, Oohira A, Braistead J E, Levine J M, Margolis R U, Rogers J H, Fawcett J W. Neurocan is upregulated in injured brain and in cytokine-treated astrocytes. J Neurosci. (2000) 20: 2427-38.

262. Deller T, Haas C A, Naumann T, Joester A, Faissner A, Frotscher M. Up-regulation of astrocyte-derived tenascin-C correlates with neurite outgrowth in the rat dentate gyrus after unilateral entorhinal cortex lesion. Neuroscience. (1997) 81: 829-46.

263. Delpech B, Maingonnat C, Girard N, Chauzy C, Maunoury R, Olivier A, Tayot J, Creissard P. Hyaluronan and hyaluronectin in the extracellular matrix of human brain tumour stroma. Eur J Cancer. (1993) 29A: 1012-7.

264. Zagzag D, Friedlander D R, Dosik J, Chikramane S, Chan W, Greco M A, Allen J C, Dorovini-Zis K, Grumet M. Tenascin-C expression by angiogenic vessels in human astrocytomas and by human brain endothelial cells in vitro. Cancer Res. (1996) 56: 182-9.

265. Lukoyanov N V, Brandao F, Cadete-Leite A, Madeira M D, Paula-Barbosa M M. Synaptic reorganization in the hippocampal formation of alcohol-fed rats may compensate for functional deficits related to neuronal loss. Alcohol. (2000) 20: 139-48.

266. Smith B N, Dudek F E. Short- and long-term changes in CA1 network excitability after kainate treatment in rats. J Neurophysiol. (2001) 85: 1-9.

267. Papadopoulos M C, Verkman A S. Aquaporin-4 gene disruption in mice reduces brain swelling and mortality in pneumococcal meningitis. J Biol Chem. (2005) 280: 13906-12.

268. Wang K, Bekar L K, Furber K, Walz W. Vimentin-expressing proximal reactive astrocytes correlate with migration rather than proliferation following focal brain injury. Brain Res. (2004) 1024: 193-202.

269. Tomas-Camardiel M, Venero J L, de Pablos R M, Rite I, Machado A, Cano J. In vivo expression of aquaporin-4 by reactive microglia. J Neurochem. (2004) 91: 891-9.

270. Hawrylak N, Fleming J C, Salm A K. Dehydration and rehydration selectively and reversibly alter glial fibrillary acidic protein immunoreactivity in the rat supraoptic nucleus and subjacent glial limitans. Glia. (1998) 22: 260-71.

271. Nagelhus E A, Veruki M L, Torp R, Haug F M, Laake J H, Nielsen S, Agre P, Ottersen O P. Aquaporin-4 water channel protein in the rat retina and optic nerve: polarized expression in Muller cells and fibrous astrocytes. J Neurosci. (1998) 18: 2506-19.

272. Binder D K, Oshio K, Ma T, Verkman A S, Manley G T. Increased seizure threshold in mice lacking aquaporin-4 water channels. Neuroreport. (2004) 15: 259-62.

273. Wen H, Nagelhus E A, Amiry-Moghaddam M, Agre P, Ottersen O P, Nielsen S. Ontogeny of water transport in rat brain: postnatal expression of the aquaporin-4 water channel. Eur J Neurosci. (1999) 11: 935-45.

274. Liberski P P, Streichenberger N, Giraud P, Soutrenon M, Meyronnet D, Sikorska B, Kopp N. Ultrastructural pathology of prion diseases revisited: brain biopsy studies. Neuropathol Appl Neurobiol. (2005) 31: 88-96.

275. Kim J H, Manuelidis E E. Serial ultrastructural study of experimental Creutzfeldt-Jacob disease in guinea pigs. Acta Neuropathol (Berl). (1986) 69: 81-90.

276. Landis D M, Williams R S, Masters C L. Golgi and electronmicroscopic studies of spongiform encephalopathy. Neurology. (1981) 31: 538-49.

277. Miyakawa T, Katsuragi S, Koga Y, Moriyama S. Status spongiosus in Creutzfeldt-Jakob disease. Clin Neuropathol. (1986) 5: 146-52.